Tectonophysics 822 (2022) 229150

Contents lists available at ScienceDirect

Tectonophysics

journal homepage: www.elsevier.com/locate/tecto

Invited Review

Opening of the Gulf of Mexico: What we know, what questions remain, and how we might answer them

Irina Filina [a,*], James Austin [b], Tony Doré [c], Elizabeth Johnson [d], Daniel Minguez [d], Ian Norton [b], John Snedden [b], Robert J. Stern [e]

[a] The University of Nebraska, Department of Earth and Atmospheric Sciences, 1215 U St., Lincoln, NE 68508, USA
[b] The University of Texas at Austin, Institute for Geophysics, 10100 Burnet Rd., Austin, TX 78758, USA
[c] Energy & Geoscience Institute (EGI), 423 Wakara Way, Suite 300, Salt Lake City, Utah 84108, USA
[d] Chevron, 1500 Louisiana St, Houston, TX 77002, USA
[e] The University of Texas at Dallas, Department of Geosciences, 800 West Campbell Rd., Richardson, TX 75080, USA

ARTICLE INFO

Keywords:
Gulf of Mexico
Basin formation
Tectonic reconstruction
Magma-rich
Magma-poor
Seafloor spreading

ABSTRACT

The Gulf of Mexico is an economically important basin with more than a century-long history of hydrocarbon exploration. However, the opening of the basin remains debated for two reasons: 1) the quality of data does not allow for reliable interpretations of crustal features beneath thick and complex overburden, and 2) most industry well and geophysical data are proprietary. The last concerted effort by industry and academia to summarize the state of knowledge regarding the Gulf of Mexico's formation was three decades ago and resulted in publication of a major volume as part of the Decade of North American Geology (DNAG). This paper reviews the key, publicly available, recently published geophysical datasets and geological observations that constrain the basin's tectonic history. We compare and contrast published tectonic models and formulate remaining controversies about the basin. These relate to tectonic affiliation of Triassic redbeds (early syn-rift vs. precursor basin[s]), the timing of seafloor spreading vs. salt deposition, the nature of breakup (magma-rich vs. magma-poor), and remaining ambiguities in restoring crustal blocks to their pre-rift positions. We then speculate on the datasets that can help resolve these controversies. We conclude that continued collaborative industry and academia partnerships are crucial for advancing our understanding of how the Gulf of Mexico formed.

1. Introduction

The Gulf of Mexico (GoM) is a prolific petroleum basin at the southern edge of the North America tectonic plate (Fig. 1) with more than a century long exploration history. Despite a vast number of wells that have been drilled and large amounts of geophysical, geochemical and geological data that have been acquired in the basin, its tectonic history remains debated by the geoscientific community. The GoM margin can be subdivided into five zones based on tectonic settings (Fig. 1). These zones also correlate with different types of rifted margins that have been proposed in the literature. Zone 1 refers to the well-accepted transform margin along the eastern coast of Mexico although its name differs in the literature (see details in section 5.4). In contrast, the nature of crust beneath Zone 2 in the northwestern GoM remains debated, with interpretations ranging from stretched and intruded continental crust, thicker than normal oceanic crust, or exhumed mantle proposed in the literature. Zone 3 in the northeastern GoM is also poorly understood, interpreted by different authors as either a magma-poor or magma-rich margin (see section 7.3). Tilted blocks imaged by seismic profiles in Zone 4, beneath the western approaches to the Florida Straits, are generally interpreted as evidence for a rifted continental margin; the presence of intruded continental crust there is confirmed by DSDP drilling (Schlager et al., 1984; sites 537 and 538A in Fig 2b; see Appendix C1). The nature of the GoM near Cuba is also poorly known, although tilted crustal blocks are observed seismically along the northwestern coast (Angstadt et al., 1985). Zone 5 north and west of the Yucatan Peninsula is another debated region, with interpretations ranging from a magma-rich rifted margin to a hyperextended one with exhumed mantle. We will refer to these zones throughout the text.

The GoM has a very thick sedimentary cover (Fig. 2a) that buries its oldest rocks and consequently obscures its formation history. Largely because of the masking effect of this thick cover, the early tectonic

* Corresponding author.
E-mail address: ifilina2@unl.edu (I. Filina).

https://doi.org/10.1016/j.tecto.2021.229150
Received 6 January 2021; Received in revised form 31 October 2021; Accepted 10 November 2021
Available online 18 November 2021

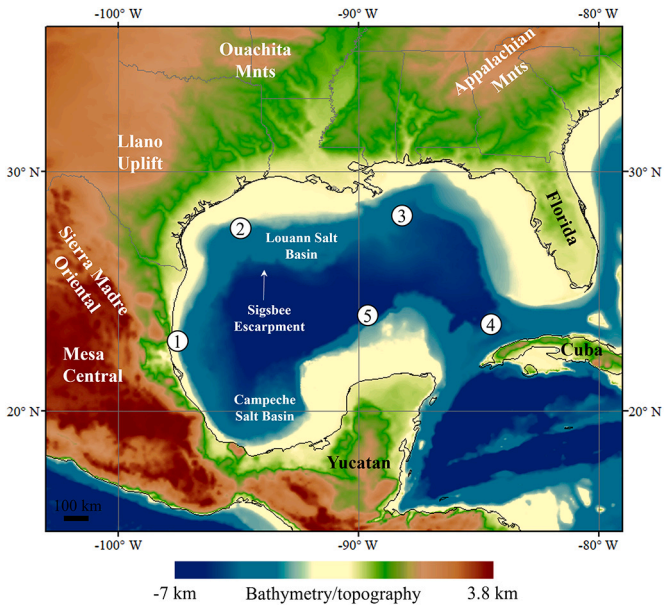

Fig. 1. Bathymetry/topography of the Gulf of Mexico from Smith and Sandwell (1997). The numbers refer to five distinct margin zones described in the text: (1) Tamaulipas transform margin, (2) the western GoM rifted margin, (3) the eastern GoM margin, (4) the western approaches to the Florida Straits, and (5) the Yucatan margin.

history of the GoM continues to be debated by the geoscientific community. Many different models for basin opening have been put forth over the years, sometimes proposing contrary ideas for opening style, pre-break-up location(s) of crustal blocks, and even the order of major tectonic events. The last integrated peer-reviewed synthesis of GoM evolution was published three decades ago as part of the Decade of North American Geology (Salvador, 1991). Since then, significant new datasets have been acquired, petroleum exploration in deepwater GoM has expanded, and new ideas about how continents rift and transition to seafloor spreading have been published, and new quantitative interpretations and models for GoM opening have been proposed. This paper brings together researchers from academia and industry with different perspectives on GoM opening to review what we know, what questions remain, and what new data are needed to answer them.

Before we describe the current state of knowledge about GoM opening and outline the range of alternative models that have been proposed for the basin, we list the key acronyms and define the terms that are most often used in the literature (section 2). We then summarize the four recognized major tectonic phases of GoM formation (section 3). We focus on earlier Mesozoic events and do not cover many important but younger Cretaceous and Cenozoic events, as all published tectonic models for the GoM agree that oceanic spreading ceased before the Barremian (128 Ma).

Deciphering how the GoM opened requires integrating different data types, observations and models, each providing constraints that collectively can be used to reduce uncertainties. In section 4, we introduce the major datasets that have been used to constrain GoM tectonic models, while more details about those datasets are provided in the Appendices. Key geological observations are summarized in section 5. We then describe recently published tectonic models, outline their differences and similarities, and tie them to key datasets, validations and observations in section 6. We do not determine which model is best and we do not propose any new model. Our intent instead is to describe the diversity of published models and to highlight key datasets and the range of interpretations proposed for the opening of the GoM, in order to encourage further research. In section 7, we identify the key controversies about the GoM opening and discuss proposed alternative scenarios. Finally, in section 8 we list missing pieces of the GoM tectonic puzzle and recommend which geological or geophysical data, methods, and analyses may help resolve remaining controversies. Our approach - involving both academic and industrial geoscientists working together - should also be useful for studying other sediment-covered oceanic basins and margins around the world.

2. Key definitions and acronyms

In Table 1 we summarize the terms and acronyms that are often used in the literature referring to various components and concepts related to passive margin evolution. The term OCB (sometimes COB) is widely used and refers to the Ocean Continent Boundary – the interpreted border between oceanic and continental crust. This boundary is often approximated by a line, but that is clearly an oversimplification, as noted by Eagles et al. (2015). Nonetheless, this approximation of a mapped line is still useful, especially as an aid to 2D modeling and tectonic restoration.

The term OCT - Ocean Continent Transition (zone) – takes into account the geologic reality that the transition between continental and oceanic crustal domains is a complex zone of varying width. There is general confusion in the geoscience community about its use. Often, OCT gets confused with the term transitional crust – crust interpreted to lie between normal (unstretched) continental crust and oceanic crust formed by seafloor spreading (e.g., Emiliani, 1965; Menard, 1967). In the GoM, this term was introduced by Buffler and Sawyer (1985) to designate crust that was stretched and possibly intruded during continental rifting. Sawyer et al. (1991) further split transitional crust into two zones: thick and thin transitional crust, as shown in Fig. 2b. While transitional crust implies stretched and thinned continental crust that may or may not have been intruded, a transition zone (i.e., OCT) may be represented by either magmatically modified continental crust, exhumed lower continental crust, or by exhumed mantle resulted from rifting processes.

All authors agree that GoM has continental and oceanic crustal zones. Some authors have suggested exhumed mantle to underlie some portion of the GoM (Pindell et al., 2016; Minguez et al., 2020). To avoid ambiguity about the nature of the crustal zone adjacent to the oceanic domain, the term LOC – Limit of Oceanic Crust has been proposed to define the landward limit of normal oceanic crust in the GoM (Hudec et al., 2013). Landward of LOC, the nature of the adjacent region can be variously ascribed – whether it be thick mafic crust, thinned continental crust or exhumed mantle. Interpreted OCBs and LOCs in the GoM vary among published tectonic models (Fig. 3). For this review, when discussing interpretations and associated models, we utilize the authors' original nomenclature.

The terms Mid-Oceanic Ridge (MOR), Extinct Spreading Ridge/Center (ESR/ESC), and Fracture Zone (FZ) relate to features produced by oceanic or seafloor spreading. In the GoM, different published notations are used for ESRs. Eddy et al. (2014) refer to them as Extinct Spreading Ridges (ESR), which is slightly misleading, as morphologically the extinct spreading centers are often topographic lows, not ridges (see Deighton et al., 2017). Publication of satellite-derived gravity by Sandwell et al. (2014) revealed the pattern of the ESRs and associated transform FZs in the GoM basin, although there remain some discrepancies in interpretations of spreading geometries (Fig. 3).

The term breakup appears to have different connotations in the geoscience community. One meaning encompasses a continuum from initial rifting to initial seafloor spreading (i.e., "the breakup of Pangea supercontinent"). Another perspective is narrower, relating the term to the interval between continental rifting and seafloor spreading/mantle exhumation, e.g., initial separation of conjugate rifted continental blocks, marked often in geophysical data by "the breakup unconformity". In this review, we retain the latter meaning of this term.

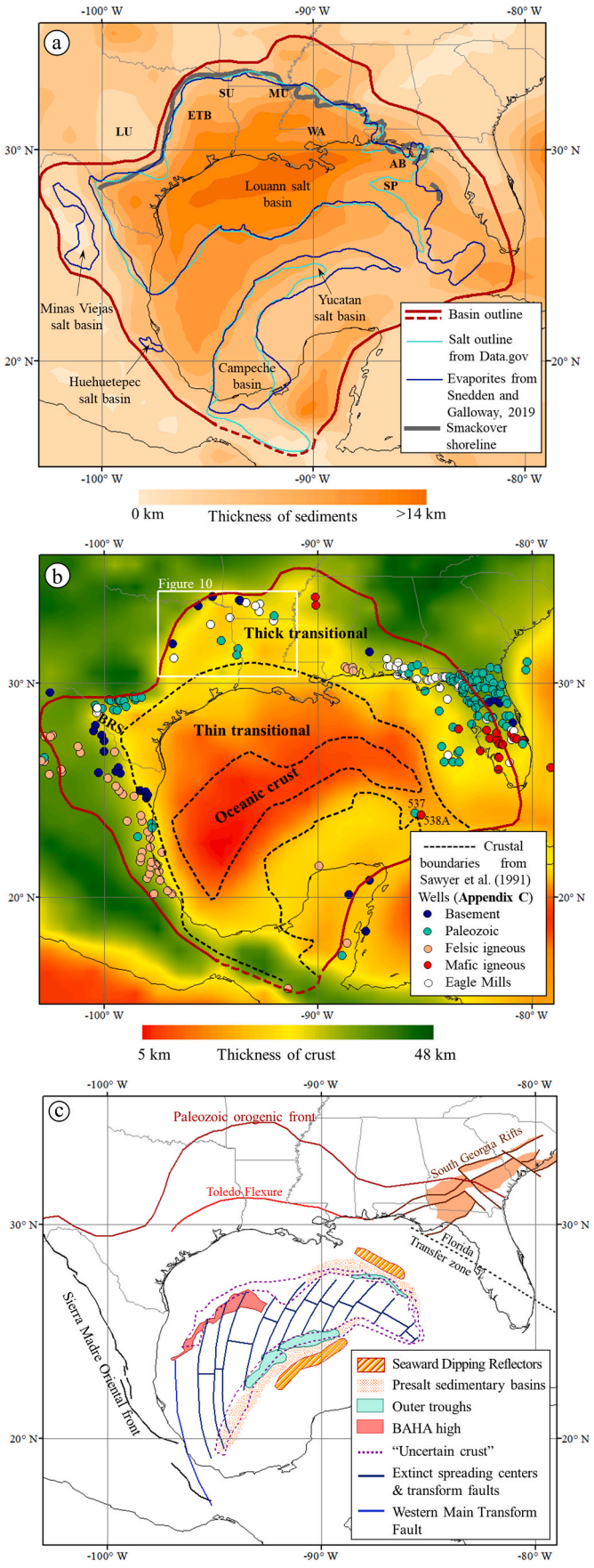

(caption on next column)

Fig. 2. The thickness of sediments (a) and crust (b) from CRUST1.0 model (Laske et al., 2013). The thick red line shows the approximate boundaries of the GoM basin outlined by the authors based on that model. Two different polygons for the Louann and Isthmian salt provinces in the north and south of the basin, respectively, are shown. The latter comprises the Yucatan and Campeche sub-basins. The dashed black lines in (b) show the location of different crustal boundaries from Sawyer et al. (1991). Wells that penetrated basement or Paleozoic rocks are shown in (b) and are described in Appendix C. Note the DSDP sites 537 and 538A (Schlager et al., 1984); the latter penetrated stretched and intruded continental crust. White box shows the extent of Fig. 10. (c) Key tectonic features in the GoM mentioned in the literature: the presalt basins and SDR provinces are interpreted from joint analysis of seismic and potential fields Filina and Beutel (2021), extinct spreading centers and associated transform faults are from joint analysis of gravity and seismic data (Deighton et al., 2017), "uncertain crust" from Curry et al. (2018) is a descendant of the basement ramp of Hudec et al. (2013), outer troughs are from Hudec and Norton (2019), BAHA high is from Hudec et al. (2020), Toledo flexure is from Anderson (1979), the Florida Transfer zone is from Pindell et al. (2020), the Western Main Transform Fault from Nguyen and Mann (2016), note that it is referred as Tamaulipas transform in Fig. 1. AB = Apalachicola Basin, BRS = Border Rift System, ETB = East Texas Basin, LU = Llano uplift, MU=Monroe Uplift, SU=Sabine Uplift, SP = Southern Plateau, WA=Wiggins Arch.

3. Generalized tectonic evolution

While there is no consensus for the opening of the Gulf of Mexico, it is accepted that the opening post-dates the end of the Late Paleozoic Ouachita-Marathon-Appalachian orogeny and that sea-floor spreading had ended by Early Cretaceous (Fig. 4). Snedden and Galloway (2019) provide a comprehensive synthesis of the pertinent tectonic and depositional history, in light of new scientific and exploration insights. Four major tectonic phases have been proposed in the literature to describe the progression of GoM opening:

1. Pre-rift, Permo-Triassic following Late Paleozoic Pangean suturing
2. Continental rifting, Early Mesozoic
3. Seafloor spreading, mostly Jurassic
4. Post-spreading thermal subsidence and sediment loading, Cretaceous and younger.

The presence of a thick sedimentary succession and mobile Jurassic salt complicates the interpretation of structures related to this 4-fold subdivision. Where salt exists (Fig. 2a), seismic imaging of underlying (i.e., syn-opening) sequences is difficult. Whether salt was deposited during the last stages of continental rifting, over oceanic crust, and/or concurrent with the first stages of seafloor spreading, remains unclear. For this reason, salt deposition is described briefly in this section, while we focus on how it fits into the simplified tectonic evolution in section 7.2.

The pre-rifting phase encompasses the time interval between the assemblage of Pangea and the start of basin-forming extension. The supercontinent Pangea assembled during the Late Paleozoic, with Laurussia (including Laurentia, comprising most of what is now North America) bounded by Gondwana to the east and south. The Ouachita-Marathon orogen (both exposed and buried, Fig.s 1 and 2) marks the Laurentia-Gondwana suture zone, as well as the continental limit of crustal thinning accomplished during the GoM formation (e.g., Marton and Buffler, 1994). Some researchers (see Snedden and Galloway, 2019) have proposed the presence of a Permo- Triassic precursor basin based on the lack of extensional features observed in pre-salt sections in the northern part of the GoM. In contrast, Stern and Dickinson (2010) have interpreted the Border rift and East Texas basin (Fig. 2) as Late Jurassic extensional structures. Consequently, these alternative interpretations suggest different affiliation for the Triassic sediments in the GoM, namely as either early rift sequences or fill within a precursor basin. This contradiction is the first of a number of GoM controversies discussed in section 7.1.

Table 1
Commonly used acronyms and definitions referred to in this synthesis. See text for details and references.

Term	Definition
OCB / COB	Ocean – Continent Boundary. An interpretation of the boundary between oceanic and continental crust.
LOC	Limit of Oceanic Crust. The landward limit of oceanic crust formed at a mid-ocean spreading center.
OCT/COT	Ocean-Continent/Continent – Ocean Transition. The transitional area between extended continental crust and oceanic crust. This can be hyper-extended continental crust, unusually thick basaltic crust, exhumed mantle or lower crust, or some combination. Not to be confused with transitional crust.
Transitional Crust	Crust that is thinner than normal continental crust and thicker than normal oceanic crust. The term defined by Buffler and Sawyer (1985) in the GoM which relates to the wide region of rifted continental crust there (see Fig. 2b). Not to be confused with much narrower transitional zone of OCT/COT.
MOR	Mid-ocean ridge, site of seafloor spreading. Fossil MORs are ESR/ESCs.
ESR/ESC	Extinct Spreading Ridge/Center. A MOR that is no longer actively spreading but can be interpreted from geophysical data, see Fig.s 2c, 3, 7, 8
Fracture Zone (FZ)	The boundary between two oceanic crust tracts formed by an offset in the MOR. The oceanic crust is of different ages on either side of the FZ, see Fig.s 2c, 3, 7
SDR	Seaward Dipping Reflectors. High amplitudes tilted/curved reflectors observed in seismic reflection data, which are generally interpreted as basalts erupted before the start of seafloor spreading, see section 5.2.
Magma-rich margin	The form at extensional margins accompanied by extensive volcanism (sometimes referred to as volcanic rifted margins). Thick basalts and/or lower crust gabbro make up this kind of transitional crust. Magma-rich margins generally show strong magnetic and gravity anomalies and have SDRs. See section 7.3.
Magma-poor margin	Extensional margin where transitional crust formed with little or no magmatic addition, dominated by hyperextended continental crust. Exhumed and serpentinized mantle is common is outboard domain of magma-poor margins. See section 7.3.
Exhumed mantle	Mantle exhumed after the continental crust has extended beyond break-up and before sea-floor spreading has started. Exhumed mantle is generally serpentinized. See section 7.3.
OMD/OMC and OMT	Outer Margin Detachment/Outer Margin Collapse – the processes hypothesized by Pindell et al. (2014) particularly for magma-poor margins. The accompanying regional large-scale structural low in crystalline basement is referred as Outer Marginal Trough. Not to be confused with “outer trough”. See section 7.3.
Outer trough	Basement trough observed at outer edge of OCT off northern Yucatan and locally along the northeastern margin (Hudec and Norton, 2019). See outline in Fig. 2c and details in section 5.3
BAHA high	Up to 3 km high and 500 km long ridge in the Western GoM described by Hudec and Norton (2019) that serves as a backstop for the Perdido Fold belt. See outline in Fig. 2c and section 5.5 for details.
BAB, HABAB	Back-Arc Basin and High-Angle Back-Arc Basin refer to the sedimentary basin formed behind a subduction-related magmatic arc.

The continental rifting phase represents an extension of the continental lithosphere before seafloor spreading began in the Jurassic. Researchers generally agree that the formation of the GoM was part of the disassembly of the late Paleozoic–early Mesozoic supercontinent Pangea (e.g., Pindell, 1985; Winterer, 1991; Adatte et al., 1996) and was broadly coincident with extensive magmatism, the Central Atlantic Magmatic Province (CAMP), of eastern North America and beyond (Marzoli et al., 2018). This brief magmatic event occurred ~ 200 Ma (e.g., Marzoli et al., 1999; McHone, 2003) and produced a large volume of mafic lava, sills, and dikes that have been mapped on four continents – from southern Georgia - northern Florida to Newfoundland in North America, northeastern South America, northwestern Africa and in parts of western Europe.

Few basement-involved major structures formed during the continental rifting phase have been identified in the GoM. The clearest example is the Triassic South Georgia Rift (Fig. 2c), which developed in the northeast prior to the GoM opening, and which is capped by CAMP flood basalts (McBride, 1991; Blount and Millings, 2011). Another tectonic structure potentially related to this phase is the NW-SE trending Florida Transfer Zone through southern Florida (Fig. 2c). Other names for this structure are found in the literature(see details in section 6); its nature remains debated. Following or even interbedded with CAMP magmatic products, Triassic redbeds (Eagle Mills Fm and its equivalents) are documented in various parts of the basin (see Fig. 2b and Appendix C2 for more details). Relevant pre-salt chronostratigraphy can be established from subsurface data across the basin (Fig. 4). As already mentioned, the tectonic affiliation of Triassic sediments is debated (section 7.1). In addition, an up to 5 km-thick pre-salt sedimentary section is interpreted in seismic data (section 5.1) along the Yucatan margin (Zone 5) and in the eastern GoM (Zone 3); these are outlined in Fig. 2c based on joint analysis of seismic data with potential fields (Filina and Beutel, 2021). In addition, adjacent regions of basinward dipping reflectors (section 5.2) are identified seismically in the same two zones; these can be interpreted either as SDRs (as in Fig. 2c) or as amagmatic extensional features (see section 7.3 for discussion).

The GoM continental rift changed to a passive margin when seafloor spreading began. Typically, seafloor spreading magnetic anomalies (section 4 and Appendix B2) are used to constrain the timing of breakup, but such data are poor in GoM and cannot be used to constrain the time of break-up in a robust way. Consequently, the proposed onset of spreading varies from ~190 Ma to ~150 Ma among published models (Fig. 4; section 6). All modern models agree that the last phase of seafloor spreading coincides with the counterclockwise rotation of the Yucatan block away from North America; the initiation of the spreading-related rotational phase varies from ~ 170 to ~ 162 Ma in literature (Fig. 4). We further discuss the complexities of the rift to drift transition in section 6.

Deposition of salt plays an important role in the formation of the GoM basin. Very thick (as much as 4 km; Hudec et al., 2013a) salt was deposited in the Jurassic; halokinesis of overlying sediments has had major influences on structural style within the basin. Salt is present on both the U.S. and Mexican sides of the GoM (Fig. 2a). The Louann Salt on the U.S. side is contained within several sub-basins. The coast-parallel Toledo Flexure (Anderson, 1979; Fig. 2c) separates onshore basins from coastal and offshore basins. Salt beneath the Sigsbee Escarpment (Fig. 1) is clearly allochthonous, having moved a substantial distance basinward in two phases (Hudec et al., 2013); the Escarpment itself is a testament to that movement. The first phase was in the Mesozoic, when salt flowed out horizontally into the basin. This became the mother salt for the second, mostly vertical phase during the Cenozoic, that today results in multiple diapirs, welds, sheets, local minibasins and other complex structures forming hydrocarbon traps that have been the target of hydrocarbon exploration wells. There are three salt basins on the Mexican side (Fig. 2a). The largest is the Isthmian Basin on the Yucatan

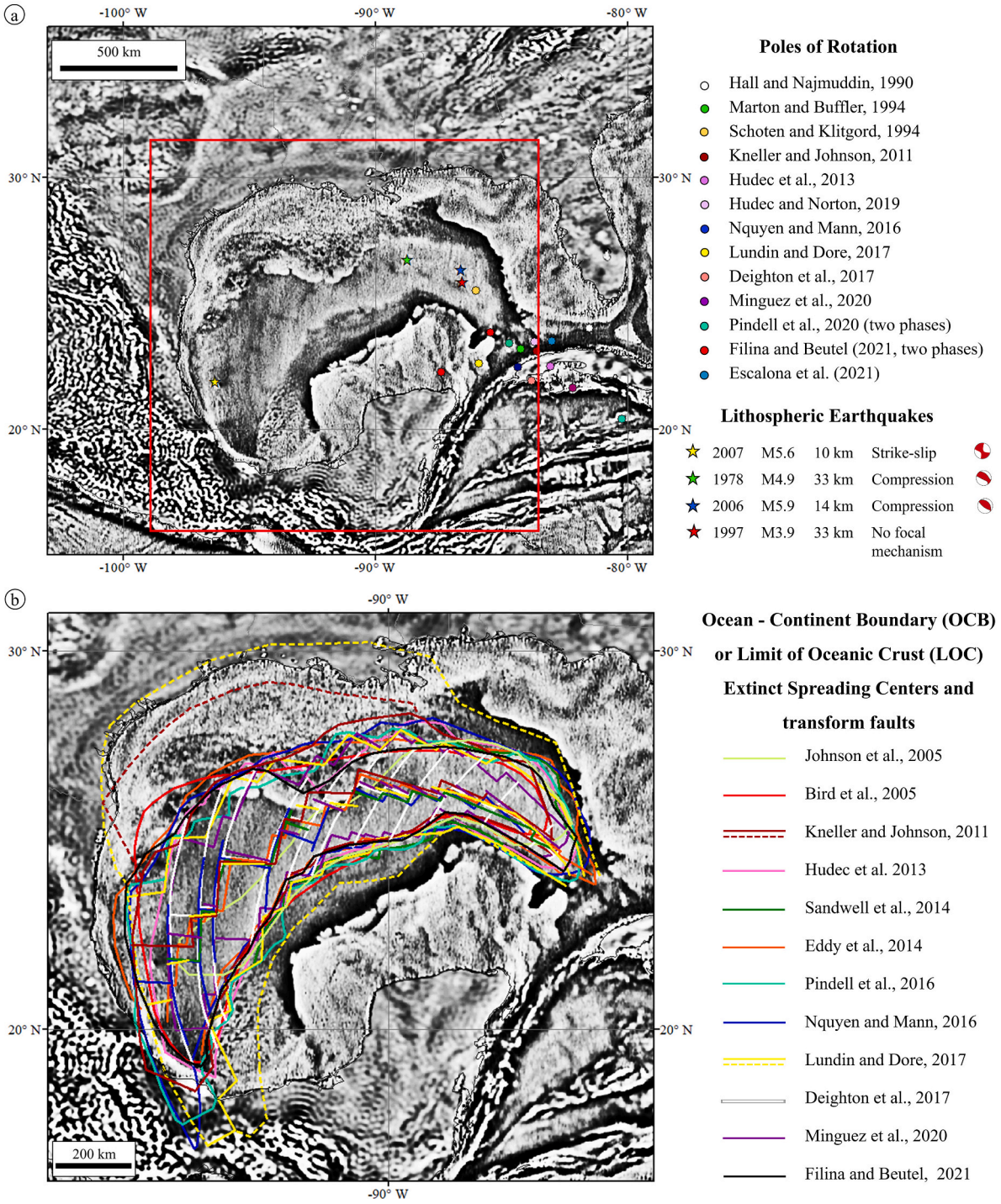

Fig. 3. (a) The first vertical derivative of gravity field from Sandwell et al. (2014). Pole of rotations from different published tectonic models are shown as circles of different color. The stars show earthquakes with focal depth within lithosphere (see Appendix D). The region within red box is shown in (b) with locations of OCB, COB, LOC and MOR from recently published tectonic models for the Gulf of Mexico plotted with different colors. Some models provide polygons for two spreading phases; for those, the OCB/LOC is shown by dashed line, while solid line of the same color shows crustal boundary for the onset of the Yucatan rotational phase.

margin that consists of the Yucatan and Campeche sub-basins (Hudec et al., 2013). Onshore in northern Mexico, salt structures collectively form the Minas Viejas salt basin (Fig. 2a; Goldhammer and Johnson, 1999 and Goldhammer and Johnson, 2001). Further south is the Huehuetepec salt, known only from well data (Salvador, 1991). In early tectonic analysis of the GoM, researchers realized that the Louann and Isthmian salts were originally deposited in one basin that subsequently was split by movement of Yucatan away from North America (e.g., Salvador, 1987 and references therein). Although almost all GoM tectonic models adopt this scenario, the depositional settings of salt (i.e., whether or not it was formed on continental or oceanic crust, or both, see section 7.2) and the relationships of onshore Mexican basins to this larger salt basin are not clear. Until recently, the age of the salt was thought to be Callovian to Oxfordian (~163 Ma; Salvador, 1991); many published tectonic models assign this timing as the transition from rifting to drifting (see section 6). Igneous inclusions with crystallization

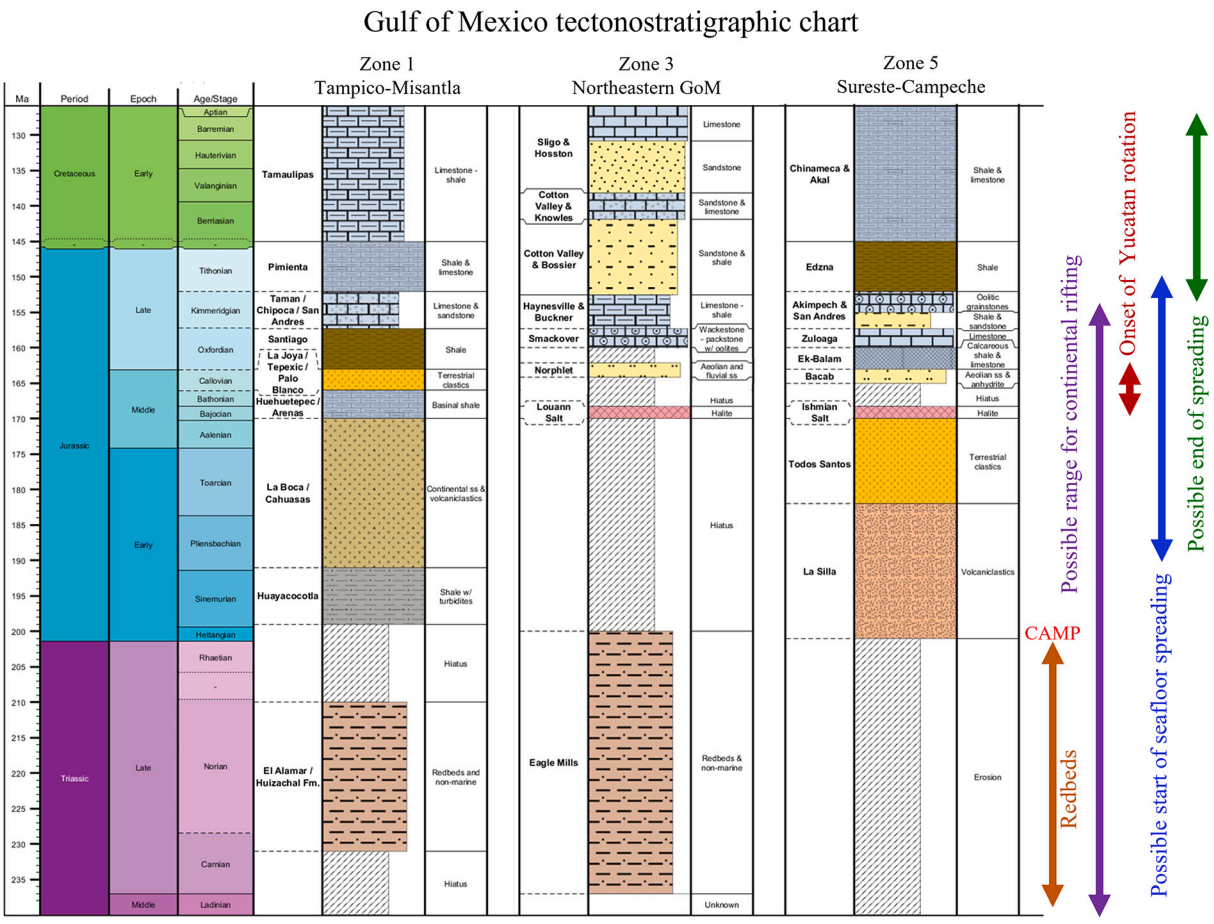

Fig. 4. Tectono-stratigraphic chart for the opening of the Gulf of Mexico. Generalized stratigraphic columns are shown for three of the major margins of GoM (see Fig. 1 for zone locations): Tampico-Misantla basin (Zone 1) to the west of the Western Main Transform (after Lawton et al., 2020 and Shann et al., 2020), Northeastern GoM margin (Zone 3; after Snedden and Galloway, 2019; Snedden et al., 2020), and Sureste-Campeche salt basin onshore and offshore Yucatan (Zone 5; after Snedden and Galloway, 2019; Snedden et al., 2020 and Shann et al., 2020). Summary of tectonic events and associated age ranges are from this review.

age of ~ 160 to 158 Ma are found in the salt from drilling in different parts of the basin (see Appendix C3). The latest estimate on salt age from Sr isotopes suggests that it was deposited during Bajocian time (~169 Ma; Pindell et al., 2019; Snedden et al., 2019; Peel, 2019). How this adjusted, younger timing affects tectonic models is addressed in section 7.2.

Arid climate conditions persisted during the initial stages of basin opening (Jurassic) and a broad belt of dryland deposition, including a prominent aeolian sand sea (erg) developed in what is now the northeastern GoM (Mancini et al., 1985; Snedden and Galloway, 2019) and along the Yucatan margin (Snedden et al., 2020). According to many tectonic models (see section 6), the Late Jurassic (Oxfordian, 163 -157 Ma) subaerial deposition (Fig. 4; Appendix C4) was coincident with early seafloor spreading. Deposition in the GoM basin during the remainder of the Mesozoic reflected thermal subsidence and sediment loading. After an initial influx of siliciclastics, the basin had attained its present size, and combined with favorable climatic conditions, carbonate systems transitioned from local grainstone shoals and thrombolite buildups to more widespread platform margin and shelf interior reefs and associated grainstone aprons (Mancini et al., 2004). Episodic local tectonism and volcanism continued through the Cretaceous, particularly onshore (Byerly, 1991).

4. Primary data constraining opening of the Gulf of Mexico

Multiple geoscience datasets have been acquired across the GoM during the last century and keeping track of these data is complicated. Still, this review seeks to highlight some of the key data that have been repeatedly invoked to support GoM tectonic models, or data that should, in our view, be taken into consideration as new models continue to be developed. We present a general summary in this section, while a more detailed description of the key datasets is provided in Appendices A-E.

A general tectonic model for the GoM evolution comprises a combination of several key factors, namely: 1) order and timing of key events, 2) modern boundaries between crustal domains, 3) modeled kinematic parameters, such as the location of the pole(s) of rotation and the total angle of rotation of the Yucatan crustal block as the GoM basin opened, and 4) pre-breakup fit of continental blocks. Table 2 lists the major datasets for each of these factors, while key geological observations drawn from these datasets are summarized in section 5. Published tectonic models and their primary constraining datasets are discussed in section 6.

The location of publicly available seismic reflection and refraction data is shown in Fig. 5. Seismic refraction data, such as the GUMBO experiment (Christeson et al., 2014; Eddy et al., 2014, 2018; Van Avendonk et al., 2015) illustrated in Fig. 6, provide important insight about crustal architecture of the basin, although the interpretations differ among authors (see Appendix A for more details). The GUMBO experiment revealed lateral variations in crustal structures along the northern GoM (Fig. 6), as well as presence of two distinct crustal zones in the oceanic domain. In particular, the oceanic crust imaged by profile GUMBO3 (Eddy et al., 2014; Fig. 6c) is up to 9 km thick and has characteristic two-layered structure interpreted as basaltic upper layer with slower acoustic velocity over the faster one of gabbroic composition. In

Table 2
Major geological and geophysical data constraining tectonic history of the Gulf of Mexico

References	Location	Method	Observation	Potential implications for tectonic reconstruction
			Constraints for the timing of tectonic events	
Scott et al., 1961; Moy and Traverse, 1986; Raymond, 1989; Frederick et al., 2020	Northern GoM, onshore	well cores, palynology analysis, U-Pb analysis	Eagle Mills redbeds (and equivalents) are non-marine, formed during Carnian (237-227 Ma) in dry climatic conditions (see section 5.1). Three paleodrainage paths identified.	Redbeds represent early syn-rift deposits. Alternatively, they may be deposited in precursor setting (see section 7.1 for more details)
Marzano et al., 1988	offshore Alabama	Core description	Norphlet Fm deposited on the Louann salt was formed in arid conditions by fluvial-aeolian deposition mechanisms	Regional depositional environment immediately post salt was aeolian and arid/fluvial
Dickinson et al., 2010	NW GoM offshore	U-Pb Zircon geochronology	Late Triassic flood of clastic sediments from the GoM region	Late Triassic uplift in Central Texas, if interpreted as an early rift-flank, provides constraints on early rift topography, sediment generation, and timing
Stern et al., 2011	Southern Louisiana	$^{40}Ar/^{39}Ar$ dating of igneous inclusions in salt	158.6 ± 0.2 Ma and 160.1 ± 0.7 M at two different salt domes, geochemical analysis is consistent with depleted mantle source (see Appendix C3)	Direct evidence of Jurassic magmatism during basin opening, serves both magma-rich and magma-poor breakup models (section 7.3)
Pindell et al., 2019	regional	Sr isotope analysis of salt	Bajocian age (170.3 -168.3 Ma) of salt deposition	Timing of salt deposition that is earlier than assumed by most models (see Fig. 9)
DSDP Leg 77, Schlager et al., 1984; Dallmeyer, 1984	NE Yucatan, offshore	Scientific Drilling	Barresian (145-139.8 Ma) age of sediment just above the "breakup unconformity" (syn-rift/post-rift seismic boundary), early Paleozoic metasedimentary basement with Jurassic (190.4 ± 3.4 Ma) intrusions (see Appendix C)	End of rifting in the eastern GoM before or during Barrresian time. Timing of magmatism that may be related to the rifting stage or may be interpreted as a syn-spreading magmatism.
			Constraints for kinematic parameters for tectonic reconstruction	
Molina-Garza et al., 1992, 2020; Godínez-Urban et al., 2011a, 2011b (see Appendix E)	Chiapas Massif, Yucatan	Paleomagnetic analysis	Total rotation of Yucatan between 75° to 40°, rotation ceasing around Oxfordian time	Constrains degree and duration of rotation phase of the Yucatan block with respect to North America
Molina-Garza and Geissman (1999)	Caborca Block	Paleomagnetic analysis	Paleomagnetic inclinations for Jurassic and Pre-Jurassic rocks in the Mexican craton indicate internal rotations, but minimal translation.	Paleomagnetic inclinations limit Jurassic deformation of Mexico to less than ~300 km along hypothetical shear zones (Mojave-Sonora), but support internal rotations during rifting.
Sandwell et al., 2014	regional	Gravity anomalies	ESC and FZ are evident (Fig.s 3 and 8) revealing asymmetry of the basin with respect to spreading centers	Constrain the motion of Yucatan relative to North America; asymmetry must be addressed in tectonic reconstruction. See Appendix B1
Bankey et al., 2002	regional	Magnetic anomalies	Multiple magnetic anomalies (see Appendix B2 and Fig. 8b)	Match in conjugate magnetic anomalies during reconstruction, although multiple variants are proposed (see section 7.3) Magnetic chrons could constrain timing of spreading, although also non-unique
			Constraints for tectonic zonation (oceanic and continental domains)	
Multiple (see Fig. 5 and Appendix A)	regional	Seismic refractions	Compiled vintage refraction velocity models across the GoM (see Fig. 5)	Can be used to delineate crustal types, map regional basement topography basin-wide and Moho in the central part only (thinner oceanic crust), although rock velocities overlap
Multiple (see Chapter 4 and Appendix A)	US sector, offshore	GUMBO refraction experiment	Crustal thinning toward the center of the basin; inhomogeneities within the crust; variations in thickness of interpreted oceanic crust (see Appendix A and Fig. 6)	Crustal thickness and type, although may be ambiguous (see section 7.4); spreading rate may be derived given some assumptions, although dependent on assumed timing. Some syn-rift section and structures are potentially observed.
Multiple (see Chapter 4)	regional	Seismic reflections	Seismic reflections showing basement topography, pre-salt section, basinward dipping reflections, etc. (see Fig. 7 and Chapter 5)	Various geological features (Chapter 5, Fig. 7) that should be explained by any tectonic model

contrast, the oceanic crust imaged by GUMBO4 (Christeson et al., 2014; Fig. 6d) is thinner (~ 5 km) and appeared to be uniform. Crustal variations revealed by the GUMBO experiment provide important constraints for understanding tectonic evolution of the GoM basin (Table 2).

The amount of seismic reflection data that has been acquired in the GoM is challenging to quantify, because most was acquired with petroleum industry support and is therefore proprietary. As already mentioned, the thick sedimentary section including mobile salt complicates seismic imaging and challenges examination of sub-salt sedimentary section and basement structures. In the last few years, major seismic vendors have acquired extensive 2D and 3D seismic surveys for sale; a series of "teaser papers" (Saunders et al., 2016; O'Reilly et al., 2017; Horn et al., 2017; Deighton et al., 2017) have been published with examples from these surveys. These sections, while not comprehensive, are useful for qualitative analysis of basin evolution. We list some of the most useful seismic reflection lines that should be considered while developing any new tectonic model of the GoM (Fig. 5). An example from the recent GIGANTE survey, acquired by TGS, is shown in Fig. 7. This pre-stack depth migrated section illustrates several key tectonic elements: pre-salt sedimentary section (see section 5.1), and basinward-dipping reflectors (section 5.2) and outer trough (section 5.3) on the Yucatan margin. This profile crosses an ESC and several interpreted

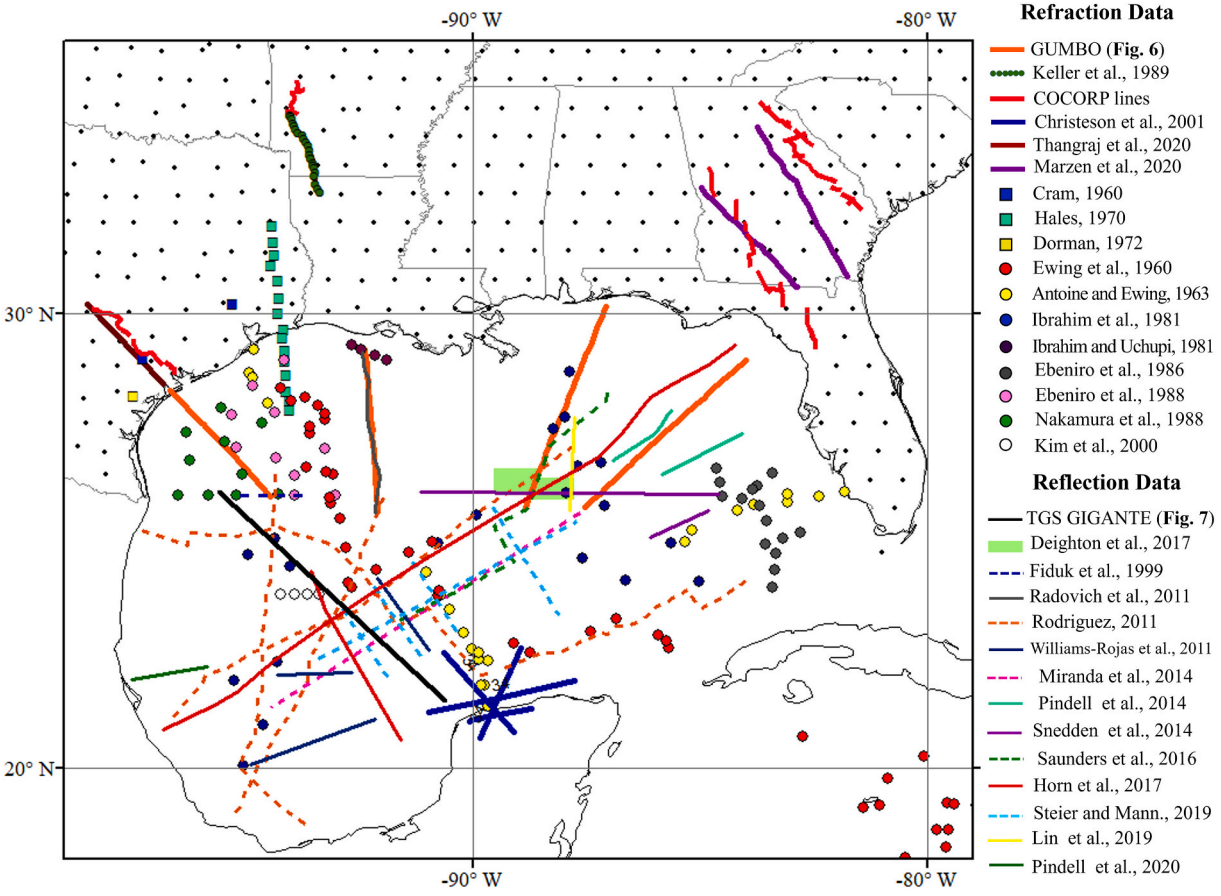

Fig. 5. Locations of published seismic reflection and refraction data. Black dots in the U.S. sector are EarthScope stations (Schmandt et al., 2015). Circles of various colors show the positions of the ocean bottom seismometers from different surveys. Some of the vintage refraction campaigns report the source locations instead, which are shown as squares. Seismic reflection profiles that are published as depth sections are shown as solid lines, while time sections are dashed. (Lin et al., 2019; Radovich et al., 2011; Rodriguez, 2011)

transform faults (Fig. 7) that are expressed as local basement troughs (see Deighton et al., 2017 for more details) and also images the BAHA high (section 5.5) in the northwestern part of the basin. In addition, this profile illustrates crustal thickness variations in the oceanic domain, with oceanic crust near the BAHA high in the northeast and near the Outer Trough in the south being thinner than the crust in the center. This interpretation is similar to two different domains in oceanic crust imaged by GUMBO3 (thicker crust, Fig. 6c) and GUMBO 4 (thinner crust, Fig. 6d); these are interpreted as having been produced during two distinct phases of oceanic spreading (Filina et al., 2020; Filina and Beutel, 2021). In addition to crustal insights, seismic reflection data provide important constraints on sequence stratigraphic and tectono-stratigraphic framework of the basin. A significant example of this was published by Snedden et al., 2014, where a series of seismic images were used to confirm the location of the ESR previously interpreted from gravity data, and to map down-laps of the Haynesville-Buckner to Cotton-Valley Knowles super sequences, as well as the overlying Sligo-Hosston super sequence. These observations imply that seafloor spreading in the eastern GoM was active from the Tithonian (152 Ma) to Valanginian (137 Ma).

Potential fields are commonly used for analysis of tectonic structures of the GoM (e.g., Mickus et al., 2009; Nguyen and Mann, 2016; Lundin and Doré, 2017; Liu et al., 2019; Minguez et al., 2020; Filina et al., 2020; Filina and Beutel, 2021). The satellite-derived gravity data published by Sandwell et al. (2014) (see Figs 3 and 8a) has revolutionized our understanding of the oceanic domain of the GoM, because it has allowed us to interpret ESCs that are offset by a series of curvilinear fracture zones (FZ; Figs 2c and 3). These FZs separate oceanic crust of different ages and therefore different cooling and subsidence histories. Differences in age-related subsidence also create measurable difference in basement topography and Free-Air gravity.

Fig. 8b shows the reduced to pole magnetic field for the GoM. There are a few significant anomalies that have been studied and discussed in the literature, namely the Gulf Coast Magnetic Anomaly (GCMA) that comprises the Houston Magnetic Anomaly (HMA) and the Florida Magnetic Anomaly (FMA), the Yucatan magnetic anomaly (YMA), the "En Echelon Anomalies" EEA, and the Extinct Spreading Ridge Anomalies (ESRA). With the exception of the ESRA, these anomalies have multiple interpretations that illuminate the spectrum of possibilities for the nature of the transition zone between continental and oceanic domains in the GoM. The reader is referred to Appendix B2 for in depth discussion of individual anomalies and their interpretations.

Petroleum exploration in the GoM has been ongoing for more than a century (Galloway, 2008), resulting in many wells drilled in the basin, primarily targeting sedimentary structures. In Appendix C, we briefly summarize the findings only of those wells that are important for constraining the GoM formation. These wells have: 1) penetrated basement and/or pre-GoM Paleozoic sediments, 2) sampled Triassic redbeds, 3) encountered volcanic inclusions in the salt, and/or 4) penetrated aeolian deposits above salt (the Norphlet and Bacab formations) that were likely deposited during seafloor spreading (see Fig.s 2, 4 and Appendix C).

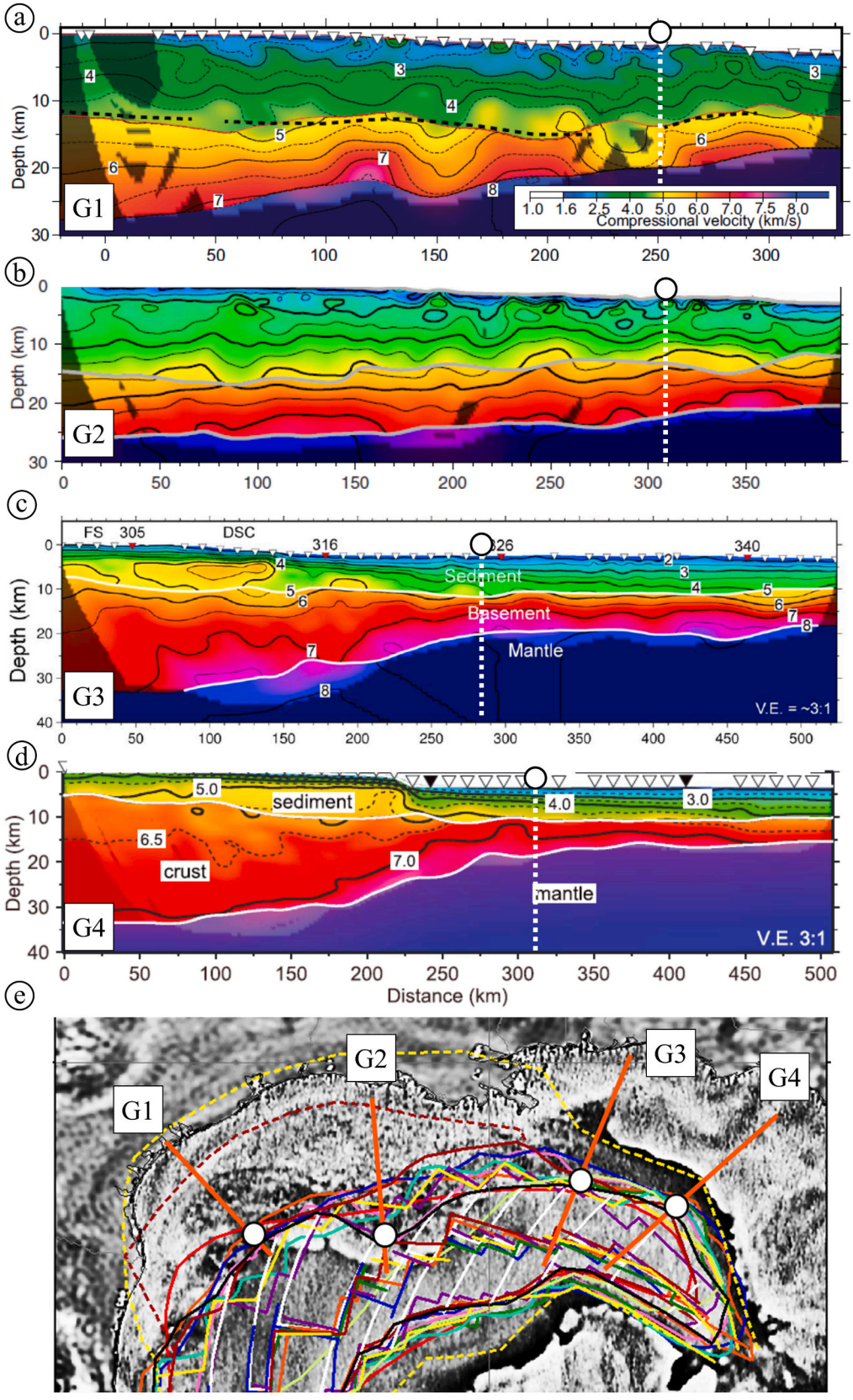

Fig. 6. (a - d) the results of the GUMBO refraction experiment from Eddy et al. (2014, 2018), Christeson et al. (2014) and Van Avendonk et al. (2015). The location of the GUMBO profiles is shown by orange lines in panel (e); see legend in Fig. 3b for different published tectonic models. White markers show the location of the Limit of Oceanic Crust interpreted by the GUMBO team.

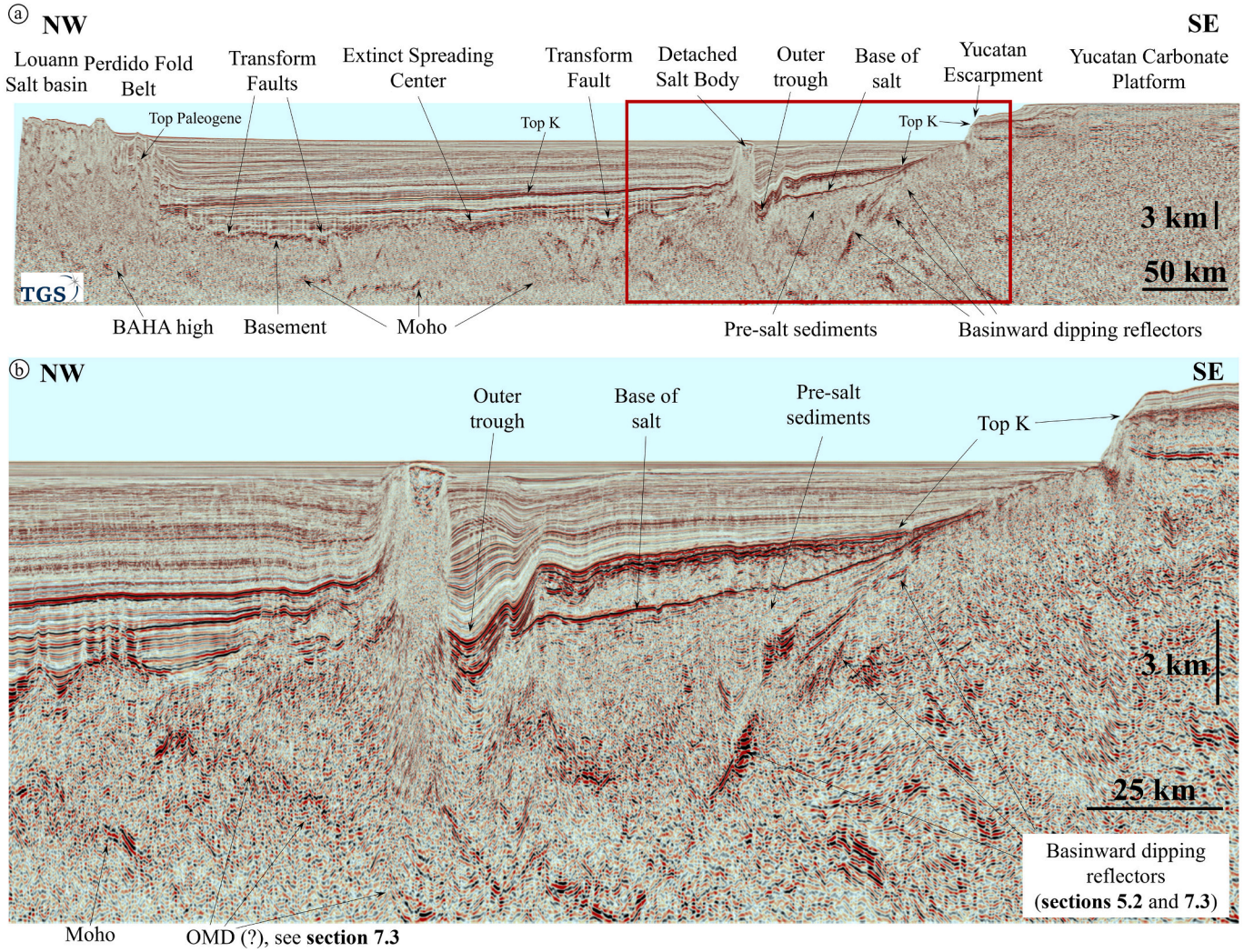

Fig. 7. a) Representative seismic reflection cross-section from the TGS GIGANTE survey, spanning from the northern Mexican shelf in the northwest to the Campeche margin in the southeast (see location in Fig. 5). The profile crosses key tectonic features, such as the BAHA high, outer trough, basinward dipping reflectors, transform faults and the extinct spreading center (ESC). The red box marks the extent of zoomed-in portion shown in panel (b). See more details about these tectonic structures in sections 5 and 7. The line is included with the permission from TGS.

5. Geological observations

5.1. *Pre-salt sedimentary section*

Several kilometer-thick pre-salt sediments are interpreted in multiple seismic surveys conducted along the Yucatan margin (Fig. 7; Williams-Rojas et al., 2011; O'Reilly et al., 2017; Horn et al., 2017), as well as in the eastern GoM (Saunders et al., 2016). The presence of these deposits in the western GoM is still debated, as the large volume of overlying mobilized salt obscures seismic imaging and challenges sub-salt interpretation. In the northwestern part of the basin, a 3D seismic reflection survey in the East Breaks and Alaminos Canyon areas (Filina et al., 2015) did not image pre-salt sediment. This contradicts Van Avendonk et al. (2015) along GUMBO1 (Fig. 6a) in the same region, who proposed a thick layer of pre-salt sediments based on seismic P velocities (Vp) between 5 and 5.5 km/s. Their conclusion was guided by a tectonic reconstruction of Eddy et al. (2014), which assumes the northwestern GoM is the conjugate to the western Yucatan margin, where thick pre-salt deposits are well imaged in seismic reflection data (Williams-Rojas et al., 2011). However, as noted in Appendix A, Filina (2019) has offered an alternative interpretation to GUMBO 1, based on results of integration with potential fields, arguing that the presence of very thick salt, known as a "salt wall" (labeled (3) in Fig. 8a), was not accounted for in the sedimentary velocities that in turn affected velocities and interpretation of deeper structures. Filina (2019) concluded that the velocity values between 5 and 5.5 km/s that Van Avendonk et al. (2015) interpreted as pre-salt sediments can also be characteristic of upper continental crust, and this alternative interpretation agrees better with observed gravity and magnetic fields. In the eastern GoM, pre-salt sediments are identified in seismic data (Eddy et al., 2014), as well as modeled in gravity and magnetics (Liu et al., 2019; Filina and Beutel, 2021). The thick pre-salt section is well imaged in multiple seismic sections along the Yucatan margin (Williams-Rojas et al., 2011; Saunders et al., 2016; O'Reilly et al., 2017; Horn et al., 2017; Steier and Mann, 2019). The seismic section of Miranda-Peralta et al. (2014) suggests a two-way traveltime through interpreted pre-salt sediments of 2 sec, which represents a thickness of 5 km if Vp of 5 km/s is assumed. Pre-salt sediments are also imaged in the TGS regional line from GIGANTE survey (Fig. 7). Williams-Rojas et al. (2011) distinguish at least two stratigraphic units in this section. The pre-salt basins interpreted in Fig. 2c are based on integrated analysis of seismic, gravity and magnetic data (Filina and Beutel, 2021).

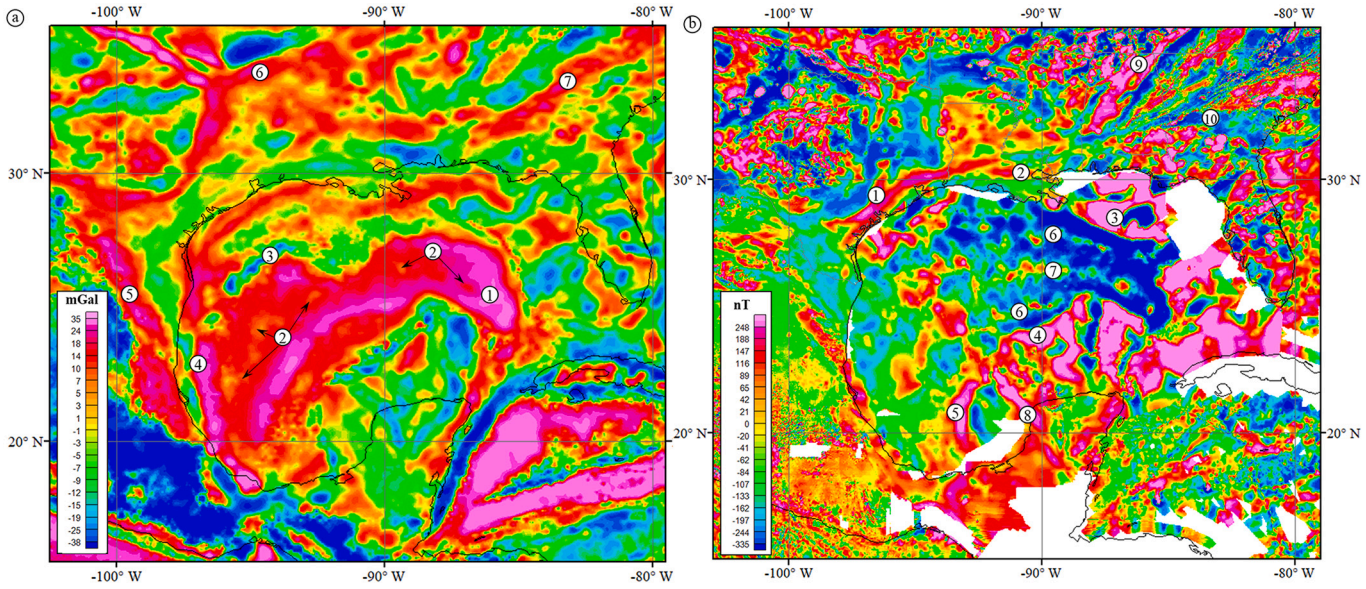

Fig. 8. (a) Residual Bouguer gravity anomaly map for the GoM. The Free-Air data from Sandwell et al. (2014) were reduced using the topography/bathymetry grid from Smith and Sandwell (1997) with assumed Bouguer densities of 2670 kg/m^3 onshore and 2000 kg/m^3 offshore. The regional trend was computed via upward continuation to an elevation of 40 km and removed. The oceanic crust in the center of the basin (1) generally corresponds to regions of pronounced gravity highs. Extinct spreading centers, labeled (2), are regions of local gravity lows (to be compared with Fig. 3). The region of thick salt (the so-called "Perdido salt wall") corresponds to a pronounced gravity low marked with (3). The Tamaulipas transform margin (4) is evident in the gravity anomaly, as well as the Sierra Madre Oriental front (5), the Paleozoic orogenic front (6) and Suwannee suture (7). (b) Reduced to pole magnetic anomaly, derived from onshore data of Bankey et al. (2002), offshore from Minguez et al. (2020). The Gulf Coast Magnetic anomaly (GCMA) is sometimes separated into several parts: (1) Houston magnetic anomaly (HMA), (2) Louisiana magnetic anomaly and (3) Florida magnetic anomaly (FMA). The Yucatan magnetic anomaly (YMA) marked as (4) refers to magnetic high over the rim of the Yucatan peninsula; the western portion of this magnetic high is known as the Campeche magnetic anomaly shown as (5). "En Echelon Anomalies" (EEA), shown with (6), are the pair of smaller magnetic highs (Minguez et al., 2020) symmetrical about the Extinct Spreading Ridge Anomalies (ESRA) that is marked by (7). (8) and (9) are two anomalies that may be used to constrain the pre-breakup fit of the Yucatan and North America (e.g., Lundin and Doré, 2017). To align these anomalies, the rotation of the Yucatan crustal block ~ 70-75° is required. (10) marks Brunswick magnetic anomaly.

5.2. Basinward - dipping reflectors

Regions of basinward-dipping reflections have been identified in the northeastern GoM and in the southwestern parts of the basin along the Yucatan margin. The seismic reflection profile in Fig. 7 shows these basinward-dipping reflectors along the Yucatan margin. They have been interpreted by some researchers as SDRs (Seaward-Dipping Reflectors, generally taken to indicate of a magma-rich margin; see Planke et al., 2000 for a general overview).

Seaward Dipping Reflectors represent a key characteristic of magma-rich margins and consist of subaerial basalt flows extruded from embryonic spreading axes during the break-up phase. SDRs are recognized along a number of margins worldwide, and their subaerial nature has been documented by two ODP legs (Eldholm et al., 1989; Larsen et al., 1994). Basalt flows are typically interbedded with sediments and may exceed 40 km (Paton et al., 2017). Early interpretations proposed that SDRs developed by landward directed lava flows from a fissure and flowed over the edge of the continental margin such that continuous subsidence landward of the active ridge allowed subsequent flows to overlap older ones (Palmason, 1980). Later models have suggested that the seaward dip is governed by structurally controlled rollover on to listric normal faults that dip landward and sole out on the intruded lower crust. These faults are described as constituting a specific type of magma-involved extension occurring at the point of break-up on magma-rich margins (e.g., Quirk et al., 2014; Geoffroy et al., 2015). Other characteristics associated with SDRs are discussed in section 7.3.1.

Many authors argue that the basinward-dipping reflectors observed on seismic data in the northeastern part of the GoM basin (Imbert and Post, 2005; Hudec et al., 2013; Eddy et al., 2014; Rowan, 2014; Pindell et al., 2011; Kneller and Johnson, 2011; Lundin and Doré, 2017; Liu et al., 2019) and along the Yucatan margin (e.g. Williams-Rojas et al., 2011; Saunders et al., 2016; O'Reilly et al., 2017; Hudec and Norton, 2019; Steier and Mann, 2019; Filina and Hartford, 2021) represent SDR complexes, as these reflectors align with strong magnetic signals such as the linear, positive Florida Magnetic Anomaly (FMA) and Yucatan Magnetic Anomaly (YMA) (Fig. 8b). Other authors have suggested alternative tectonic models to explain the basinward-dipping reflections in the eastern GoM, not involving magma-rich breakup (Curry et al., 2018; Minguez et al., 2020). A full discussion of alternative ideas, specifically on magma-rich versus magma-poor breakup, is provided in section 7.3.

5.3. Northern Yucatan outer trough

Another geological observation from seismic reflection data that should be included in GoM tectonic model constraints is the ~ 50x300 km region offshore northern Yucatan that is referred to as the outer margin by Hudec and Norton (2019). This is a zone associated with at least a 2 km deepening of acoustic basement immediately landward of interpreted oceanic crust (see outlines in Fig. 2c and the seismic cross-section in Fig. 7). This trough is interpreted to be filled with salt and a thickened overlying Jurassic section that Hudec and Norton (2019) attribute to unconfined basinward salt and overlying cover flow during the last stage of continental rifting. According to Hudec and Norton (2019), this structure is observed in the northern part of the Yucatan margin only; there is no similar feature in the Campeche salt basin to the south. This outer trough is also evident in seismic sections published by Williams-Rojas et al. (2011) and O'Reilly et al. (2017) and is also imaged by the GIGANTE profile (Fig. 7). Hudec and Norton (2019) state that this trough overlies crust of "unknown nature" (Fig. 2c). Filina and Hartford (2021) have modeled seismic and potential field data associated with the trough and

conclude that it coincides with a region of nearly exhumed lower continental crust. They suggest that exhumation occurred during the final (post-salt) phase of continental rifting and led to local subsidence that triggered the seaward flow of Jurassic salt observed by Hudec and Norton (2019).

5.4. The western GoM transform margin

The Tamaulipas margin in the western GoM (Zone 1 in Fig. 1) along the eastern continental margin of Mexico is marked by a sharp change in crustal thickness over the OCB/LOC. This buried structure has many names in the literature. It was called the Tehuantepec Transform by Dickinson et al. (2010) and the Western Main Transform (Fig. 2c) by Nguyen and Mann (2016). Padilla Sánchez (2016) refer to this as the Tamaulipas-Oaxaca Fault, while Hudec and Norton (2019) use the term Tamaulipas margin. Pindell et al. (2020) refer to it as the East Mexico Transform. Whatever its name is, the structure is generally interpreted as a major transform fault that allowed Yucatan to slide southward to open the GoM. Pindell et al. (2020) present a seismic section over this margin showing the classic configuration of a transform margin with ~ 27 km-thick continental crust abruptly juxtaposed against thin, presumably oceanic crust, over a distance of ~15 km. Integrated geophysical modeling of seismic and potential fields (Ramos et al., 2009; Nguyen and Mann, 2016; Filina and Beutel, 2021) also indicate the presence of thin oceanic crust outboard of the transform, which is interpreted as a distal lateral boundary of "windshield wiper" motion of Yucatan during GoM opening.

5.5. The northwestern GoM BAHA high

The high ridge outbound of the Perdido fold belt offshore Texas has been mentioned by a number of previous authors (e.g., Peel et al., 1995; Trudgill et al., 1999; Hudec et al., 2013), but Hudec and Norton (2019) were first to outline the extent of this feature (see Fig. 2c). The BAHA high is a 500 km-long region, with relief up to 3 km in seismic data, that was named after the first well drilled on it by Shell and partners in 1996. BAHA is an acronym derived from named exploration prospects along the high. According to Hudec and Norton (2019), this ridge formed at the same time as salt (~170 Ma) and forms the landward dam against which Louann salt pinches out. Hudec et al. (2020) have described the BAHA high as a part of the western GoM transform margin (marked as Zone 1 in Fig. 1) that dies out to the northeast at the transition to a wider rifted margin (Zone 2 in Fig. 1). Tectonic reconstruction by Hudec and Norton (2019) restores the Texas margin to the Campeche (see details in section 7.4.). There is no similar structure on the presumed Yucatan conjugate margin, where there is no basement high and where interpreted base salt is actually higher and shallower than the outboard, presumably oceanic crust (e.g., Miranda-Madrigal and Chávez-Cabello, 2020).

The nature of the BAHA high remains debated. Many tectonic models place it in the oceanic domain (Fig. 3). Hudec and Norton (2019) suggest that it formed synchronously with salt deposition (~170 Ma). Alternatively, the BAHA high structures have been interpreted as tilted blocks of rifted continental crust by Fiduk et al. (1999). However, seismic refraction data (Nakamura et al., 1988; Fig. 5) coincident with the

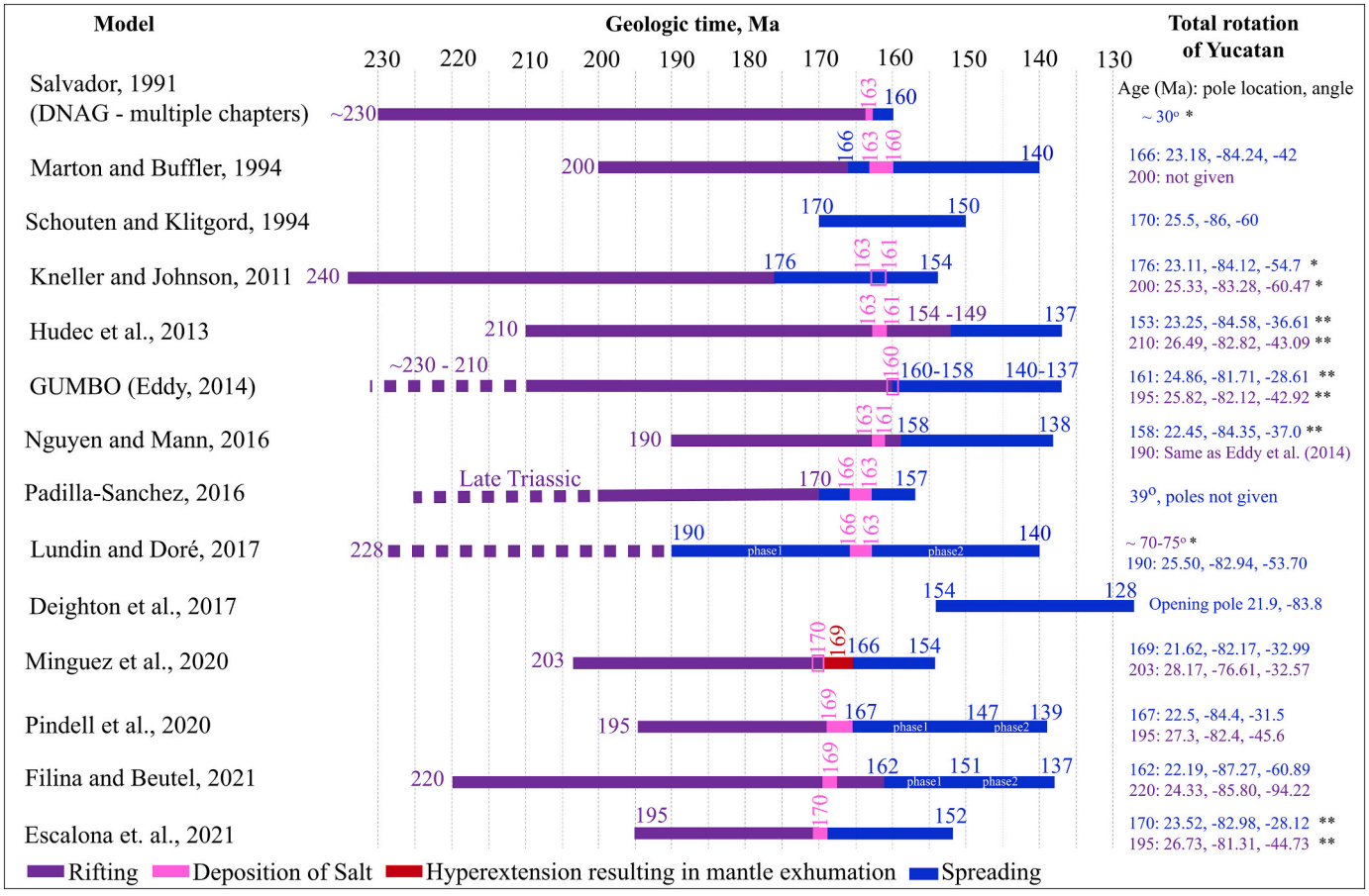

Fig. 9. A chart summarizing the major published tectonic reconstructions of the Gulf of Mexico. Where known, the kinematic parameters for the motion of the Yucatan crustal block are included with the total rotation angles from the start of rifting to a present day noted in purple and rotation from the begining of the spreading phase(s) to a present day given in blue. Not all models explicitly mention kinematic parameters as well as the age of salt deposition. Inferred age of salt is shown as an unfilled rectangle, single asterisks mark the parameters that were estimated from the georeferenced figuress, double asterisks denote the evolution of the Plates model. Rotations are given as latitude (N positive), longitude (E positive), angle (counterclockwise positive).

seismic profile analyzed by Fiduk et al. (1999) indicate that the crust of the BAHA high is 6 km thick and has a seismic velocity structure characteristic for oceanic crust. In contrast, Pindell et al. (2016) interpret this region as either a hyperextended (continental crust) margin or exhumed mantle. Hudec et al. (2020) suggest that the BAHA high could be a volcanic ridge formed in the early stages of seafloor spreading (but before salt deposition, which is why salt now onlaps the high). In their scenario, the outer troughs in the northern Yucatan and Florida (see Fig. 2c and section 5.3.) could be formed by seafloor spreading under salt. Norton et al. (2016) have proposed this latter scenario for South Atlantic passive margins. Filina and Beutel (2021) attribute this region to the initial phase of oceanic spreading. Clearly, further study of this feature is needed.

6. Major published tectonic models of the GoM

Many tectonic models have been proposed for GoM formation. Although most modern models agree on the broad framework for the opening, all differ in some aspects. As already mentioned in section 4, a robust tectonic model combines several factors 1) order and timing of key tectonic events, 2) identification of present-day boundaries between various crustal domains, 3) identification of pertinent kinematic parameters for the basin, and 4) pre-breakup fit of now-separated continental blocks. These model components allow derivation of remaining model parameters, such as the total amount of crustal stretching and the corresponding oceanic spreading rate. Fig. 3 shows different poles of rotations, LOCs and ESRs, while Fig.s 4 and 9 illustrate the uncertainty in key tectonic stages proposed by published models. Ideally, all of these elements should agree with each other, and with geological, geochemical and geophysical data. Many published quantitative plate kinematic models are based on digital reconstructions using software such as GPlates (Boyden et al., 2011). However, a large number of these plate models have only been published in non-peer-reviewed extended abstracts, and the digital reconstructions are not freely available for validation. To date, published digital models for GoM opening have also used only rigid plates (note that Kneller and Johnson (2011) use a deformable plate model for the Central Atlantic, but a rigid one for the GoM), and have not described full margin deformation, which is important for a tight "full-fit" reconstruction. We describe the major published tectonic models (Fig. 9) that either have kinematic parameters published, or those that we could infer from the accompanying text or figures. Notably, not all models list the age of salt deposition (shown with pink bars in Fig. 9, unfilled rectangles indicate inferred time of salt deposition for those models that do not mention it explicitly). Table 3 lists additional publications for other interpretations or conceptual models that do not include a unique tectonic reconstruction, or for

Table 3
Other published tectonic interpretations without kinematic reconstruction for the GoM opening.

Author	Governing datasets and interpretation methods	Constraints for major tectonic elements and crustal domains	Continent-Ocean Transition / basinward dipping reflectors
Bird et al., 2005	Gravity and seismic refraction 2D gravity models Plate reconstruction using Hall and Najmuddin (1994)	Oceanic crust is bounded by three features: two high amplitude gravity anomalies on conjugate margins that are interpreted as L. Jurassic hot spot tracks. (Keathley Canyon anomaly, Yucatan parallel anomaly)	Third gravity anomaly (Tamaulipas - Golden Lane - Chiapas anomaly) is interpreted as a marginal ridge formed along ocean-continent transform fault.
Johnson et al., 2006	Gravity and seismic refraction (pre-Sandwell, pre-GUMBO) 2D gravity models	Geophysical data is equivocal regarding the extent, or even existence of true oceanic crust. Only a limited area of crust has geophysical properties consistent with true oceanic crust observed elsewhere on the globe.	High crustal densities and velocities in the U.S. Gulf of Mexico may be indicative of extreme extension and attenuation, not true "drift phase" crust.
Mickus et al., 2009	Potential fields data in the northwestern GoM Models constrained by seismic refraction data Features correlated with detrital zircon ages	Interpret a triple junction between rifted and transform margin.	Large-amplitude coast-parallel magnetic maximum associated with a small Bouguer gravity high modeled as high density, high susceptibility outer transitional crust, interpreted as volcanic rifted margin of Triassic age.
Huerta and Harry, 2012	2D Thermal-mechanical model applicable to NE GoM. Compare modeled vs. observed crustal thickness for different heat flow scenarios. Show, but do not model, gravity data.	Use Pindell and Kennan (2009) outline of oceanic crust	Two Wilson cycles - influence of preexisting structure on the style of Mesozoic rifting. Strong lithosphere beneath orogen, causing extension to initiate adjacent to, rather than within, the orogen, resulting in unusually broad region of extension.
Snedden et al., 2014	2D seismic reflection data including 2D lines coincident with GUMBO refraction lines. oceanic crust spreading center and downlap of regional surfaces onto basement.	Axial valley typical of slow spreading systems. Isolated basement highs that reflect localized magma supply. Limit of oceanic crust defined at transition to in place salt. Downslope gliding of parautochthonous salt is excluded.	SDR's noted on several 2D sections but not discussed in this paper
Pindell et al., 2014	Long-offset 2D depth-imaged seismic reflection data. Compared GoM, eastern India and southern Brazil margins. Outer marginal detachment and consequent collapse is interpreted in both magma-rich and magma-poor margins.	Normal oceanic crust is outboard of the margin collapse. Kinematics and rotation of margin collapse and exhumation similar to seafloor spreading. Seafloor spreading begins with magmatic infiltration of exhumed mantle.	Rapid outer-margin collapse at the rift to drift transition. Collapse post-dates rifting and causes rapid subsidence prior to the start of seafloor spreading. Hanging wall associated with landward-dipping shear zone. Magma-poor margin. Footwall interpreted to be serpentinized, exhumed, sub-continental mantle, Rapid subsidence allows deposition of mega-salt basins.
Filina, 2019	GUMBO1 and GUMBO2 and potential fields data. Tested competing hypotheses with modeling	OCB interpreted near the Sigsbee escarpment.	Crust in NW and central GoM is stretched continental with multiple magmatic additions, potentially associated with rifting. Thick pre-salt sediments not supported.
Filina et al., 2020	Gravity, magnetic and seismic data (GUMBO Line 3 and Fugro line from Eddy et al., (2014)); gravity filtering	Asymmetric nature of oceanic crust relative to observed extinct spreading centers. Two spreading centers with two phases of spreading, a jump with a change in spreading direction, and magma supply are interpreted. Recent seismicity observed within oceanic domain.	OCB is mapped coincident with pronounced gravity gradient. The SDRs are acknowledged based on Liu et al. (2019) in Zone 3 in the eastern GoM and Filina and Hartford (2021) in Zone 5 of the Yucatan margin.

which we were not able to determine kinematic parameters. Differences between the models, related to Triassic redbeds interpretation, the timing of salt with respect to oceanic crust, the mode of break-up, and pre-GoM fit of the crustal blocks are discussed in section 7.1.

We begin our review of published models with the model of Salvador (1991) in the DNAG volume that integrated multiple geophysical data to determine crustal stretching parameter (beta factor) and to map tectonic boundaries (Fig. 2b). That model revealed the pronounced asymmetry of the basin, with the northern margin being up to three times wider than the southern one. This tectonic restoration was based on a multidisciplinary synthesis but represents a simple geometric model rather than a true kinematic reconstruction. Marton and Buffler (1994), in contrast, used Plates 2.0 software available at the University of Texas at Austin for a rigid plate model, and the Canvas graphics software to produce a non-rigid reconstruction of Central Atlantic. This model used detailed regional geological observations, especially knowledge of the occurrence of Paleozoic rocks, as well as discussed influence of preexisting structural trends and foldbelts. Their model utilized a published time-kinematic framework for Central Atlantic opening (Klitgord and Schouten, 1986) and proposed a "jumped" spreading center that split the salt province in two, producing the modern observed configuration. This model also assumes a left-lateral displacement along the Bahamas FZ during continental rifting. This structure is mentioned in the literature under different names, such as the Sunniland Transform (Pindell and Dewey, 1982) or Florida Transfer Zone (see Fig. 2c) in multiple tectonic reconstructions by Pindell and his co-authors (1982, 1985, 2001, 2019, 2016 and 2020) that imply significant (~500 km) displacement along this structure. In contrast, Heatherington and Mueller (1991) called this potential structure the Jay Fault and argued against its transform nature based on three basement-penetrating wells in Florida. They suggested instead that this structure may be a normal fault related to Triassic breakup of Pangaea that experienced little to no lateral displacement. Dobson and Buffler (1991) mapped this fault using poor quality seismic data, again referring to it as the Bahamas FZ. Recently, Erlich and Pindell (2020) traced this structure from south-central Florida into southern Mississippi based on multiple basement wells. However, most published tectonic models do not imply significant lateral displacement in Florida while reconstructing the GoM basin, so the presence of this transform fault continues to be debated.

Hall and Najmuddin (1994) used magnetic anomaly data and models in the central part of the GoM to identify considerably more oceanic crust than previously suggested. The authors interpreted discontinuities in the magnetic anomaly patterns as NNE-SSW fossil fracture zones. Their extensional phase is associated with 30-35° of counterclockwise rotation during rifting with an additional 25° of counterclockwise rotation during spreading. Schouten and Klitgord (1994) also utilize magnetic anomalies to interpret the "edge" of oceanic crust. They propose two conceptual mechanistic models for the GoM, namely: 1) a piggyback version, where Yucatan moves with South America and 2) a "Rack and Pinion" version, in which Yucatan is forced to rotate counterclockwise by forces on its southern edge. This model has a strike-slip western margin for the GoM basin and assumes symmetric spreading that is faster in the west due to pole location.

Stern and Dickinson (2010) argued that the GoM opened as a Jurassic backarc basin (BAB) behind the Nazas Arc of Mexico. This model highlights the significance of the Border Rift System (BRS, see Fig. 2a) and the East Texas Basin (ETB in Fig. 2b) that are interpreted as Jurassic aulacogens. They point out that continental BABs develop spreading ridge orientations that are often at high angles to the associated convergent margin. Examples of such BABs are the Miocene Sea of Japan and the modern Andaman Sea in the eastern Indian Ocean; both have spreading ridges that trend perpendicular to the associated arc. Such geometries reflect the presence of extensional stresses that are not orthogonal to the subduction zone, a situation proposed by Stern and Dickinson (2010) for the GoM region during the Late Jurassic. According to them, the BRS is associated with the Nazas magmatic arc (and equivalents to the north), acting as a "swinging door" that opened in southwestern North America during the Jurassic, from a hinge in California that widened progressively eastward into the GoM. Subsequent thermotectonic subsidence created an extensive depositional domain along the U.S.–Mexico border region. Late Jurassic marine transgression advanced northwest up the Sabinas Basin, part of the BRS, from the nascent GoM during Oxfordian time (161–156 Ma) and up the Chihuahua Trough, another part of the BRS during Kimmeridgian time (156–151 Ma; Dickinson and Lawton, 2001).

The model of Kneller and Johnson (2011) is the first based on the GUMBO refraction experiment (Fig. 6). This model utilizes GUMBO and other geophysical datasets to constrain a deforming Central Atlantic and rigid GoM plate model that uses isostatic back-stripping from proprietary sedimentary isopachs and palinspastically restored refraction profiles. According to this model:1) spreading propagates south in the Central Atlantic, 2) as the proto-Caribbean opens, rotation of Yucatan begins, and 3) Yucatan stays coupled with South America as the South Atlantic opens. This model does not infer lateral displacement along the Florida transform. Volcanic addition in the northeastern GoM (i.e., SDRs in Fig. 2c, section 5.2) is acknowledged, along with ultra-slow lithospheric stretching in the northern GoM.

A number of models have evolved out of the industry-supported Plates consortium at the University of Texas (https://www.ig.utexas.edu/marine-and-tectonics/plates-project). The Plates model has not yet been published, but different versions of this model have been used in several published reconstructions, including those from the GUMBO campaign. So, before we describe the models generated using the Plates consortium restorations (marked with double asterics in Fig. 9), it is important to understand the evolution of the Plates model and its impact on publications. The Plates work in the GoM has been aided by support from the industry-sponsored Applied Geodynamics Laboratory (AGL, https://www.beg.utexas.edu/agl) consortium and the Gulf of Mexico Basin Depositional Synthesis (GBDS, https://ig.utexas.edu/energy/gbds) Project of the University of Texas, as well as collaborations with the Conjugate Basins, Tectonics and Hydrocarbons (CBTH, http://cbth.uh.edu) consortium at the Universities of Houston and Stavanger. These industry-sponsored projects have different philosophies about publication of data, analyses, and models. The Plates model has evolved, so there are subtle, but important differences between successive GUMBO papers, especially as interpretations of crustal boundaries also evolved. Recently, the Plates model has undergone another significant change, as new data has revised the age of salt from 162 to 170 Ma (section 3).

Hudec et al. (2013) used proprietary seismic reflection profiles throughout the basin to constrain the Plates model with the following observations: 1) a basement ramp was interpreted as the LOC (this was the predecessor of the polygon of "uncertain crust" proposed by Curry et al. (2018), see Fig. 2c); 2) various deep salt provinces were mapped with respect to the ramp (such as parautochthonous salt); (3) paleodepth of the post-salt sequence was interpreted as evidence that a basin was filled by salt to ambient sea level; and (4) Late Jurassic post-salt strata had salt-detached extension not balanced by equivalent salt-detached shortening (the earliest description of outer trough structures, see Fig. 2c and section 5.3). Their model also proposed that continental stretching continued for another 6 to 12 Myr after salt was deposited. The NW-SE trending Brazos transfer fault in the north-central GoM is emphasized as a key factor in the LOC (i.e., the NW-SE oriented segment of "uncertain crust" region in Fig. 2c). Spreading initiated simultaneously in the eastern and the western parts of the GoM, while the Walker Ridge (the region in the central GoM; it corresponds to the widest "uncertain crust" in Fig. 2c) was a salient in the center of the basin, as the final part of the GoM basin to break apart.

The first of the GUMBO publications (Eddy et al., 2014) serves as a representative for the GUMBO model mentioned in Fig.s 9 and 11. Follow-up GUMBO publications (Christeson et al., 2014; Van Avendonk et al., 2015; Eddy et al., 2018) suggest similar tectonic reconstructions

with progressively modified LOC. Eddy et al. (2014) utilize the Plates consortium reconstruction model valid for that time, with kinematic parameters similar to those in Hudec et al. (2013), while the LOC was constrained by GUMBO3 profile (Fig. 6c). Based on these parameters, a slow full spreading rate of 23-25mm/yr that increased to the west was predicted. The timing of spreading is constrained by stratigraphic observations from Snedden et al. (2014), based on seismic stratigraphy tied to industry wells. Morphological observations of spreading centers as axial valleys (e.g., Fig. 7) are consistent with a slow rate of spreading and are also consistent with estimates from GUMBO4 (Christeson et al., 2014) combined with timing from Snedden et al. (2014). Eddy et al. (2014) reported both seaward and landward dipping reflectors in the Apalachicola Basin (see location in Fig. 2a) that are interpreted as the "inner wedge" of syn-rift basins, although an alternative interpretation for these reflectors related to earlier orogenic structures is also mentioned. Potential pre-salt sediments are proposed based on the seismic reflection profile accompanying GUMBO3. SDR succession was interpreted near the LOC along GUMBO3 (coincident with the SDR polygon in Fig. 2c). High velocity lower crust was interpreted as substantial intrusions of melt into the lower, middle and upper crust during continental rifting. Notably, the interpreted mode of breakup varies between magma-rich for Zone 3 in the eastern GoM (Eddy et al., 2014), and magma-poor are northwestern GoM (Van Avendonk et al., 2015). A general west to east increase in magmatic material during rifting and breakup was proposed by Eddy et al. (2018).

The model of Nguyen and Mann (2016) was also based on a Plates consortium reconstruction at that time, with the use of the ESCs and transform faults derived from Sandwell et al. (2014) gravity (Fig. 3). This model assumes asymmetrical spreading in the eastern GoM, with a faster rate to the north of ESC and a right-lateral Western Main Transform fault as an OCB offshore eastern Mexico (Fig. 2c, section 5.4).

The model of Padilla Sánchez (2016) is the only one that proposes deposition of salt onto oceanic crust in two separate basins. According to this model, formation of the oceanic crust in the GoM started in the Bajocian (170.3 – 168.3 Ma) via a 39° counterclockwise rotation of the Yucatan block that was completed by the time of salt deposition (assumed to be Oxfordian, 163.5-157.4 Ma, per Salvador, 1991).

A rigid plates reconstruction of Pindell et al. (2016) was based on unpublished proprietary magnetic data in the Mexican sector of the GoM. This model proposes one extensional stage of continental rifting and two phases of oceanic spreading, with a syn-drift change in the pole of rotation ~150 Ma. The model includes potential episode of mantle exhumation. This model was revised in Pindell et al. (2020), as a new salt age (Bajocian) became available from Sr isotopes (i.e., Pindell et al., 2019). The new salt age, as well as detrital zircon data were used to constrain the age of seafloor spreading. The model has a slightly different kinematic concept for the rift stage that includes magmatism during the syn-rift phase, and two boundary systems, the Florida Transform Zone and North Oaxaca Transfer, which were active during the syn-rift stage. The model also includes an updated reconstruction in the Equatorial Atlantic. Salt was deposited during the transition from rift to drift. Three poles of rotation are proposed – the one for syn-rift extension, one for initial rotation of the Yucatan crustal block, with one for the change in rotation at 147 Ma. There is a wide zone of "uncertain basement" in the northern GoM, while both phases of spreading are denoted as oceanic crust, i.e., no exhumed mantle being proposed.

Lundin and Doré (2017) suggested a break-up near 190 Ma base on reconstruction of the HMA and YMA (see Fig. 8b and Appendix B2), both of which were considered to be COBs marked by SDR successions. A second phase of seafloor spreading with a distinctly different pole of rotation was proposed for the post-salt opening (ca 163-140 Ma). Their model was placed in a mega-regional (Pangean) context, applied rigid plate restoration with GPlates and correlation of magnetic lineaments (Fig. 8b). It reached a similar conclusion as Stern and Dickinson (2010) and introduced the term "high-angle back arc basin" (HABAB) to describe the GoM and potentially analogous Pacific Rim ocean basins, such as the Canada Basin, Weddell Sea and South China Sea. In the case of the GoM, the line of break-up formed where the Suwannee and Appalachian-Ouachita-Marathon sutures converged on the Pacific margin. Lundin and Doré (2017) also remark on the striking similarity between the GoM and the Canada Basin at the opposite (northern) end of the North American continent. Both re-opened Late Paleozoic sutures between major continents, both are small, pie-shaped ocean basins with axes intersecting the paleo-Pacific margin at high angles, and both were periodically confined, resulting in important source rock developments and (in the GoM) evaporites.

The model of Deighton et al. (2017) focuses only on the spreading phase, which they interpreted to be 154 – 128 Ma, based on modeling of high-resolution magnetic anomalies along a transect in the western GoM. Mapping of the mid-ocean ridge and transform faults were further refined based on industry proprietary seismic, magnetics and gravity data, resulting in a pole of rotation in western Cuba. Their plate kinematic model was also used to derive paleo-bathymetry at the end of spreading, which led them to compare opening of the GoM to the Gulf of Aden.

Alvey et al. (2018) is primarily a crustal architecture model that used satellite-derived gravity data and bathymetry/topography to derive crustal thickness and thinning factor to locate the LOC and interpret the ESR and TZ's. They propose two phases for opening: extension from 175 – 165 Ma, and rotation with seafloor spreading form 163 – 153 Ma, with a pole of rotation on the western edge of Cuba.

Minguez et al. (2020) rigorously utilizes gravity data to derive plate motion (i.e., flow lines, spreading centers and pole of rotation) and magnetic data for timing and location of LOC. Minguez et al. (2020) made the kinematic reconstruction available as supplemental material. Initially, the GoM opens as a rift between South and North America. At 169 Ma, the Yucatan began to rotate away from North America. Seafloor spreading started in the west and propagated eastward, ending at 154 Ma. This model did not interpret basinward-dipping reflectors as SDR complexes. Instead, these complexes are interpreted as a consequence of fault driven accommodation (as in Curry et al., 2018). The EEA (Fig. 8b) were modeled as serpentinized exhumed continental mantle. An average full spreading rate of 2.4 cm/yr in the northeastern GoM was derived based on modeling of magnetic chrons M23 to M38n.2n (166 -154 Ma), constrained by the timing of the opening of the Central Atlantic and decoupling of North and South America. Conversely, the tectonic model of Deighton et al. (2017), which also was based on interpreted magnetic chrons, proposed that oceanic spreading starting at 154 Ma and ceased at 128 Ma (M25 to M3) – the youngest end of spreading among all published tectonic models (Fig. 9).

Escalona et al. (2021) also provides a plate kinematic model of CBTH as supplemental material and utilized potential fields, seismic, and well data to update the most recent Plates consortium model. They focus on reconstructions of the Caribbean Plate relative to North and South America, with the timing of the spreading phase constrained by magnetic chrons. This model acknowledges the presence of the Florida transform (Fig. 2c). Deposition of Louann salt coincides with initiation of rotation of Yucatan; the oceanic spreading associated with this rotation ceases at 152 Ma.

The tectonic reconstruction by Filina and Beutel (2021) is based on integration of potential fields and seismic data. Interpreted SDR regions and presalt basins (Fig. 2c) in the eastern GoM (Zone 3) and on the Yucatan margin (Zone 5) were treated as conjugate features that guide tectonic reconstruction. Their model used the timing scheme from Snedden et al. (2014) and acknowledged two phases of oceanic spreading, with a ridge propagation at ~151 Ma. Filina and Beutel (2021) postulate temporal variability of magmatic regime during GoM opening ranging from CAMP (~200 Ma) presumably responsible for SDR complexes (Fig. 2c) to initial amagmatic ultra-slow spreading (~ 162 -151 Ma, estimated full spreading rate 0.9 cm/yr by Filina et al., 2020) that produced thin and uniform crust imaged by GUMBO4 (Fig. 6d). The second spreading phase was faster (~ 1.1 cm/yr) and

characterized by increases in magmatic input, as it produced thicker and layered oceanic crust imaged by GUMBO3 (Fig. 6c).

While recent geophysical data have reduced uncertainties about the nature and geometry of seafloor spreading in the GoM, published models still illustrate a range of potential timing and areal extent of oceanic crust (Fig. 3b), in addition to variations in the nature of the OCT. Regardless of timing differences, most models agree that the rift phase resulted from the south-southeast translation of South America and Yucatan from North America, while the latest phase of seafloor spreading was due to counterclockwise rotation of the Yucatan away from North America. On the other hand, models differ in the relationship of salt deposition to seafloor spreading, the type of the crust under the salt (see section 7.2), the nature of break-up (section 7.3), shifts in poles of rotation and symmetry or asymmetry of spreading. Further refinement of the duration of seafloor spreading, as well as compositional heterogeneities in the GoM, awaits unequivocal identification of magnetic chrons, direct sampling of the crust, thermo-mechanical modeling of GoM beak-up, and/or additional sequence stratigraphic mapping and chonostratigraphic control of sediment downlaps onto new oceanic crust.

7. Key unanswered questions in the GoM

This section lists major questions that the authors believe are still unresolved for the tectonic evolution of the GoM. These include: 1) whether Triassic redbeds (and equivalent non-marine facies in Mexico) represent the latest stage of Late Paleozoic collision (i.e., successor basin) or the initial stage of rifting (section 7.1), 2) the order of oceanic crust formation and salt deposition, and the extent to which these overlapped in time and space (section 7.2), 3) the mode of break-up, i.e., magma-rich or magma-poor, or both (section 7.3), and what are the spatial and temporal variations in these processes across the basin, and 4) pre-breakup location of continental blocks (section 7.4).

7.1. Triassic redbeds: Early syn-rift deposits or successor basin?

The Triassic section of the GoM region represents a transition between the Paleozoic Ouachita-Marathon orogeny and Mesozoic rifting that ultimately led to formation of the GoM (Fig. 4). Most GoM tectonic models have rifting starting in the Late Triassic (Fig. 9, Table 3). This interpretation is based on limited well data along the northern rim of the basin, and from observations in Mexico. Many wells have encountered a continental clastic section generally described as 'redbeds' below Jurassic or Cretaceous sediments (see Fig. 4 and Appendix C2). This section, known as the Eagle Mills, is similar in age and lithology to well-known rift sections in eastern North America (such as South Georgia Rift, Fig. 2c) leading to early suggestions that the Triassic section was deposited in grabens formed during early Pangea rifting (e.g. Woods and Addington, 1973). When seismic reflection data became available, rift faults and grabens were not observed. Unfortunately, most of these seismic lines are not publicly available. However, two of the co-authors of this paper (Norton and Snedden) have seen several hundred such profiles that never show rift structures associated with presumed Triassic extension along the northern margin. Instead, several published seismic images, e.g., Nicholas et al. (1989), Milliken (1988), Snedden and Galloway (2019), consistently show that Triassic deposits overlie Late Pennsylvanian and Permian sections that together represent a southward-thickening wedge below a mid-Jurassic unconformity. Fig. 10 shows a structure map on top of the Paleozoic section (Milliken, 1988) representing the mostly unfaulted base of the Triassic and younger sections. The "base of salt" seismic horizon (Horn et al., 2016) appears mostly unfaulted as well, although the geometry of the underlying Triassic and older section is not apparent from current data. These observations have led to the alternative interpretation that there was little Triassic rifting in the northern GoM, and that the Triassic represents a successor basin deposited as part of the succession following the Ouachita-Marathon orogeny (Nicholas et al., 1989; Snedden and Galloway, 2019). More research is needed to fully establish the relationship between these apparently unfaulted basins and extension that led to Pangea breakup.

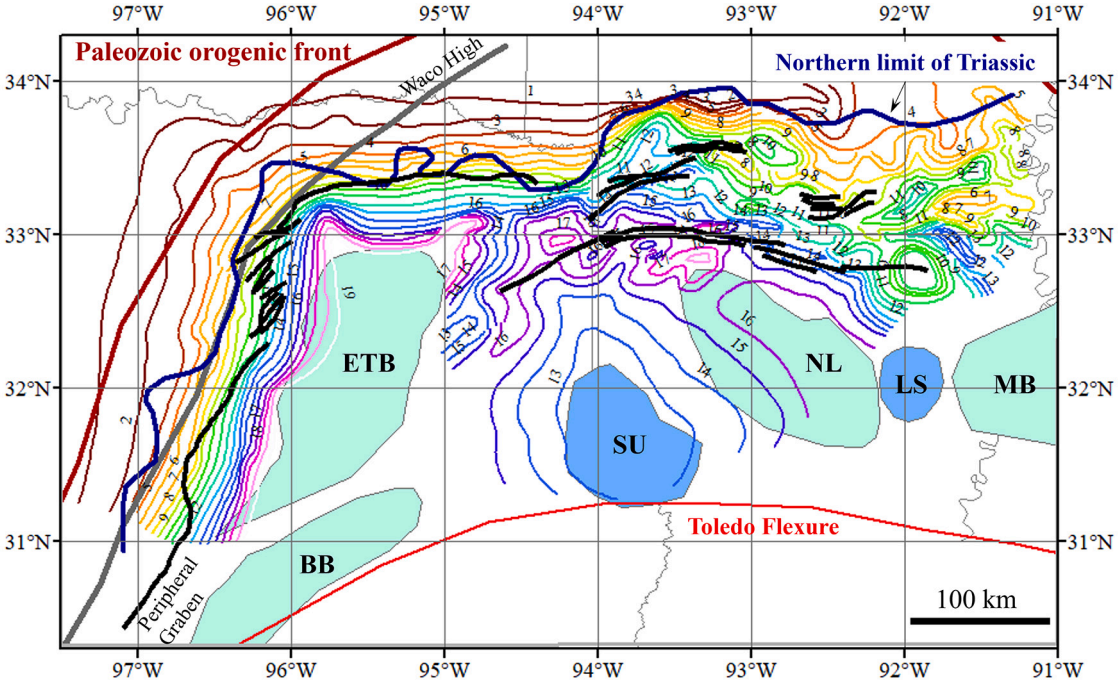

Fig. 10. Structure map on top Paleozoic from Milliken (1988). Contours in thousands of feet. Basins (light blue) and Arches (dark blue) from Ewing (2009). ETB = East Texas Basin; BB = Brazos Basin; SU = Sabine Uplift; NL = North Louisiana Basin; LS = La Salle Arch; MB = Mississippi Basin.

The Triassic section of northern Mexico is also mostly redbeds, although there are more volcanics since the tectonic setting is very different from the northern GoM (see section 3 and Fig. 4). However, these deposits are poorly dated, and this has led to some confusion in nomenclature as geologic knowledge has evolved. The reader is referred to Salvador (1991) for an excellent summary of early interpretations of the Triassic of Mexico.

In the southern GoM, more recent studies separate the section related to the Nazas arc from backarc rift sections (Barboza-Gudiño et al., 2010; Rubio-Cisneros and Lawton, 2011; Peña, 2016). The backarc Huizachal Group is interpreted to have been deposited from Triassic through Early Jurassic time (Fig. 4), with the later part of the group being represented by the La Boca and La Joya formations (see Appendix C2). There are no known well penetrations of the Early Jurassic sediments in the northern GoM, but this time span is well-represented by deposits in northern Mexico. This observation is presumably linked to opening of the GoM basin, i.e., extension (of poorly constrained geometry and debated nature) in the northern GoM, while Mexico tectonic blocks were being realigned as South America and Yucatan pulled away from North America. Furthermore, Mexico may have experienced significant strike-slip deformation as the GoM opened during the Jurassic (Centeno-García, 2017).

7.2. Salt deposition – before, after or during oceanic spreading?

Regardless of the absolute age of the GoM salt, published models differ on the timing of salt deposition relative to the initiation of seafloor spreading (Fig. 9). Salt deposition represents the first marine incursion into the GoM after the Permian and the first recognized basin-wide stratigraphic unit (Fig. 4; Snedden and Galloway, 2019). Salt overlies poorly-dated Late Triassic continental clastics (see section 3) and is in turn locally overlain by Jurassic clastics of the Norphlet Fm followed by carbonates of the Smackover Fm in the northern GoM and the Zuloaga Fm in Mexico. Oxfordian (~158 Ma; Olson et al., 2015) ages for these carbonates has led to the natural assumption that salt was immediately older, i.e., Callovian (~162 Ma; Salvador, 1991), but recent Sr-isotope data have suggested an older, Bajocian, age of 169-170 Ma (Fig. 4; Snedden et al., 2019; Peel, 2019; Pindell et al., 2020).

It is believed that the salt was deposited very rapidly, in less than a million years (e.g., Warren, 2006). This estimate is consistent with numerical modeling of salt deposition in the South Atlantic (Montaron and Tapponnier, 2010), and also with estimates from stratigraphy of the Santos Basin, Brazil (Dias, 2005). The hypothesis of rapid deposition also matches modern rates from the few regions of current salt deposition (see Davison et al., 2012) and with the known ~640,000-year duration of up to 3 km thick Messinian salt deposition in the Mediterranean (e.g., Krijgsman et al., 1999). If GoM salt deposition was completed within one million years of the Sr age dates of 169-170 Ma, ~10 million years elapsed before the first fossil-dated carbonate sediments were deposited. One explanation is that salt was deposited throughout this interval (Godo, 2017; Rives et al., 2019). Rives et al. (2019) further suggest that salt was deposited contemporaneously with a sedimentary section they named the 'SAKARN Series' (an acronym for the expected lithological sequence of salt – anhydrite – carbonate - Norphlet Fm clastics). This 10 million year age gap is remarkable given that in the northern GoM, the updip limit of salt, which is likely to mark the salt-time shoreline, is almost coincident with the Smackover Fm shoreline (Fig. 2a), pointing to apparent tectonic stability over this time interval. In contrast, many tectonic models propose substantial concurrent movement of the Yucatan crustal block relative to North America during this time (see Fig. 9 and section 6).

Many authors have noted that the interpreted base of salt in the northern GoM is generally smooth in seismic data (Horn et al., 2016). The updip limit of salt is marked by a 'Peripheral Graben' in the post-salt succession (Fig. 10; Anderson, 1979; Ewing, 2018) and runs from central Texas to Alabama; this structure represents a breakaway extensional feature formed by downslope motion of the post-salt sedimentary column, with the salt as an underlying weak detachment. This motion is unlikely to have occurred if the original base of salt had much rugosity, and it therefore suggests that the salt was deposited in a large, flat basin. The structural implication of this smooth base salt is that the salt may not represent a 'syn-rift' deposit, as was suggested in early papers on the GoM (see Fig. 9) but may have been deposited instead after oceanic spreading began (e.g., Padilla Sánchez, 2016; Lundin and Doré, 2017). This scenario is consistent with the lack of rift faults observed in seismic data (Fig. 10), although seismic imaging is challenging. In the western GoM, very thick sediments obscure deep structures in seismic data; even in the eastern GoM, where imaging is better, few rift faults are mapped (e.g., Pindell and Miranda, 2011; Rowan, 2014). The salt could also have been deposited at the onset of seafloor spreading (e.g., Rowan, 2014; Pindell et al., 2020; Hudec et al., 2020).

In contrast to the generally unstructured base of salt, the basinward salt edge shows some large structures (see Fig. 2c). In the western GoM, this edge is marked by the BAHA high (see Fig. 2c and section 5.5), while in the eastern GoM a basement ramp is mapped by Hudec et al. (2013) based on proprietary seismic data (coincident with the region of "uncertain crust" in Curry et al. (2018) in Fig. 2c). In Florida and the northern Yucatan margins, the outboard edge of salt coincides with this outer trough (see Fig. 2c and section 5.3). There is little doubt that crust outboard of salt is oceanic (see seismic refractions, section 4 and Appendix A), especially since publication of the gravity dataset by Sandwell et al. (2014); Fig. 3 and Appendix B1). In fact, the edge of authochthonous salt is generally used to define the LOC (e.g., Hudec et al., 2013). The troughs and ridges marking the edge of presumed autochthonous salt could be stretched continental crust (Hudec et al., 2013; Eddy et al., 2014; Nguyen and Mann, 2016; Filina, 2019), exhumed mantle (Van Avendonk et al., 2015; Pindell et al., 2016; Minguez et al., 2020), or the oldest oceanic crust (Kneller and Johnson, 2011; Rowan, 2014; Padilla Sánchez, 2016; Lundin and Doré, 2017; Hudec et al., 2020; Pindell et al., 2020). In this latter scenario, the BAHA high (section 5.5) could be a volcanic ridge formed in the early stages of sea floor spreading (i.e., before the salt, which is why salt onlaps the high; Hudec et al., 2020); the troughs could also be formed by sea floor spreading under salt. Therefore, the question of crustal type below the outer rim of the autochthonous salt vs. crustal type outboard of that salt is key to understanding the GoM tectonic evolution.

7.3. Magma-poor vs magma-rich origins of the GoM

Understanding the mechanisms for transition from continental extension (rifting) to sea floor spreading is a focus of modern geodynamics research (e.g., Franke, 2013; Doré and Lundin, 2015; Lundin et al., 2018; Cadenas et al., 2020). Due to thick sediment cover in the GoM and the general lack of wells reaching basement, the GoM rifting, nature of the crust, and the mode of break-up remain uncertain.

The term "break-up" broadly applies to the span of geologic time and mechanisms that accomplish the transition from continental rifting/extension to sea floor spreading. Broadly, two end-member rifted margin types have been identified, magma-rich and magma-poor (e.g., Franke, 2013 and references therein). The terms focus on the influence of magmatism on the transition, but differences also include styles of deformation, resulting paleobathymetry, subsidence, and mechanisms leading to break-up. The degree of magmatic influence varies significantly between margin end members, as does the timing of magmatism. At magma-rich margins, the lithospheric mantle breaks up approximately at the same time as magmatism takes place, while at magma-poor margins the crust breaks before the lithosphere, thereby thinning the crust and offten exhuming the mantle. Summaries of margin end members are provided by Franke (2013), Doré and Lundin (2015) and Tugend et al. (2018).

Authors studying the early evolution of the GoM have argued for both magma-poor and magma-rich modes of break-up, and both types

may be present. The margins of the GoM have experienced both intrusive and extrusive magmatic activity during rifting, and igneous rocks are known from well penetrations (see Fig. 2b, Table 2 and Appendix C3). However, limited magmatism is documented to occur even on the "type margin" for the magma-poor end member, Iberia-Newfoundland, (e.g., Cornen et al., 1999), and thus the current observations of GoM magmatism alone are not enough to constrain the breakup mechanism. Geophysical and geodynamic investigations are also important to characterize potential magma-rich and magma-poor scenarios.

7.3.1. Arguments favoring a magma-rich hypothesis in the central to northeast GoM

Magma-rich margins are well-known worldwide, exemplified by the southern South Atlantic (e.g., Austin Jr. and Uchupi, 1982; Franke et al., 2007; Koopmann et al., 2014), the Central Atlantic (e.g., Austin Jr. et al., 1990; Holbrook et al., 1994; Talwani et al., 1995), and the Northeastern Atlantic (e.g., White et al., 1987; Eldholm et al., 1987). Perhaps the most diagnostic geologic features associated with magma rich margins are SDRs that consist of subaerial basalt flows extruded from embryonic spreading axes during the break-up phase.

A commonly held view is that SDRs, together with underlying intrusions, represent initial subaerial oceanic crust although with thicknesses above the "steady state" 7 km thickness (e.g., White et al., 1987). The "above-normal" subaerial oceanic crustal thickness typically thins in the direction of the evolving submarine spreading axis toward "steady-state" oceanic crustal thickness (e.g., Kelemen and Holbrook, 1995; Mjelde et al., 2008; Funck et al., 2017; Paton et al., 2017).

Another characteristic of magma-rich margins is high-velocity lower crustal intrusions, often referred to as underplating (e.g., Austin Jr. et al., 1990; Mjelde et al., 2008; White and Smith, 2009). Together, the SDRs and lower crustal intrusions result in an abnormally thick, presumably completely subaerially accreted crust that transitions rapidly into classic submarine oceanic crust, as seen in the northeastern Atlantic (e.g., Hinz, 1981; Mjelde et al., 2008; Funck et al., 2017). A Moho reflection is often observed beneath the landward part of accreted crust marked by SDRs (e.g., Franke, 2013), in addition to beneath adjacent thinned continental and oceanic crust. In contrast, a Moho reflection is generally not observed at the COT along magma-poor margins, which instead displays a velocity gradient (e.g., Sibuet and Tucholke, 2013; Davy et al., 2016). The mechanism causing the "above-normal" melt thickness of magma-rich margins is a much-debated topic; such melts have been attributed to elevated mantle temperatures (e.g., White et al., 1987). However, alternatives to elevated mantle temperature exist such as small-scale convection (Mutter et al., 1988), mantle fertility (e.g., Foulger, 2002), and variations in extension rate (Lundin et al., 2014; Gallahue et al., 2020).

In the GoM, candidate SDRs have been observed in seismic reflection profiles both along the US margin and off northern and western Yucatan (Fig. 7; section 5.2 and references therein). Steier and Mann (2019) also published seismic reflection profiles over the Yucatan margin. Although SDRs were not a focus of the paper, the high-quality profile shown in their Fig. 7 reveals pronounced basinward-dipping reflections beneath the salt layer. Empirically, these reflectors bear a good comparison to known SDRs, for example those identified along the Argentina margin (Franke, 2013). Liu et al. (2019) performed integrated geophysical modeling of seismic and potential fields data in the eastern GoM and concluded that these basinward-dipping reflectors require dense and highly magnetic rocks to explain observed gravity and magnetic anomalies. In the southern GoM, analysis by Filina and Hartford (2021) also indicates a similar region of dense and highly magnetic rocks coincident with the seismically mapped basinward-dipping reflectors. Filina and Beutel (2021) proposed that the GoM regions identified as SDRs provide constraints for tectonic restorations, as they should be come together at reconstructed conjugate margins (see outlines in Fig. 2c). This idea will be further discussed in section 7.4.

A key element of the magma-rich argument for the GoM is the spatial coincidence of the candidate SDRs with high-amplitude positive linear magnetic anomalies. As described in section 4, the strong, linear positive FMA (Fig. 8b) coincides with SDRs interpreted from seismic data in the northern GoM. This compares to the Central Atlantic where the ECMA is also coincident with marginal SDRs (e.g., Austin Jr. et al., 1990; Holbrook et al., 1994; Talwani et al., 1995) and with similar geometries in other magma-rich margins such as the Vøring margin off mid-Norway (e.g., Hinz, 1981; Mjelde et al., 2008) and South Atlantic (e.g., Franke, 2013). Along strike from the FMA to the west, Mickus et al. (2009) have also modelled the Houston Magnetic Anomaly (HMA) as a magma-rich margin. Although implied by the model, the body causing the HMA is buried too deeply to determine whether or not the SDR pattern is present. To the south, the SDRs imaged off Yucatan are also coincident with a positive magnetic anomaly, the YMA (Steier and Mann, 2019; Filina and Hartford, 2021; Filina and Beutel, 2021). Importantly, the refraction velocity model of Eddy et al. (2014) over the FMA demonstrates high-velocity lower crust in the same region as the interpreted SDRs, as well as a Moho associated with velocity step (Fig. 6c).

In summary, the magma-rich interpretation benefits from an empirical comparison between the GoM anomalies (FMA, HMA and YMA) with the ECMA, and also provides a link between the typical magma-rich margin process that generates SDRs, high-velocity lower crust, and the associated major, linear positive magnetic anomalies.

7.3.2. Arguments favoring a magma-poor breakup of the GoM

Magma-poor margins have been characterized on the Iberia-Newfoundland conjugates (e.g., Péron-Pinvidic and Manatschal, 2009; Mohn et al., 2015), Nova Scotia (Funck et al., 2004), the Labrador Sea (e.g., Chian et al., 1999), and an obducted paleomargin in the eastern Swiss Alps (Manatschal and Müntener, 2009; Nirrengarten et al., 2016). Key characteristics of magma-poor margins are widths up to several hundred kilometers, a hyperextended margin crustal architecture and sequential, low-angle, basinward dipping listric faults bounding rotated fault blocks (e.g., Lavier et al., 2019). Hyperextension can give way to exhumed mantle, and eventually to oceanic crust (e.g., Péron-Pinvidic et al., 2008; Pérez-Gussinyé, 2013). As the name implies, magmatism is limited compared with magma-rich margins (e.g., Whitmarsh et al., 2001), which is also reflected in the subsidence pattern (e.g., Karner et al., 2012; Mohn et al., 2015). On the Iberian margin, peridotite ridges exist at the COT. These ridges were sampled on Galicia margin by ODP leg 103 (Boillot et al., 1987) and are characterized by ~100nT magnetic anomalies (Miles et al., 1996). A contiguous Moho is not generally recorded across the transition to oceanic crust, presumably due to serpentinization of the exhumed continental mantle (Davy et al., 2016).

In the GoM, the primary observation that supports a magma poor breakup is a seismic reflection bounding a ridge-like basement high (Fig. 7b) in the central to northeastern GoM, and in some places along the Yucatan margin (Rowan et al., 2012; Pindell et al., 2014; Miranda-Madrigal and Chávez-Cabello, 2020). Pindell et al. (2014) interpret this reflection as an outer marginal detachment (OMD), essentially a mechanical boundary separating the crust and mantle that allowed mantle exhumation. In its original formulation, the OMD was proposed to accommodate slip between continental crust and mantle, yielding rapid accommodation and related subsidence (outer marginal collapse, OMC) which could potentially explain thick accumulations of salt in other parts of the basin.

The basement high bounded by the OMD also forms the outboard side of a trough, referred to by Pindell et al. (2014) and Curry et al. (2018) as the "Outer Marginal Trough" (OMT). The trough and basement high are related to a regional magnetic low and set of EEA magnetic anomalies, respectively (Fig.s 7b and 8b, Appendix B2). Some authors have modeled these anomalies as the OCB/LOC (Liu et al., 2019; Pindell et al., 2020; Filina and Beutel, 2021), while others suggest that the EEA may be evidence of mantle exhumation (Pindell et al., 2016; Minguez et al., 2020). Minguez et al. (2020) modeled this basement step-up as a peridotite ridge that has a conjugate on the Yucatan margin.

Thus, this inferred peridotite ridge may rim the oceanic crust, at least in the eastern part of the basin. A correlative basement high may exist in the western GoM (i.e., the BAHA high, see section 5.5 and Fig. 2c), but fault relationships to this feature remain unclear. In the western GoM, Kneller and Johnson (2011) interpreted a zone of ultra-slow lithospheric stretching, while Van Avendonk et al. (2015) have interpreted exhumed mantle at the rift to drift transition. Kneller and Johnson (2011) discuss the implications of their interpretation from the plate kinematic perspective, but do not provide any geophysical evidence to support their interpretation of "possible ultra-slow spreading lithosphere". Van Avendonk et al. (2015) provide a refraction velocity model in the region discussed by Kneller and Johnson (2011); Fig. 6a) that includes a window in the upper crust, essentially a graben that has opened a hole in the crust to mantle below (see alternative interpretations in Appendix A). If correct, their interpretation provides a novel method to "exhume" the mantle that is distinct from the Iberian and Alpine analogues already mentioned.

The basinward dipping reflectors in the magma-poor model can be explained as structurally controlled packages of rift fill (Minguez et al., 2020). The associated strong magnetic signature was modeled by Minguez et al. (2020) as thick lower crust, without introducing the highly magnetic material in the upper crust (i.e., without an SDR complex). Minguez et al. (2020) have modeled the transition from oceanic crust, through the basement high in the eastern GoM (i.e., Southern Plateau, see location in Fig. 2a), to attenuated continental crust in the eastern GoM using analogue rock properties for oceanic crust, exhumed mantle, and continental crust, respectively. Their model provides a good fit to the data, and supports crustal types represented at magma-poor margins. Lastly, circumstantial support for a magma-poor interpretation is derived from rather thin (~ 5 km) and uniform oceanic crust imaged by GUMBO 4 (Fig. 6d), and slow plate spreading rates suggested in some studies, typical of low magma supply during oceanic crust formation (Eddy et al., 2014; Minguez et al., 2020).

While a magma-poor breakup mechanism that exhumes the mantle can be envisioned in parts of the GoM, there are several caveats to consider. First, the refraction velocity model of Eddy et al. (2014) would have to be interpreted as evidence of attenuated continental crust rather than intruded lower crust. In this case, high velocity structures in the lower continental crust are explained as preexisting crustal fabric related to Paleozoic collision, or as evidence for a decompression melt introduced during magma-poor continental rifting (as in Van Avendonk et al., 2015). This interpretation is possible given the overlap between the acoustic velocities of crustal rocks (Christensen and Mooney, 1995), but it is not the preferred interpretation of Eddy et al. (2014). Alternative interpretations of velocity models are not uncommon. The Samba project, for example (in the Santos basin, Brazil), has authors suggesting both exhumed mantle and lower crustal intrusions for the same velocity anomalies (Evain et al., 2015; Rigoti, 2015). On the Iberian margin, significantly different velocity models fit refraction data where exhumed mantle is known (Dean et al., 2000; Minshull et al., 2014). A significant ambiguity in the crustal structure of the GoM is also a potential challenge for magma-poor interpretations. Magma-poor margin analogues, like the Iberia-Newfoundland conjugates, demonstrate pervasive brittle deformation in the attenuated crust that is only debatably resolved in existing public domain reflection data within the GoM (Culotta et al., 1992; Trudgill et al., 1999; MacRae and Watkins, 1995; Pindell et al., 2011).

7.4. Pre-breakup location of crustal blocks

There is little controversy about the final phase of rotational opening of the GoM, due to the persuasiveness of the spreading structures delineated by satellite gravity (Sandwell et al., 2014; Fig. 3a). As shown in Fig. 3b, all post-Sandwell interpretations agree on the approximate location of the ESC, although interpretations vary in some details, such as the position of the Euler Pole, geometries of the OCB/LOC and oceanic transforms/fracture zones. Many models agree that rotation of the Yucatan crustal block with respect to North America initiated near the time of salt deposition (Fig. 9) previously thought to be Callovian (166.1-163.5 Ma), but now older, Bajocian (169-170 Ma, see section 3).

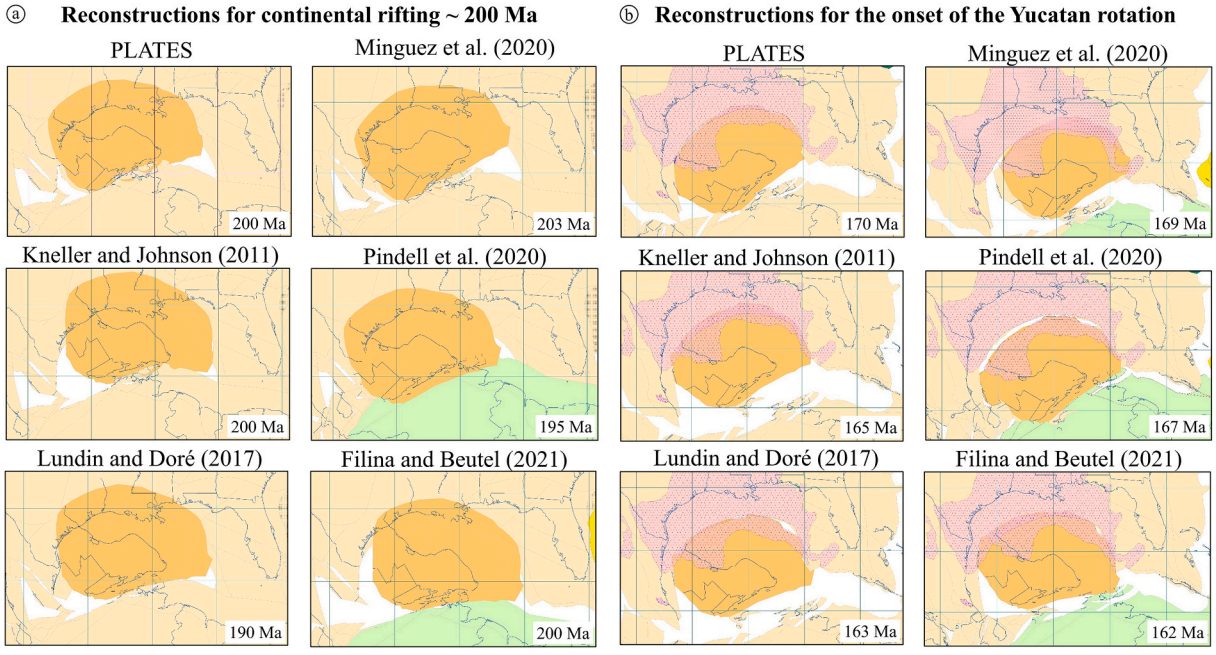

Fig. 11. (a) Plate reconstructions for various models near ~ 200 Ma. Not all models give kinematic parameters for the earliest pre-rift geometries, but all do give parameters for the time shown here. Yucatan is colored darker tan; the light tan shows tectonic blocks that are rotated with the parameters from the Plates database. South America in green shows that the quoted model provided rotations for South America, and similarly yellow for Africa. Please note that these reconstructions use the latest Plates LOC and are meant to illustrate the variations in the pole of rotations only, not the variations in LOC/OCB (see Fig. 3b for that) (b). Reconstructions for times in each model for the onset of rotation of Yucatan about poles near the Florida Straits, i.e., the onset of the 'rotational phase' of opening of the GoM. The pale pink color denotes salt.

Pre-spreading reconstructions, however, differ between the models (Fig. 11).

As illustrated, for example, by gravity inversion of crustal thickness (Alvey et al., 2018) a significant expanse of thinned crust remains, all contained within the present GoM area. This "remaining crust" needs to be accounted for in order to achieve a tight Pangaea fit between North and South America. Awareness of this thinned crust has led many authors to propose a two-stage model for GoM opening, with an earlier (Early to Middle Jurassic) phase consisting of either continental rifting (i.e., resulting in thinned continental crust, e.g., Hudec et al., 2013; Eddy et al., 2014; Nguyen and Mann, 2016; Filina and Beutel, 2021), exhumation of continental mantle (Pindell et al., 2016; Minguez et al., 2020), or formation of oceanic crust (Imbert et al., 2005; Kneller and Johnson, 2011; Lundin and Doré, 2017; Snedden and Galloway, 2019; Pindell et al., 2020). Regardless of whether a single-stage or two-stage model is used, all models place the original Yucatan and the U.S. continental margins closer together, but precise positions vary (Fig. 11).

Various geological observations are used to constraint pre-breakup locations of continental blocks, such as magnetic anomalies (Imbert et al., 2005; Lundin and Doré, 2017; Minguez et al., 2020), alignment of pre-salt sedimentary basins (Van Avendonk et al., 2015; Filina and Beutel, 2021), and/or regions of presumed SDRs (Imbert et al., 2005; Lundin and Doré, 2017; Filina and Beutel, 2021). The latter interpretation – that basinward dipping reflectors aligned with pronounced magnetic anomalies are interpreted as evidence of rift-related magmatism near the onset of seafloor spreading (i.e., SDR) - has been proposed by Imbert et al. (2005) for the eastern GoM and then extended by Lundin and Doré (2017) to other pronounced magnetic anomalies, namely HMA, FMA, and YMA (Fig. 8b). This interpretation assumes that crust outward of interpreted SDR complexes is oceanic (Hinz, 1981; Lundin and Doré, 2017; Snedden and Galloway, 2019). Alternatively, the thin crust under the northeastern GoM (see Fig. 6 and Appendix A) has also been proposed to represent stretched and intruded continental crust (Eddy et al., 2014, 2018; Christeson et al., 2014; Filina, 2019; Filina and Beutel, 2021) exhumed mantle (Van Avendonk et al., 2015; Pindell et al., 2016; Minguez et al., 2020), or a combination of both, presumably formed at a slow-spreading margin (e.g., Kneller and Johnson, 2011; Eddy et al., 2014; Christeson et al., 2014; Filina et al., 2020). Hyper-extended crust would produce a less tight fit between the margins, using a rigid plate model, since the remaining continental crust must be restored using a deformable margin, and therefore the alignment of magnetic character pointed out above would be different (Fig. 11). Exhumed mantle (Rowan, 2014; Minguez et al., 2020) could yield a tight fit, but this may require different explanations for the HMA, FMA, and YMA. For example, Hall (1990) have proposed that the GCMA (including the FMA and HMA) relate to ultramafic or mafic bodies entrained in the suture between Gondwana and Laurentia. More recently, Minguez et al. (2020) have suggested that the FMA could be explained by a horst-like crustal block (i.e., Southern Plateau, see Fig. 2a for location), with a lower crustal igneous component contributing to its magnetic signature.

As the pre-breakup match of crustal blocks based on magnetic anomalies is not unique (Fig. 11), more matching observations on presumed GoM conjugate margins are necessary. The plate reconstruction underpinning the restoration by Lundin and Doré (2017) has used the USGS aeromagnetic data of Bankey et al. (2002) shown in Fig. 8b, to illustrate that the "tight" fit of the HMA and YMA, which also aligns a pronounced NNE-trending linear magnetic anomaly marking the Appalachian front (Steltenpohl et al., 2013) with a similar linear anomaly crossing Yucatan. Additionally, matching anomaly patterns between Yucatan and the Suwannee Terrane of southern Florida suggest that these elements originally formed a single terrane on the northern margin of Gondwana (Fig. 11). Filina and Beutel (2021) have outlined regions of SDR complexes and pre-salt sedimentary basins on both Yucatan and the eastern GoM margins (see Fig. 2c) that were interpreted as conjugate features that should be aligned during pre-breakup reconstruction. In addition, the outer trough identified on both the Yucatan and Florida margins (Fig. 2c) may also represent conjugate geological structures that would guide tectonic restoration. Much remains to be confirmed by new data in these critical regions.

Clearly, the "best" fit of the crustal blocks bordering the GoM will ultimately be resolved by not only by a fully deformable margin model, but also by establishing the composition(s) of the crustal substrate in the northern GoM. Drilling to these depths and stratigraphic levels is unlikely in the near future. Therefore, the most revealing information is likely to come from new or newly-available seismic – reflection, refraction and wide-angle – with particular emphasis on velocity analysis (e.g., Vp/Vs analyses).

8. How we can answer the remaining questions

Based on our synthesis of published models, we have outlined three major questions that remain debated in the scientific community. Question 1 addresses the Triassic history of the basin and the origin of early redbeds and sedimentary equivalents – do they represent the initial phase of Gulf of Mexico rifting, or were these sediments deposited in post-orogenic, pre- basin settings? To answer this question, joint deep-penetration seismic reflection surveying and targeted core studies are necessary. Onshore seismic reflection data exist in the northern part of the basin, but those data are proprietary or of poor quality. Cores from Triassic redbeds along the rim of the basin were recovered in the 1950s and 60s, but the status of the most of these cores is unknown. Acquisition of 3D seismic data would help us figure out where it would be best to put a scientific drillhole, but that hole would be deep and very expensive.

Question 2 relates to the timing of salt deposition relative to seafloor spreading. As outlined in section 7.2, some models call for salt to be deposited during the last stage of continental rifting, while others suggest that oceanic spreading already was underway when salt was deposited. In order to answer this question, better constraints on the age of oceanic crust are needed. Technologically, sampling of oceanic crust is not possible in the center of the basin, as it is too deep. The Gulf of Mexico lacks high quality, high resolution magnetic data to constrain seafloor spreading models. Sager et al. (1998) have demonstrated the utility of deep-tow magnetic data to map M-series anomalies east of the Mariana Trench. Sibuet et al. (2007) employ deep-towed data on the Newfoundland-Iberia rift in the North Atlantic to discriminate M-series anomalies from similar features created by serpentinized, exhumed mantle. A deep-towed magnetics survey across the expanse of interpreted oceanic crust in the GoM, perhaps along a series of transects acquired across ESCs and between FZs interpreted from satellite-derived gravity (Sandwell et al., 2014), will serve two purposes: 1) clarify magnetic chron character (presuming that they are somewhere within the M-series, Gee and Kent, 2007) in order to pin down the time span within the Jurassic-Early Cretaceous during which seafloor spreading took place, and 2) refine the extents and orientations of ESCs suggested by gravity data. Modeling of these deep-towed data will not remove all uncertainty: sediments within the central basin are thick, deep-towed data will contain complex features not all of which may be explained, and modeling of portions of M-series anomalies remains controversial (Tominaga and Sager, 2010), but acquisition of such new data in the deep GoM basin would likely be a step forward in refining both the timing of seafloor spreading and defining the limits of oceanic crust. Additional age dating of salt and surrounding stratigraphy would be also beneficial, as all the new age dating of salt (Pindell et al., 2019) are from the edges of the basin.

Question 3 addresses the nature of basin opening - magma poor vs. magma rich, or both. Coring one or more basinward dipping complexes to determine their nature and age would help address this question. However, the industry wells are unlikely to target the OCT, while scientific drilling in the GoM is currently limited due to environmental concerns. Therefore, the major effort should be on 2D and 3D seismic studies that allow recovery of both Vp and Vs variations in the crust of the disputed region, as well as to study the continuity of Moho in seismic

records to test the mantle exhumation hypotheses. Crustal refraction surveys like the GUMBO experiment in the Mexican sector would also be desirable. A passive seismic experiment similar to EarthScope for the offshore GoM would allow better determination of crustal and lithospheric structures in the basin.

The GoM basin is a unique place that hosts several academic research projects, like Tectonic Analysis, Ltd. (https://www.tectonicanalysis.com), CBTH, Plates, GBDS, AGL and others that are industry-sponsored. Several recently published tectonic reconstructions using the Plates models (Hudec et al., 2013; Eddy et al., 2014; Nguyen and Mann, 2016; Escalona et al., 2021) not only illustrate the evolution of the Plates model, but also demonstrate the increased collaboration across these consortia. However, we also acknowledge that there have been less than desirable scientific consequences of these arrangements. Particularly, data owners have been generous in allowing consortia researchers access to proprietary data, but the data themselves are generally not publicly available, which limits scientific advancement. In addition, digital plate kinematic models have been used for paleogeographic reconstructions but have not been fully published or peer-reviewed. Many consortia publication policies limit broader dissemination of the results to the general geoscience community, so new data, interpretations and models generated by joint collaborations are often inadequately documented and reviewed in the open literature. This funding model, i.e., industry-sponsored academic consortia, has worked well for about 40 years, but is now struggling due to the changing business environment; so, the future of research funding for GoM research is at risk.

Furthermore, there are many other sediment-filled extensional basins around the world that need to be better understood, such as the Caspian Sea, the Black Sea, the Aleutian Basin, the Baltic Sea, and the Sea of Japan. The approach of combining the perspectives of both industry and academic geoscientists followed in the GoM, made possible by both joint research and the use of internet conferencing, provides a model for studying those basins.

The geoscience community as a whole significantly benefits greatly when collaborative research and publication programs are in place to acquire and analyze new data and publish more comprehensive tectonic models. Therefore, we encourage future academic-industry collaboration and jointly funded research projects to explore ways to openly share significant data and results in the peer-reviewed literature. Through the continued partnership of industry and academia the remaining questions about the formation of the GoM basin can be investigated productively.

9. Conclusions

The Gulf of Mexico is a challenging sedimentary basin to investigate from a plate tectonic point of view, because its deep crustal and lithospheric geometry is largely hidden beneath a thick and complex overburden and most data in the basin are proprietary. Nevertheless, significant progress in understanding GoM opening has been made in recent years with the help of several major publicly available datasets, such as industry-sponsored GUMBO refraction experiment in the U.S. sector of the basin that have enabled significant advances in our understanding of the basin's evolution. High-quality satellite gravity data led to a near-consensus on the last, Middle Jurassic to Early Cretaceous rotational spreading episode. In this review we have assessed the current level of understanding and compared the many published tectonic models. We have highlighted some key areas where significant controversy remains, and where work remains to be done. These include:

1) The nature of the Triassic redbed basin preceding GoM opening - whether these units represent a successor basin to the Ouachita-Marathon orogeny or precursor rifting to GoM formation. The issue is tied to the challenge of identifying firm evidence of pre-breakup rifting, which is currently sparse compared to other rifted margins;
2) The timing of salt deposition with respect to the Middle Jurassic seafloor spreading – specifically whether the salt predated, was synchronous with, or just postdated the initial spreading;
3) Whether GoM opening was facilitated by magma-rich breakup associated with SDRs, or it was mantle-poor and resulted in exhumed mantle close to the ocean-continent boundary;
4) The related issue of continental restoration of pre-GoM crustal blocks. The newly mapped geological structures within and adjacent to the OCT, such as interpreted SDR complexes with adjacent presalt sedimentary basins and outer troughs, in addition to magnetic anomalies may further constrain tectonic reconstruction of the basin.

In considering what data can help resolve these controversies, we stress the importance of the academia-industry partnerships both in terms of releasing more proprietary data to the general geoscience community, and via joint gathering, analysis and interpretation of new datasets. Publication of model parameters improves researchers' ability to compare and improve tectonic models for the benefit of science. We encourage authors to provide the numerical parameters (poles of rotation, timing, tectonic zonation) used in kinematic plate reconstructions and recommend that reviewers and editors publish these digital models and constraining data for the benefit of future research in the Gulf of Mexico, as well as other, similar basins around the world.

Declaration of Competing Interest

None.

Acknowledgements

The authors are extremely grateful to TGS and particularly to Jim Howell for allowing us to show the regional seismic reflection line from their recent GIGANTE survey. Many thanks go to Eric Lundin for his immense efforts with this paper and for many constructive discussions. The Editors and anonymous reviewers are thanked a lot for their valuable comments. The authors are grateful to Lawrence Febo for assistance with TSCreator Pro used for tectonostratigraphic chart shown in Fig. 4. This is UTD Geosciences contribution number 1381and UTIG contribution number 3835.

Appendix A. Seismic Refraction Studies

The first seismic refraction studies conducted offshore Gulf of Mexico were collected by Ewing et al. (1960) and revealed the presence of oceanic crust in the center of the basin. In the same year, Cram Jr (1961) collected onshore data from multiple stations along the Texas coast from two explosive sources near Cleveland, TX and Victoria, TX. This experiment revealed four subsurface layers, in particular two sedimentary units over the upper and lower continental crust layers on top of the upper mantle with a depth to Moho of 33 km. Similar structure was revealed in an experiment conducted by Dorman et al. (1972), mapping Moho at a depth at 30 km (see shotpoint location in Fig. 5). Later offshore expeditions by Antoine and Ewing (1963), Hales et al. (1970), Ibrahim et al. (1981), Ibrahim and Uchupi (1982), Ebeniro et al. (1986, 1988), Sawyer et al. (1986); Nakamura et al. (1988), Kim et al. (2000), and Christeson et al. (2001) have resulted in more than a hundred refraction datasets within the basin (Fig. 5). Marton and Buffler (1994) have presented an overview of prior seismic refraction data in the GoM. Onshore seismic data were collected as a part of Consortium for Continental Reflection Profiling (COCORP; Lillie et al., 1983; Nelson et al., 1985; Culotta et al., 1992) and in PASSCAL experiment (Keller et al., 1989). Recent studies of Thangraj et al. (2020) and Marzen et al. (2020) study crustal architecture onshore (see location in Fig. 5). Some of these crustal studies incorporate various types of receiver function analysis. Stations from the EarthScope project ('https://www.earthscope.org/'), which cover the onshore U.S. in a network with instruments ~100 km

apart, are shown as black points in Fig. 5. Interpretations of crustal structure from EarthScope have been published by Schmandt et al. (2015). Another study in the southeastern U.S. that used seismic stations supplementing the EarthScope array was called SESAME; these results were published by Wagner et al. (2018).

In 2010, the University of Texas at Austin Institute for Geophysics, supported by industry, carried out the GUMBO (GUlf of Mexico Basin Opening) experiment, with the primary objective to reveal crustal architecture and provide constraints for basin opening. That experiment consisted of four regional profiles crossing the U.S. sector of the basin (Fig. 6).

In the northwestern GoM (Zone 2 in Fig. 1), GUMBO1, a 350-km long profile (Fig. 6a), crosses a region of thinned, heterogeneous crust that different authors have interpreted variously as hyper-extended continental covered by thick pre-salt sediments (Van Avendonk et al., 2015), ultra-slow spreading lithosphere (Kneller and Johnson, 2011), transitional (i.e., stretched and intruded continental; Filina, 2019), or oceanic crust (Imbert and Post, 2005; Lundin and Doré, 2017). Some tectonic models suggest that GUMBO1 is located entirely over oceanic crust (Fig. 3b). The published cross-section (Fig. 6a) implies a 40 km wide zone of interpreted exhumed mantle adjacent to inferred oceanic crust at the very southeastern end of the profile (Van Avendonk et al., 2015). Filina (2019) has reported that this zone is adjacent to a region of thick salt (known as a "salt wall" in the Perdido fold belt, labeled (3) in Fig. 8a) that is missing in the seismic refraction interpretation (Fig. 3a). The lack of this salt in the GUMBO1 refraction model leads to significant deviations in seismic raypaths and results in the inaccurate velocities that were interpreted by Van Avendonk et al. (2015) as exhumed mantle. Filina (2019) proposed an alternative interpretation, based on analysis of GUMBO1 refraction data integrated with potential fields, suggesting ~10 km thick stretched and intruded continental crust, instead of exhumed mantle immediately adjacent to oceanic crust.

Most of GUMBO2 in Zone 2 (Eddy et al., 2018; Fig. 6b) has been interpreted to lie over stretched and intruded continental crust with a total thickness on the order of 10 km. The contact with the oceanic domain is interpreted to occur at the southern end of the profile near the Sigsbee Escarpment (Fig. 1). This LOC challenges many tectonic models (Fig. 3b) that position that boundary more than 100 km to the north, which allows for a tighter fit between the Yucatan crustal block and the Texas-Louisiana margin during tectonic reconstructions (more details in section 7.4). However, that northern location is not supported by either GUMBO2 (Eddy et al., 2018) or potential fields (Filina, 2019). Furthermore, results from GUMBO2 do not support the presence of pre-salt sedimentary section in the central GoM (see location in Fig. 6e; note published tectonic models range the most there). Lack of pre-salt basin in that region further challenges tectonic reconstructions proposing that the Texas-Louisiana margin is conjugate to western Yucatan (i.e., Kneller and Johnson, 2011; Eddy et al., 2014; Van Avendonk et al., 2015; Pindell et al., 2020) where up to 5 km thick section of pre-salt sediments is imaged in reflection seismic (see section 5.1).

The crust along GUMBO3 in Zone 3 (Eddy et al., 2014) is interpreted to vary from 23 km-thick transitional crust in the northeast to up to 9 km-thick oceanic crust in the center of the basin (Fig. 6c). This profile crosses regions of basinward and landward dipping reflections, some of which are interpreted as SDRs by multiple authors (Imbert and Post, 2005; Pindell and Heyn, 2011; Kneller and Johnson, 2011; Hudec et al., 2013; Rowan, 2014; Eddy et al., 2014; Lundin and Doré, 2017; Filina and Beutel, 2021). Furthermore, this region coincides with a pronounced magnetic anomaly (FMA, labeled (3) in Fig. 8b), which may support the presence of associated magmatism (Liu et al., 2019); FMA may also be related to relatively thick crust and a basement high known as the Southern Plateau (see location in Fig.2b; Minguez et al., 2020). Notably, there is up to a 3 km mismatch in Moho depth interpreted from seismic reflection and refraction data along GUMBO3 (Eddy et al., 2014). This Moho discrepancy is located immediately basinward of interpreted transitional crust (Fig. 6c) and is believed to be oceanic crust by some researchers (Eddy et al., 2014; Nguyen and Mann, 2016; Liu et al., 2019; Filina and Beutel, 2021) and a zone of exhumed mantle by others (Pindell et al., 2016; Minguez et al., 2020). Notably, in the most recent model, Pindell et al. (2020) refer to this region as an older oceanic crust. Thicker than normal oceanic crust in the center of the basin has a characteristic two-layered structure – an upper basaltic layer with slower seismic compressional velocities (Vp) over an interpreted, faster gabbroic layer. An interpreted ESC is evident at the southwestern end of GUMBO3, expressed as a 3 km deep, ~20 km wide valley. The ESC is associated with an overall decrease in seismic velocities (Fig.s 6c, d).

Another profile in Zone 3, GUMBO4, appears to have the most homogeneous transitional crust of all four refraction lines (Fig. 6d; Christeson et al., 2014). Interpreted crust is >30 km thick at the landward end of the profile, presumably continental, to a ~5 km thick, presumably oceanic crust, at the southwestern (seaward) end. Remarkably, this oceanic domain is drastically different from the one imaged by GUMBO3 – much thinner (~ 5 km) and more uniform, with relatively high compressional seismic velocities (Fig. 6c), suggesting complex lithologic domains toward the center of the basin. GUMBO4 also contains a high velocity body near 225 to 275 km (Fig. 6d), which may reflect a magmatic addition associated with continental rifting and/or breakup.

The GUMBO experiment represents one of the most important geophysical datasets acquired in recent decades in the U.S. sector of the GoM. Unfortunately, there is no similar comprehensive seismic refraction survey in the Mexican part of the basin, so the crustal structures there remain less constrained.

Appendix B. Potential Fields

Section B1 Satellite-derived gravity data

Satellite-derived gravity data published by Sandwell et al. (2014) allowed to interpret ESCs that are offset by a series of curvilinear fracture zones (FZ; Fig.s 2c and 3). The interpreted ESCs, crossed by the GUMBO experiment, show overall decreases in seismic velocity with respect to adjacent oceanic crust (Fig. 6c, d). These velocity decreases likely correspond to decreases in density for the rocks composing the ESCs, leading to apparent negative gravity anomalies, so the ESC/FZs can be mapped in the gravity field (Fig. 3). The FZs form concentric arcs of circles, from which the pole(s) of rotation for ocean-spreading in the GoM can be derived (different published poles are shown in Fig. 3a). Multiple interpretations of ESCs and associated FZs have been published since Sandwell et al. (2014) became available (Christeson et al., 2014; Nguyen and Mann, 2016; Pindell et al., 2016; Lundin and Doré, 2017; Minguez et al., 2020), demonstrating some variations in detail despite being based on the same gravity data (Fig. 3b). The location of ESCs and OCB/LOC's in the eastern GoM reveals an apparent asymmetry of the basin, as the width of interpreted oceanic crust in some models north of the interpreted ESC is much wider than to the south; this observation led to the hypothesis of asymmetrical basin opening proposed by Hudec et al. (2013). Filina et al. (2020) have instead proposed a ridge propagation in the eastern part of the basin that explains the observed asymmetry. Alternatively, Minguez et al. (2020) have explained the observed asymmetry with an episode of mantle exhumation in the northeastern part of the basin preceding symmetrical oceanic spreading.

Section B2. Magnetic data

The most complete public domain compilation of digital magnetic anomaly data in the GoM region to date is the USGS open file report published by Bankey et al. (2002), which includes a merged grid of thousands of ground-based observations onshore, and dozens of marine track-line datasets offshore. This synthesis extends across international borders, offering one of the few quantitative public domain data sets for both Mexico and the U.S. Onshore, the quality of the data merge is excellent, and the results have been interpreted in terms of both continental structure and as a guide to plate reconstructions (e.g., Mickus et al., 2009; Lundin and Doré, 2017). Offshore, both the quality of the data processing and the data density, are reduced. Still, the anomalies

have been used to aid interpretations of crustal type, locations of oceanic crustal boundaries, spreading centers, and as kinematic markers for plate reconstructions (Imbert and Post, 2005; Eddy et al., 2014; Liu et al., 2019; Minguez et al., 2020).

One of the downsides of the existing offshore data merge is the significant along-line corrugation of the anomaly data. As a result, individual ship tracks can be observed in the anomaly grid centered on various ports and radiating throughout the GoM. Recently, Minguez et al. (2020) have re-levelled the offshore portion to provide a decorrugated grid useful for single-profile extractions, 2D and 3D modelling, and plate kinematic analysis. Unfortunately, the quality of the public domain magnetic data is not adequate to observe magnetic chrons in the central GoM, where oceanic crust is sure to exist (see Appendix A), due to both spatial resolution and water depth, as well as thick sedimentary overburden. Modern magnetic survey technologies (i.e., near-bottom surveys) might have the ability to map these critical anomalies, which we discuss in section 8. Fig. 8b shows the reduced to pole magnetic field for the GoM combined from two sources Bankey et al. (2002) offshore and Minguez et al. (2020) offshore. There are a few significant anomalies that have been studied and discussed in the literature, namely the Gulf Coast Magnetic Anomaly (GCMA) that comprises the Houston Magnetic Anomaly (HMA) and the Florida Magnetic Anomaly (FMA), the Yucatan magnetic anomaly (YMA), the "En Echelon Anomalies" EEA, and the Extinct Spreading Ridge Anomalies (ESRA). With the exception of the ESRA, these anomalies have multiple interpretations that illuminate the spectrum of possibilities for the nature of the transition zone between continental and oceanic domains in the GoM.

The GCMA name was coined by Hall (1990) and included the Houston (HMA), Louisiana Magnetic anomaly (LMA) and Florida (FMA) magnetic anomalies (Fig. 8b) that extends further to northeast as the East Coast magnetic anomaly (ECMA). Hall (1990) related them all to remanent mafic to ultra-mafic bodies emplaced along the mega-suture associated with assembly of Pangea. These anomalies are now recognized as different features. The ECMA relates to SDRs associated with the opening of the Central Atlantic (e.g., Talwani et al., 1995), while the FMA has also been interpreted to be related to SDRs by some authors, although alternative interpretation related to the Southern Plateau, a relatively thick block of interpreted extended continental crust between the Apalachicola basin and GoM ocean basin (see location in Fig. 2a) is also proposed (see section 5.2). Mickus et al. (2009) have modeled the HMA as a single intrusive body within continental crust. The Brunswick anomaly to the north of FMA marks a low-angle boundary between two peri-Gondwana terranes (Knapp et al., 2017).

The EEA are a set of segmented magnetic highs outboard of the FMA in the central and eastern GoM (Fig. 8b). These anomalies are present on the U.S. and Mexico sides of the basin and are flanked landward by a distinct magnetic low. Potential continuations of these anomalies exist in the western GoM; however, the data quality is generally lower and there appear to be additional anomalies superimposed with the EEA equivalents, complicating the pattern. Many interpreters use the EEA to constrain the OCB/LOC (e.g., Kneller and Johnson, 2011; Eddy et al., 2014; Liu et al., 2019; Pindell et al., 2020; Filina and Beutel, 2021). Minguez et al. (2020) have proposed that the crust outboard of the EEA is consistent with oceanic crust of Jurassic age, while the EEA are not seafloor spreading anomalies, but instead mark a peridotite ridge, as this anomaly is aligned with a basement step up (Hudec et al., 2013; coincident to region of "uncertain crust" in Fig. 2c). Pindell et al. (2016) also suggest that the EEA may indicate the presence of exhumed mantle. Pindell et al. (2016) and Minguez et al. (2020) show that conjugate EEA anomalies reconstruct to collinear positions prior to the beginning of sea floor spreading, implying some degree of symmetry in the structures formed by breakup of the GoM. Pindell et al. (2020), however, interpret that the region that used to be interpreted as presumed exhumed mantle near EEA (Pindell et al., 2016), is now instead older oceanic crust. More details on these various interpretations are given in section 7.3.

In the center of the GoM ocean basin, a long, segmented, magnetic high, the ESRA, runs from the easternmost to the westernmost extent of interpreted oceanic crust (labeled (7) in Fig. 8b). The high coincides with gravity and basement lows interpreted by most as an ESC. The seismic reflection profile of Eddy et al. (2014) shows that the ESC corresponds to a basement low, while the magnetic anomaly associated with the ESC is a pronounced high. Minguez et al. (2020) provide a 2D forward model that demonstrates that the ESRA could be achieved with a normal polarity Jurassic magneto-chron at an ESC, with an age of ~153.6 Ma (Cron M24n; Gee and Kent, 2007), and a full spreading rate of 2.4 cm/yr. The relatively subdued magnetic anomalies landward of the ESRA are matched by the younger, shorter Jurassic chrons, M23 to M38n.2n (164 Ma), which largely merge at the observation level. In contrast, similar magnetic modeling by Deighton et al. (2017) suggests a much younger age for spreading by modeling chrons M25 (154 Ma) to M3 (128 Ma), illustrating a non-uniqueness of the magnetic chrons interpretations.

Magnetic anomalies observed on the periphery of the GoM may not speak directly to the nature of the crust within the basin; however, they may represent important kinematic constraints on plate reconstructions (anomalies (8) and (9) in Fig. 8b). For example, Lundin and Doré (2017) have used the USGS magnetic anomaly compilation (Bankey et al., 2002) to illustrate that a reconstruction of the HMA and YMA to collinear positions also aligns a pronounced NNE-trending linear magnetic anomaly marking the Appalachian front (Steltenpohl et al., 2013), with a similar linear anomaly crossing Yucatan. More details on magnetic structures as a guide for tectonic reconstructions are provided in section 7.4.

Appendix C. Well data

Section C1. Wells sampling basement and Paleozoic sediments

Only a limited number of wells have penetrated either basement or pre-GoM Paleozoic sediments (Fig. 2b). These wells, located primarily along the rim of the basin, were drilled in the 1950s and 60s (Scott et al., 1961; Ramos, 1975; Ball et al., 1988; Dobson and Buffler, 1991; Woods et al., 1991; MacRae and Watkins, 1995; Coombs et al., 2019; Erlich and Pindell, 2020); the status of cores and logs from these wells is unknown. Erlich and Pindell (2020) provide a digital database of 168 wells drilled in Florida and along the Florida margins, both on the GoM and Atlantic sides, compiled from published industry wells and from scientific drilling (Deep Sea Drilling Project, DSDP), with the lithology description and ages for the deepest rocks for each well. The new age data for sedimentary rocks, as well as for igneous and metamorphic basement samples for three wells from this database, have revealed the presence of multiple terranes. According to these authors, peak igneous activity and accommodation in the region began in the north during the Early Jurassic and ended in the south in the Early–Middle Jurassic, which is consistent with findings of DSDP Leg 77 (Schlager et al., 1984) in the western Florida Straits (Zone 4 in Fig. 1) that penetrated acoustic and economic basement. Two sites – holes 537 and 538A (see location in Fig. 2b) – encountered pre-Mesozoic crystalline phyllitic metasedimentary basement rocks (Dallmeyer, 1984). $^{40}Ar/^{39}Ar$ dating revealed early Paleozoic metamorphism (at ~ 500 Ma), with an earliest Jurassic (~ 200 Ma) later thermal overprint. A diabase dike with an $^{40}Ar/^{39}Ar$ crystallization age of 190.4 ± 3.4 Ma was recovered from the Hole 538A. This intrusive sample showed both positive and negative magnetic polarity and is likely to have been intruded during continental rifting at this location. A total of 18 vintage basement-penetrating wells in Mexico, along the western coastline of the GoM basin, are described in Coombs et al. (2019). Geochronology and geochemistry analyses of basement core samples from these wells reveal three distinct magmatic episodes. The earliest, represented by Early Permian granitoids, is related to a continental arc prior to final assemblage of Pangaea. Granitoids of the second Late Permian–Early Triassic phase are interpreted as representing post-collisional magmatism, while the third

Early–Middle Jurassic phase consists of mafic porphyries that could be related to magmatism associated with the Nazas arc.

Section C2. Wells sampling Triassic - Early Jurassic redbeds

Evidence of Late Triassic to early Jurassic pre-salt sediments is found on both sides of the basin. The presence of a post-Paleozoic, pre-Louann interval has been known in the northern GoM since the 1930's (Weeks, 1938; Scott et al., 1961; Woods and Addington, 1973; Gawloski, 1983; Salvador, 1987, 1991). Lithologies include red bed successions, known as the Eagle Mills Fm (named after a well in southern Arkansas) that have been encountered in a large number of oil and gas and even water wells (Salvador, 1991; Frederick et al., 2020). Most published models explain the Eagle Mills and equivalent redbeds as the earliest syn-rift deposits marking the onset of the GoM rifting, ~237 Ma. A Triassic age has been assigned by the identification of a leaf fossil (Macrotaeniopteris magnifolia) in the Humble #1 Royston in Arkansas (Scott et al., 1961). Later palynological analyses of the fossil algae Coenobium Plaesiodictyon in a Cass County, TX well has suggested a Triassic (Carnian) age for the Eagle Mills (Wood and Benson Jr, 2000). This was confirmed by palynological analyses in the Upshur County TX well Fina LV Ray Gas Unit #1-2 well, as~237 Ma (Snedden and Galloway, 2019). There are mafic lavas and sills in the Eagle Mills, but none have as yet been radiometrically dated.

Recent extensive sampling and a related detrital zircon U-Pb age study of the Eagle Mills from 16 subsurface wells (Frederick et al., 2020) did not tightly constrain the maximum depositional age. This study showed distinct paleo-drainage pathways in three regions across the northern GoM: (1) A western paleodrainage extended from the Central Texas highlands (Llano Uplift, see location in Fig. 2a) to the submarine Potosi Fan on the western margin of Laurentia, with local tributary sources from the East Mexico Arc, Yucatán/Maya, and Marathon-Ouachita provinces of peri-Gondwanan (~700−500 Ma), Appalachian/Ouachita (500−280 Ma), Grenville (1250−950 Ma), and Mid-Continent/Granite-Rhyolite Province (1500−1300 Ma) detrital zircon ages. Isochore and associated geophysical well and seismic data suggest that by Early Jurassic time, this depocenter had shifted into the western GoM as Nazas Arc development continued. (2) A southerly paleo-drainage in the north-central GoM region bifurcated around the Sabine and Monroe uplifted terranes (see location in Fig. 2a) with southwestern flow characterized by peri-Gondwanan detrital zircon ages from late Paleozoic accreted basement and/or successor basins, and southeastern fluvial networks distinguished by traditional North American basement province sources, including Grenville, Mid-Continent, and Yavapai-Mazatzal. (3) An eastern GoM paleo-drainage, with regional southward flow, resulted in almost all pre-salt detrital zircon ages, dominated by local Gondwanan/peri-Gondwanan sources, including the proximal Suwannee terrane and Osceola Granite complex. Eagle Mills sediments in these wells contain few first cycle or syndepositional zircons, suggesting that there was little igneous activity on uplifted rift flanks.

Equivalents to the Eagle Mills are found to the east, west, and south. To the east, the Wood River Formation of the south Florida basin has yielded zircons with a maximum depositional age of 235 to 195 Ma from U-Pb analyses (Wiley, 2017). South Florida basin zircons show an affinity with Gondwana sources (i.e., the Suwannee terrane), indicating proximity to Florida, a pattern that continues into the Oxfordian (163 -157 Ma; Lovell and Weislogel, 2010; Lisi, 2013; Wiley, 2017). North and west of the Ouachita-Marathon orogenic belt, outcrops of the Dockum Group stand in contrast to the entirely subsurface Eagle Mills of Texas. These sediments are thought to have been eroded from a rift flank uplift in Central Texas. To the south, in Mexico, the Triassic to Middle Jurassic record, mainly archived in outcrop intervals, includes the Zacatecas, Nazas, and La Joya formations of Mesa Central and Huizachal Group of the Sierra Madre Oriental (Barboza-Gudiño et al., 2010). An extensive review of this phase is provided by Martini and Ortega-Gutiérrez (2016). Fossil plants from red beds of the Eagle Mills equivalent La Boca Formation (Huizachal Group) in northern Mexico are generally non-age diagnostic, broadly indicating a Late Triassic to Early Jurassic age (Mixon, 1963). However, the Plomosas Formation has more recently been radiometrically dated as Early to Middle Jurassic (Lawton et al., 2018). Further south, the Potosi submarine fan is believed to be connected to the El Alamar paleo-river system whose depositional products are the Huizachal Group, influenced by the tectonics of the East Mexico Permo-Triassic continental arc (Stern and Dickinson, 2010; Frederick et al., 2020). Unfortunately, all of these units are poorly age constrained, given either their non-marine origin or intense tectonic deformation. In Chiapas, Mexico, the La Silla and Todos Santos formations are exposed (Godínez-Urban et al., 2011a, 2011b); these unnamed Triassic-Jurassic(?) red beds were penetrated in several onshore wells in the Yucatan Peninsula (Ramos, 1975). Seismic evidence for pre-salt deposits, presumably including Triassic redbeds, is further discussed in section 5.1.

Section C3. Wells that encountered igneous rocks encased in salt

An interesting relationship between some salt diapirs and igneous activity related to the Mesozoic evolution of GoM has been documented. Lock and Duex (1996) have reported that three salt diapirs from southern Louisiana contain samples of igneous rocks. Stern et al. (2011) studied three samples from two of the domes; they are altered but preserve igneous minerals including strongly zoned clinopyroxene (diopside to Ti-augite) and Cr-rich spinel rimmed with titanite; $^{40}Ar/^{39}Ar$ ages of 158.6 ± 0.2 Ma and 160.1 ± 0.7 Ma for Ti-rich biotite and kaersutite from samples from two different salt domes are interpreted to represent the times that the igneous rocks solidified. Trace element compositions are strongly enriched in incompatible trace elements, indicating that the igneous rocks are low-degree melts of metasomatized upper mantle; isotopic compositions of Nd and Hf indicate derivation from depleted mantle. This information supports the hypothesis that crust beneath southern Louisiana formed as a magma-starved rifted margin on the northern flank of the GoM basin ~160 Ma. These results also confirm that some magnetic highs flanking GoM margin mark accumulations of mafic igneous rocks now buried beneath thick sediments.

Another example of salt diapirs containing xenoliths of Jurassic igneous rocks is reported from the northeastern Mexico (Lawton and Amato, 2017). Crystallization ages of three xenoliths entrained in a salt diapir in the La Popa basin have U-Pb zircon ages from 158 - 154 Ma (Oxfordian–Kimmeridgian). Phaneritic textures, hydrothermal alteration, zircon zonation, and previously published $^{40}Ar/^{39}Ar$ cooling ages from a nearby diapir, which are younger than Upper Jurassic strata overlying the salt, combine to suggest that these samples were intruded into salt and exhumed during diapirism. A porphyritic mafic rock with a U-Pb zircon age of 150 Ma (Tithonian) is interpreted by Lawton and Amato (2017) as a shallow intrusion into salt. Clearly more salt domes should be studied to see if they contain igneous xenoliths and these should be studied using modern petrologic and geochronologic techniques.

Section C4. Wells sampling eolian and dry fluvial sequences potentially deposited during the oceanic spreading phase (Norphlet Fm and equivalents)

The Norphlet Fm (Fig. 4) is a largely non-marine section in the northeastern GoM that is thought to be late Callovian to early Oxfordian in age, (~163 Ma), though this is poorly constrained by the lack of marine fauna and flora (Olson et al., 2015; Snedden and Galloway, 2019). The vast majority of published tectonic models (section 6) acknowledge that this sedimentary sequence was deposited during seafloor spreading. Norphlet Fm sediments were deposited in a vast dryland system, including an aeolian sand sea (aeolian erg), rimmed to the north by the Appalachians, and to the east by the Suwannee Terrane of Florida. This arid depositional system and adjacent sahbka probably transition westward to a marine shelf that was likely bordered to the south by the new GoM oceanic crust. Tidal deposits in a cored interval of the Norphlet equivalent of the northwest GoM (Snedden and Galloway, 2019) confirm that the basin was not entirely subaerial, as earlier suggested by Salvador (1987). Preservation of dune deposits under a distinctive iron-rich dolomitic transgressive horizon between the

Norphlet and overlying sediments of the northeastern basin (Brand, 2016) implies a gradual deepening of the marine seaway from the Atlantic during the Oxfordian. Evolution of GoM seawater from hypersalinity, associated with Louann Salt deposition, to normal marine conditions associated with platform margin reefs of the Kimmeridgian – Tithonian Stages (Haynesville-Buckner to Cotton Valley-Bossier Supersequences, Snedden and Galloway, 2019; Fig. 4) indicates an open connection through or near the modern Florida Straits as sea floor spreading continued. However, there is no consensus on a Tethyan (Atlantic) source for Louann seawater, as a Pacific marine connection as also been proposed (e.g., Martini et al., 2016a, 2016b vs. Padilla Sánchez, 2016).

Lovell (2010) has studied U-Pb detrital zircon geochronology and thin section petrology of core samples taken from onshore and offshore Alabama. Previous research of the Norphlet Fm in onshore Alabama suggests that these northern sediments originated from metamorphic rocks of the Talladega slate belt and Appalachian Piedmont province, while southern sediments were of primarily igneous origin. Detrital zircons from twelve Norphlet core and cutting samples yield major U-Pb age populations between 500-300, 650-500, 1,900-950, and 3,000-2,500 Ma. These correspond with known ages of source terranes in the Appalachian Mountains and foreland basin, including plutonic, metasedimentary and metavolcanic rocks. In contrast, age populations of 580-540, 625-600, and 2,200-2,000 Ma zircons indicate Gondwanan (Suwannee Terrane) sources for southern wells.

Smaller, dryland systems similar to those characterizing Norphlet facies are exposed in tectonically transported GoM sediments exposed in western Cuba (San Cayetano Fm; Haczewski, 1976), the only place where Norphlet-like sequences are exposed. These siliciclastic sediments were studied by Rojas-Agramonte et al. (2008), who interpreted them to reflect syn-rift sedimentation coeval with the breakup of Pangaea. U-Pb SHRIMP dating of detrital zircon grains from two samples of San Cayetano micaceous sandstone have provided concordant ages ranging from 2479 to 398 Ma, though the limited number of zircons (n = 19) limits statistical significance. The oldest zircon population is of Paleoproterozoic age (2479-1735 Ma), but most zircons have early Mesoproterozoic and Grenvillian ages (1556-985 Ma), whereas still younger ages are Pan-African (561 Ma), Ordovician (451 Ma) and Early Devonian (398 Ma). Rojas-Agramonte et al. (2008) argue that the most likely source terranes are Precambrian and Early Paleozoic massifs in northern South America (Colombia and/or Venezuela) and Yucatan. Paleo-wind directions measured by Haczewski (1976), when corrected for tectonic rotation, suggest transport from the Mayan (Yucatan) block, at least partially confirmed by the Pan-African ages of the detrital zircons.

Siliciclastic strata of Oxfordian age occur beneath the northern Yucatan shelf, where they are known as the Bacab Sandstone (Snedden et al., 2020). Sedimentary characteristics described from cores show that the Bacab Sandstone is comparable to the Norphlet Fm, including similar depositional processes and paleoclimate regimes, with aeolian dunes reflecting strong winds, significant sediment supply and arid climate. Detrital zircons in the sandstone are consistent with source terranes of Gondwanan crust of Yucatan (Snedden et al., 2020), suggesting wind and ephemeral stream transport from the north and east. However, U-Pb zircon age spectra are dissimilar to those documented for the Norphlet (Weislogel et al., 2015), suggesting that the Bacab was not contiguous with the Norphlet dryland system.

Most tectonic models propose that seafloor spreading occurred in the GoM during deposition of these Oxfordian sediments (Norphlet, San Cayetano, and Bacab strata), implying interesting facies changes between these environments and the basin center near the spreading axis. These Oxfordian non-marine to marginal marine siliciclastic sediments represent key constraints for seismic stratigraphy tied to well control in the northern part of the GoM (Snedden et al., 2014). While we do not know exactly how far into the U.S. sector of the GoM basin the Norphlet dryland facies exist, new industry drilling continues to advance into the basin center and will ultimately provide more answers.

Appendix D. Recent lithospheric earthquakes, potentially indicative of reactivation of old tectonic structures

The GoM is considered to have been tectonically quiescent, at least on a plate tectonics scale, since the Cretaceous. However, USGS earthquake records show that a number of seismic events with focal depths within the lithosphere continue to occur in the basin (shown with stars in Fig. 3a). Some authors have discussed the possibility that some of these earthquakes could trigger landslides and related tsunami (Ten Brink et al., 2009), although none are known to have occurred. A magnitude 5.9 earthquake in the northeastern part of the basin was recorded in 2006 (Fig. 3a), interpreted by the USGS as a mid-plate event, located away from active tectonic boundaries. That event is also far away from salt structures. Angell and Hitchcock (2007) have argued that this event was associated with possible motion along hypothesized NW-SE oriented transfer faults crossing the basin. Conversely, Gangopadhyay and Sen (2008) and Franco et al. (2013) attribute this earthquake to distal salt tectonics, although both have stated that a lithospheric origin of this earthquake cannot be ruled out. Another sizable earthquake (M 4.9, with the focal depth 33 km - an automatic value assigned by USGS when the depth uncertainty is high) was recorded in 1978; this event is described by Frohlich (1982) as a lithospheric event, with a similar focal mechanism to the 2006 event (i.e., reverse fault striking NW-SE, Fig. 3a). Although this fault plane solution aligns with the orientation of ESCs mapped from gravity, the earthquake epicenter was located ~ 60 km north of the nearest ESC (Fig. 3b). None of the tectonic models we have documented use these "lithospheric" earthquakes as a constraint. Filina et al. (2020) have tied these events with two distinct oceanic zones in the eastern GoM mapped by the GUMBO experiment, thereby proposing two distinct episodes of spreading – an initial, ultra-slow one in the Late Jurassic, with an estimated full spreading rate of 0.9 cm/yr producing thin and uniform oceanic crust imaged by line GUMBO4 (Fig. 6d), and an Early Cretaceous one with a full spreading rate of ~1.1 cm/yr that produced thicker crust with characteristic two-layered structure as documented by GUMBO3 (Fig. 6c). An interpreted ridge reorganization responsible for the change in the spreading regimes occurred ~150 Ma (consistent with Pindell et al., 2016). The boundary between the two oceanic zones, referred to as a pseudofault in Filina et al. (2020), is marked by a change in crustal thickness (such as the one imaged in Fig. 7) that is further aligned with the lithospheric earthquakes mentioned above and, thus, represents a zone of weakness that appears to have been reactivated under current compressional stress (Snee and Zoback, 2020).

Appendix E. Paleomagnetic studies

Paleomagnetic studies have been conducted in the GoM to investigate two major tectonic questions: 1) the Mojave-Sonora megashear hypothesis, and 2) timing and magnitude of rotation of the Maya Block (Yucatan Peninsula). The Mojave-Sonora megashear hypothesis is a proposed zone of strike slip along which much of central Mexico was translated (going backward in time) towards the Pacific Ocean to avoid overlaps in early Pangea reconstructions (Anderson and Schmidt, 1983). Early paleomagnetic tests compared the groupings of paleomagnetic poles from Triassic and Jurassic rocks on either side of the proposed shear, before and after the ~800 km of proposed displacement (Cohen et al., 1986). Later study of rocks from the Caborca Block in Mexico (Molina-Garza and Geissman, 1999) have demonstrated that the region proposed to be transported along the megashear has inclinations that are inconsistent with the proposed transport distance, but that they had been rotated sometime before the Cretaceous by 12 to 50°. Although a decisive study regarding the Mojave-Sonora megashear has not yet come forth, additional studies from structural and petrological disciplines appear to be converging on the understanding that the megashear did not play a major role in tectonic history of the GoM (Amato et al., 2009). Nevertheless, understanding of how to fit Mexico into a Pangaea

reconstruction remains one of the major outstanding puzzles in models of tectonic evolution of the region.

Prior to observation of the extinct ridges in satellite gravity data (Sandwell et al., 2014), paleomagnetic data provided some key constraints on the rotation of the Yucatan Peninsula (Maya Block) during basin opening, as well as some constraints on timing of rotation. A key study was that of Molina-Garza et al. (1992), who recovered igneous and sedimentary rocks spanning the history of GoM opening, from Late Permian intrusions, Late Triassic - Jurassic redbeds (Todos Santos FM), and Middle - Late Jurassic dikes. Paleomagnetic vectors from these rocks suggest a total clockwise rotation of the Yucatan Peninsula of ~75°, which ceased by the Oxfordian. New sampling of the Todos Santos FM and Jurassic dikes (Godínez-Urban et al., 2011a, 2011b) has confirmed the regional results and refined the amount of rotation occurring since the earliest Jurassic to ~45°. However, the latest analysis of Molina-Garza et al. (2020), performed on the Eocene El Bosque Fm in central Chiapas, indicates another ~20° of clockwise rotation that affected the massif's lithosphere, which is interpreted to be related to the subducting Cocos Plate. Various tectonic models use different paleomagnetic analyses to constrain Yucatan rotation. Lundin and Doré (2017) refer to the Yucatan rotation angle of 78±11° of Molina-Garza et al. (1992), while Pindell et al. (2016, 2020) and Nguyen and Mann (2016) use ~40° rotation, based on analysis of Godínez-Urban et al., 2011a, 2011b (see Figs. 9 and 11).

References

Adatte, T., Stinnesbeck, W., Keller, G., 1996. Lithostratigraphic and mineralogic correlations of near K/T boundary clastic sediments in northeastern Mexico: implications for origin and nature of deposition. Geol. Soc. Am. Spec. Pap. 307, 211–226.

Alvey, A., Kusznir, N.J., Roberts, A., 2018. Regional crustal structure of the Gulf of Mexico from gravity inversion. In: AAPG Annual Convention and Exhibition.

Amato, J.M., Lawton, T.F., Mauel, D.J., Leggett, W.J., González-León, C.M., Farmer, G.L., Wooden, J.L., 2009. Testing the Mojave-Sonora megashear hypothesis: evidence from paleoproterozoic igneous rocks and deformed Mesozoic strata in Sonora. Mexico. Geol. 37 (1), 75–78.

Anderson, E.G., 1979. Basic Mesozoic study in Louisiana: The northern coastal region and the Gulf Basin province. Louisiana Geological Series Folio Series 3, 58 p.

Anderson, T.H., Schmidt, V.A., 1983. The evolution of Middle America and the Gulf of Mexico–Caribbean Sea region during Mesozoic time. Geol. Soc. Am. Bull. 94 (8), 941–966.

Angell, M., Hitchcock, C., 2007. A geohazard perspective of recent seismic activity in the Northern Gulf of Mexico. In: Offshore Technology Conference. Offshore Technology Conference.

Angstadt, D.M., Austin Jr., J.A., Buffler, R.T., 1985. Early late cretaceous to holocene seismic stratigraphy and geologic history of southeastern Gulf of Mexico. AAPG Bull. 69 (6), 977–995.

Antoine, J., Ewing, J., 1963. Seismic refraction measurements on the margins of the Gulf of Mexico. J. Geophys. Res. 68 (7), 1975–1996.

Austin Jr., J.A., Uchupi, E., 1982. The continental-oceanic crustal transition off southwest Africa. AAPG Bull. 66, 1328–1347.

Austin Jr., J.A., Stoffa, P.L., Phillips, J.D., Oh, J., Sawyer, D.S., Purdy, G.M., Reiter, E., Makris, J., 1990. Crustal structure of the Southeast Georgia embayment-Carolina trough: Preliminary results of a composite seismic image of a continental suture(?) and a volcanic passive margin. Geology 18, 1023–1027.

Ball, M.M., Martin, R.G., Foote, R.Q., Applegate, A.V., 1988. Structure and stratigraphy of the western Florida shelf. In: Part I, Multichannel reflection seismic data (No. 88-439). US Geological Survey.

Bankey, V., Cuevas, A., Daniels, D., Finn, C.A., Hernandez, I., Hill, P., Kucks, R., Miles, W., Pilkington, M., Roberts, C. and Roest, W., 2002. Digital data grids for the magnetic anomaly map of North America (No. 2002-414).

Barboza-Gudiño, J.R., Zavala-Monsiváis, A., Venegas-Rodríguez, G., Barajas-Nigoche, L. D., 2010. Late Triassic stratigraphy and facies from northeastern Mexico: Tectonic setting and provenance. Geosphere 6 (5), 621–640.

Bird, D.E., Burke, K., Hall, S.A., Casey, J.F., 2005. Gulf of Mexico tectonic history: Hotspot tracks, crustal boundaries, and early salt distribution. AAPG Bull. 89 (3), 311–328.

Blount, G., Millings, M., 2011. Reconnaissance Assessment of CO2 Sequestration Potential In the Triassic Age Rift Basin Trend of South Carolina, Georgian and Northern Florida (No. SRNL-STI-2011-492).

Boillot, G., Recq, M., Winterer, E.L., Meyer, A.W., Applegate, J., Baltuck, M., Bergen, J. A., Comas, M.C., Davies, T.A., Dunham, K., Evans, C.A., 1987. Tectonic denudation of the upper mantle along passive margins: a model based on drilling results (ODP leg 103, western Galicia margin, Spain). Tectonophysics 132 (4), 335–342.

Boyden, J.A., Müller, R.D., Gurnis, M., Torsvik, T.H., Clark, J.A., Turner, M., Ivey-Law, H., Watson, R.J., Cannon, J.S., 2011. Next-Generation Plate-Tectonic Reconstructions using GPlates.

Brand, J.H., 2016. Stratigraphy and mineralogy of the Oxfordian Lower Smackover Formation in the eastern Gulf of Mexico. In: Mesozoic of the Gulf Rim and Beyond: New Progress in Science and Exploration of the Gulf of Mexico Basin. 35th Annual Gulf Coast section SEPM Foundation Perkins-Rosen Research Conference, GCSSEPM Foundation, Houston, TX, USA, Vol. 14, p. 35.

Buffler, R.T., Sawyer, D.S., 1985. Distribution of Crust and Early History. Gulf of Mexico basin.

Byerly, G.R., 1991. Igneous activity. The Gulf of Mexico basin: Boulder, Colorado, Geological Society of America. Geol. North America 108–191.

Cadenas, P., Manatschal, G., Fernández-Viejo, G., 2020. Unravelling the architecture and evolution of the inverted multi-stage North Iberian-Bay of Biscay rift. Gondwana Res. 88, 67–87.

Centeno-García, E., 2017. Mesozoic tectono-magmatic evolution of Mexico: an overview. Ore Geol. Rev. 81, 1035–1052.

Chian, D., Louden, K.E., Minshull, T.A., Whitmarsh, R.B., 1999. Deep structure of the ocean-continent transition in the southern Iberia Abyssal Plain from seismic refraction profiles: Ocean Drilling Program (Legs 149 and 173) transect. J. Geophys. Res. Solid Earth 104 (B4), 7443–7462.

Christensen, N.I., Mooney, W.D., 1995. Seismic velocity structure and composition of the continental crust: A global view. J. Geophys. Res. Solid Earth 100 (B6), 9761–9788.

Christeson, G.L., Nakamura, Y., Buffler, R.T., Morgan, J., Warner, M., 2001. Deep crustal structure of the Chicxulub impact crater. J. Geophys. Res. Solid Earth 106 (B10), 21751–21769.

Christeson, G.L., Van Avendonk, H.J.A., Norton, I.O., Snedden, J.W., Eddy, D.R., Karner, G.D., Johnson, C.A., 2014. Deep crustal structure in the eastern Gulf of Mexico. J. Geophys. Res. Solid Earth 119 (9), 6782–6801.

Cohen, K.K., Anderson, T.H., Schmidt, V.A., 1986. A paleomagnetic test of the proposed Mojave-Sonora megashear in northwestern Mexico. Tectonophysics 131 (1–2), 23–51.

Coombs, H., Kerr, A., Pindell, J., Buchs, D., Weber, B., Solari, L., 2019. Petrogenesis of the crystalline basement along the western Gulf of Mexico: Postcollisional magmatism during the formation of Pangea. In: Southern and Central Mexico: Basement Framework, Tectonic Evolution, and Provenance of Mesozoic-Cenozoic basins. GSA Special Paper.

Cornen, G., Girardeau, J., Monnier, C., 1999. Basalts, underplated gabbros and pyroxenites record the rifting process of the West Iberian margin. Mineral. Petrol. 67 (3-4), 111–142.

Cram Jr., I.H., 1961. A crustal structure refraction survey in south Texas. Geophysics 26 (5), 560–573.

Culotta, R., Latham, T., Sydow, M., Oliver, J., Brown, L., Kaufman, S., 1992. Deep structure of the Texas Gulf passive margin and its Ouachita-Precambrian basement: Results of the COCORP San Marcos arch survey. AAPG Bull. 76 (2), 270–283.

Curry, M.A., Peel, F.J., Hudec, M.R., Norton, I.O., 2018. Extensional models for the development of passive-margin salt basins, with application to the Gulf of Mexico. Basin Res. 30 (6), 1180–1199.

Dallmeyer, R.D., 1984. 16. 40Ar/39Ar Ages From A Pre-Mesozoic Crystalline Basement Penetrated At Holes 537 AND 538A OF The Deep Sea Drilling Project Leg 77, Southeastern Gulf Of Mexico: Tectonic Implications1.

Davison, I., Anderson, L., Nuttall, P., 2012. Salt deposition, loading and gravity drainage in the Campos and Santos salt basins. Geol. Soc. Lond., Spec. Publ. 363 (1), 159–174.

Davy, R.G., Minshull, T.A., Bayrakci, G., Bull, J.M., Klaeschen, D., Papenberg, C., Reston, T.J., Sawyer, D.S., Zelt, C.A., 2016. Continental hyperextension, mantle exhumation, and thin oceanic crust at the continent-ocean transition, West Iberia: New insights from wide-angle seismic. J. Geophys. Res. Solid Earth 121 (5), 3177–3199.

Dean, S.M., Minshull, T.A., Whitmarsh, R.B., Louden, K.E., 2000. Deep structure of the ocean-continent transition in the southern Iberia Abyssal Plain from seismic refraction profiles: The IAM-9 transect at 40 20′ N. J. Geophys. Res. Solid Earth 105 (B3), 5859–5885.

Deighton, I.C., Winter, F., Chisari, D., 2017. Recent high-resolution seismic, magnetic and gravity data throws new light on the early development of the Gulf of Mexico. In: AAPG Annual Meeting Abstracts, Houston.

Dias, J.L., 2005. Tectônica, estratigrafia e sedimentação no Andar Aptiano da margem leste brasileira. Boletim de Geociências da PETROBRAS 13 (1), 7–25.

Dickinson, W.R., Lawton, T.F., 2001. Tectonic setting and sandstone petrofacies of the Bisbee basin (USA–Mexico). J. S. Am. Earth Sci. 14 (5), 475–504.

Dickinson, W.R., Gehrels, G.E., Stern, R.J., 2010. Late Triassic Texas uplift preceding Jurassic opening of the Gulf of Mexico: Evidence from U-Pb ages of detrital zircons. Geosphere 6 (5), 641–662.

Dobson, L.M., Buffler, R.T., 1991. Basement rocks and structure, northeast Gulf of Mexico.

Doré, T., Lundin, E., 2015. Research focus: hyperextended continental margins—knowns and unknowns. Geology 43 (1), 95–96.

Dorman, J., Worzel, J.L., Leyden, R., Crook, T.N., Hatziemmanuel, M., 1972. Crustal section from seismic refraction measurements near Victoria, Texas. Geophysics 37 (2), 325–336.

Eagles, G., Pérez-Díaz, L., Scarselli, N., 2015. Getting over continent ocean boundaries. Earth Sci. Rev. 151, 244–265.

Ebeniro, J.O., O'Brien, W.P., Shaub, F.J., 1986. Crustal structure of the South Florida Platform, eastern Gulf of Mexico: An ocean-bottom seismograph refraction study. Mar. Geophys. Res. 8 (4), 363–382.

Ebeniro, J.O., Nakamura, Y., Sawyer, D.S., O'Brien Jr., W.P., 1988. Sedimentary and crustal structure of the northwestern Gulf of Mexico. J. Geophys. Res. Solid Earth 93 (B8), 9075–9092.

Eddy, D.R., Van Avendonk, H.J., Christeson, G.L., Norton, I.O., Karner, G.D., Johnson, C. A., Snedden, J.W., 2014. Deep crustal structure of the northeastern Gulf of Mexico:

implications for rift evolution and seafloor spreading. J. Geophys. Res. Solid Earth 119 (9), 6802–6822.
Eddy, D.R., Van Avendonk, H.J., Christeson, G.L., Norton, I.O., 2018. Structure and origin of the rifted margin of the northern Gulf of Mexico. Geosphere 14 (4), 1804–1817.
Eldholm, O., Faleide, J.I., Myhre, A.M., 1987. Continent-ocean transition at the western Barents Sea/Svalbard continental margin. Geology 15 (12), 1118–1122.
Eldholm, O., Thiede, J., Taylor, E., 1989. Evolution of the Vøring volcanic margin. Proc. ODP Sci. Results 1033–1065.
Emiliani, C., 1965. Precipitous continental slopes and considerations on the transitional crust. Science 147 (3654), 145–148.
Erlich, R.N., Pindell, J., 2020. Crustal Origin of the West Florida Terrane, and Detrital Zircon Provenance and Development of Accommodation during Initial Rifting of the Southeastern Gulf of Mexico and western Bahamas. Geological Society, London, Special Publications, p. 504.
Escalona, A., Norton, I.O., Lawver, L.A., Gahagan, L., 2021. Quantitative plate tectonic reconstructions of the Caribbean region from Jurassic to present, in C. Bartolini, ed., Eastern Caribbean–northeastern South American boundary: Tectonic evolution, basin architecture, and petroleum systems. AAPG Mem. 123.
Evain, M., Afilhado, A., Rigoti, C., Loureiro, A., Alves, D., Klingelhoefer, F., Schnurle, P., Feld, A., Fuck, R., Soares, J., De Lima, M.V., 2015. Deep structure of the Santos Basin-São Paulo Plateau System, SE Brazil. J. Geophys. Res. Solid Earth 120 (8), 5401–5431.
Ewing, T.E., 2009. The Ups and Downs of the Sabine Uplift and the Northern Gulf of Mexico Basin: Jurassic Basement Blocks, Cretaceous Thermal Uplifts, and Cenozoic Flexure.
Ewing, T.E., 2018. The Peripheral Graben System in Texas: An Overview.
Ewing, J., Antoine, J., Ewing, M., 1960. Geophysical measurements in the western Caribbean Sea and in the Gulf of Mexico. J. Geophys. Res. 65 (12), 4087–4126.
Fiduk, J.C., Weimer, P., Trudgill, B.D., Rowan, M.G., Gale, P.E., Phair, R.L., Korn, B.E., Roberts, G.R., Gafford, W.T., Lowe, R.S., Queffelec, T.A., 1999. The Perdido fold belt, northwestern deep Gulf of Mexico, part 2: seismic stratigraphy and petroleum systems. AAPG Bull. 83 (4), 578–612.
Filina, I., 2019. Crustal architecture of the northwestern and central Gulf of Mexico from integrated geophysical analysis. Interpretation 7 (4), T899–T910.
Filina, I., Beutel, E., 2021. Geological and geophysical constraints guide new tectonic reconstruction of the Gulf of Mexico. In: Çemen, I., Catlos, E. (Eds.), "Tectonic Processes: a Global View", Volume I. Extensional Tectonics: Continental Breakup to Formation of Oceanic Basins. John Wiley & Sons Inc, Hoboken, NJ, USA.
Filina, I., Hartford, L., 2021. Subsurface structures along western Yucatan from integrated geophysical analysis. Mar. Pet. Geol. 127, 104964.
Filina, I., Delebo, N., Mohapatra, G., Coble, C., Harris, G., Layman, J., Strickler, M., Blangy, J.P., 2015. Integration of seismic and gravity data—A case study from the western Gulf of Mexico. Interpretation 3 (4). SAC99-SAC106.
Filina, I., Liu, M., Beutel, E., 2020. Evidence of ridge propagation in the eastern Gulf of Mexico from integrated analysis of potential fields and seismic data. Tectonophysics 775, 228307.
Foulger, G.R., 2002. Plumes, or plate tectonic processes? Astron. Geophys. 43 (6), 6–19.
Franco, S.I., Canet, C., Iglesias, A., Valdés-González, C., 2013. Seismic activity in the Gulf of Mexico. A preliminary analysis. Boletín de la Sociedad Geologíca Mexicana 65 (3), 447–455.
Franke, D., 2013. Rifting, lithosphere breakup and volcanism: Comparison of magma-poor and volcanic rifted margins. Mar. Pet. Geol. 43, 63–87.
Franke, D., Neben, S., Ladage, S., Schreckenberger, B., Hinz, K., 2007. Margin segmentation and volcano-tectonic architecture along the volcanic margin off Argentina/Uruguay, South Atlantic. Mar. Geol. 244 (1-4), 46–67.
Frederick, B.C., Blum, M.D., Snedden, J.W., Fillon, R.H., 2020. Early Mesozoic synrift Eagle Mills Formation and coeval siliciclastic sources, sinks, and sediment routing, northern Gulf of Mexico basin. Geol. Soc. Am. Bull. 131 (11–12), 2631–2650.
Frohlich, C., 1982. Seismicity of the central Gulf of Mexico. Geology 10 (2), 103–106.
Funck, T., Jackson, H.R., Louden, K.E., Dehler, S.A., Wu, Y., 2004. Crustal structure of the northern Nova Scotia rifted continental margin (eastern Canada). J. Geophys. Res. Solid Earth 109 (B9).
Funck, T., Geissler, W.H., Kimbell, G.S., Gradmann, S., Erlendsson, Ö., McDermott, K., Petersen, U.K., 2017. Moho and basement depth in the NE Atlantic Ocean based on seismic refraction data and receiver functions. Geol. Soc. Lond., Spec. Publ. 447 (1), 207–231.
Gallahue, M., Stein, S., Stein, C.A., Jurdy, D., Barklage, M., Rooney, T., 2020. A compilation of igneous rock volumes at volcanic passive continental margins from interpreted seismic profiles. Mar. Pet. Geol. 122, 104635 https://doi.org/10.1016/j.marpetgeo.2020.104635.
Galloway, W.E., 2008. Depositional evolution of the Gulf of Mexico sedimentary basin, in A. D. In: Miall, Sedimentary Basins of the World, 5. Elsevier Science, pp. 505–549.
Gangopadhyay, A., Sen, M.K., 2008. A possible mechanism for the spatial distribution of seismicity in northern Gulf of Mexico. Geophys. J. Int. 175 (3), 1141–1153.
Gawloski, T., 1983. Stratigraphy and Environmental Significance of Continental Triassic Rock of Texas. AAPG Bull. 67 (3), 469.
Gee, J.S., Kent, D.V., 2007. Source of Oceanic Magnetic Anomalies and the Geomagnetic Polarity Time Scale.
Geoffroy, L., Burov, E.B., Werner, P., 2015. Volcanic passive margins: another way to break up continents. Sci. Rep. 5 (1), 1–12.
Godínez-Urban, A., Lawton, T.F., Molina-Garza, R.S., Iriondo, A., Weber, B., López-Martínez, M., 2011a. Jurassic volcanic and sedimentary rocks of the La Silla and Todos Santos Formations, Chiapas: Record of Nazas arc magmatism and rift-basin formation prior to opening of the Gulf of Mexico. Geosphere 7 (1), 121–144.
Godínez-Urban, A., Molina-Garza, R.S., Geissman, J.W., Wawrzyniec, T., 2011b. Paleomagnetism of the Todos Santos and La Silla Formations, Chiapas: implications for the opening of the Gulf of Mexico. Geosphere 7 (1), 145–158.
Godo, T., 2017. The Appomattox Field: Norphlet aeolian Sand Dune Reservoirs in the Deep-Water Gulf of Mexico.
Goldhammer, R.K., Johnson, C.A., 1999. Mesozoic sequence stratigraphy and paleogeographic evolution of northeast Mexico. Special Papers Geol. Soc. Am. 1–58.
Goldhammer, R.K., Johnson, C.A., 2001. Middle Jurassic-Upper Cretaceous paleogeographic evolution and sequence-stratigraphic framework of the northwest Gulf of Mexico rim. Memoirs-Am. Associat. Petrol. Geol. 45–82.
Haczewski, G., 1976. Sedimentological reconnaissance of the San Cayetano Formation: an accumulative continental margin in the Jurassic of western Cuba. Acta Geol. Pol. 26 (2), 331–353.
Hales, A.L., Helsley, C.E., Nation, J.B., 1970. Crustal structure study on Gulf Coast of Texas. AAPG Bull. 54 (11), 2040–2057.
Hall, D.J., 1990. Gulf Coast-East Coast magnetic anomaly I: Root of the main, crustal decollement for the Appalachian-Ouachita orogen. Geology 18 (9), 862–865.
Hall, S.A., Najmuddin, I.J., 1994. Constraints on the tectonic development of the eastern Gulf of Mexico provided by magnetic anomaly data. J. Geophys. Res. Solid Earth 99 (B4), 7161–7175.
Heatherington, A.L., Mueller, P.A., 1991. Geochemical evidence for Triassic rifting in southwestern Florida. Tectonophysics 188 (3-4), 291–302.
Hinz, K., 1981. A hypothesis on terrestrial catastrophes: Wedges of very thick oceanward dipping layers beneath passive margins. Geologisches Jahrbuch, ser. E 22, 5–28.
Holbrook, W.S., Purdy, G.M., Sheridan, R.E., Glover III, L., Talwani, M., Ewing, J., Hutchinson, D., 1994. Seismic structure of the US Mid-Atlantic continental margin. J. Geophys. Res. Solid Earth 99 (B9), 17871–17891.
Horn, B.W., Goswami, A., Haire, B.R., McGrail, A., Pindell, J., 2016. Regional Interpretation Across the Entire Gulf of Mexico Basin–A New Perspective.
Horn, B., Hartwig, A., Faw, J., Novianti, I., Goswami, A., McGrail, A., 2017. Refining exploration opportunities in Mexico. GEOExPro 14, 64–69.
Hudec, M.R., Norton, I.O., 2019. Upper Jurassic structure and evolution of the Yucatán and Campeche subbasins, southern Gulf of Mexico. AAPG Bull. 103 (5), 1133–1151.
Hudec, M.R., Norton, I.O., Jackson, M.P., Peel, F.J., 2013. Jurassic evolution of the Gulf of Mexico salt basin. AAPG Bull. 97 (10), 1683–1710.
Hudec, M.R., Dooley, T.P., Peel, F.J., Soto, J.I., 2020. Controls on the evolution of passive-margin salt basins: structure and evolution of the Salina del Bravo region, northeastern Mexico. Bulletin 132 (5-6), 997–1012.
Ibrahim, A.B.K., Uchupi, E., 1982. Continental Oceanic Crustal Transition in the Gulf Coast Geosyncline: Rifted Margins: Field Investigations of Margin Structure and Stratigraphy.
Huerta, A.D., Harry, D.L., 2012. Wilson cycles, tectonic inheritance, and rifting of the North American Gulf of Mexico continental margin. Geopsphere 8 (2), 374–385.
Ibrahim, A.K., Carye, J., Latham, G., Buffler, R.T., 1981. Crustal structure in Gulf of Mexico from OBS refraction and multichannel reflection data. AAPG Bull. 65 (7), 1207–1229.
Imbert, P., Post, P.J., 2005. December. The Mesozoic opening of the Gulf of Mexico: Part 1, Evidence for oceanic accretion during and after salt deposition. In: Transactions of the 25th Annual GCSSEPM Research Conference: Petroleum Systems of Divergent Continental Margins, pp. 1119–1150.
Imbert, P., Philippe, Y., Post, P.J., Rosen, N.C., Olson, D.L., Palmes, S.L., Lyons, K.T., Newton, G.B., 2005. The Mesozoic opening of the Gulf of Mexico: Part 2. Integrating seismic and magnetic data into a general opening model. In: Transactions of the 25th Annual GCSSEPM Research Conference: Petroleum Systems of Divergent Continental Margins. SEPM, Tulsa, Okla, pp. 1151–1189.
Johnson, E.A., Blickwede, J.F., Huston, H.H., Kacewicz, M., 2006. An interpretation of the crustal framework and continent-oceanic boundary in US OCS of the Gulf of Mexico, Based on gravity and refraction data analysis. In: 25th Annual Bob F. Perkins Research Conference: Petroleum Systems of Divergent Continental Margin Basins. GCSSEPM, pp. 1091–1103.
Karner, G.D., Johnson, C.A., Mohn, G., Manatschal, G., 2012. Depositional environments and source distribution across hyperextended rifted margins of the North Atlantic: Insights from the Iberia-Newfoundland margin: Trinity College Dublin. In: Third Central & North Atlantic Conjugate Margin Conference, 22–24, pp. 7–17.
Kelemen, P.B., Holbrook, S.W., 1995. Origin of thick, high-velocity igneous crust along the U.S. East Coast Margin. J. Geophys. Res. v. 100, B7, 10077–10094.
Keller, G.R., Braile, L.W., McMehan, G.A., Thomas, W.A., Harder, S.H., Chang, W.-F., Jardine, W.G., 1989. Paleozoic continent-ocean transition in the Ouachita Mountains imaged from PASSCAL wide-angle seismic reflection- refraction data. Geology 17, 119–122.
Kim, S.D., Nagihara, S., Nakamura, Y., 2000. P-and S-Wave Velocity Structures of the Sigsbee Abyssal Plain of the Gulf of Mexico from Ocean Bottom Seismometer Data.
Klitgord, K.D., Schouten, H., 1986. The western north Atlantic region. The Decade North Am. Geol. 1000, 351–378.
Knapp, J.H., Boote, S., Mueller, P.A., 2017. The Neoproterozoic Osceola Arc and Brunswick Suture Zone: Preserved Continental Collision in the Southeastern US. AGUFM 2017, T14A–04.
Kneller, E.A., Johnson, C.A., 2011. Plate Kinematics of the Gulf of Mexico Based on Integrated Observations From the Central and South Atlantic.
Koopmann, H., Franke, D., Schreckenberger, B., Schulz, H., Hartwig, A., Stollhofen, H., di Primio, R., 2014. Segmentation and volcano-tectonic characteristics along the SW African continental margin, South Atlantic, as derived from multichannel seismic and potential field data. Mar. Pet. Geol. 50, 22–39.
Krijgsman, W., Hilgen, F.J., Raffi, I., Sierro, F.J., Wilson, D.S., 1999. Chronology, causes and progression of the Messinian salinity crisis. Nature 400 (6745), 652–655.

Larsen, H.C., Saunders, A.D., Clift, P.D., 1994. Introduction: Breakup of the southeast Greenland margin and the formation of the Irminger Basin: background and scientific objectives. Proceed. Ocean Drilling Progr. Initial Rep. 152, 5–16.
Laske, G., Masters, G., Ma, Z., Pasyanos, M., 2013, April. Update on CRUST1. 0—A 1-degree global model of Earth's crust. Geophys. Res. Abstr. 15, 2658.
Lavier, L.L., Ball, P.J., Manatschal, G., Heumann, M.J., MacDonald, J., Matt, V.J., Schneider, C., 2019. Controls on the Thermomechanical Evolution of Hyperextended Lithosphere at Magma-Poor Rifted Margins: The Example of Espirito Santo and the Kwanza Basins. Geochem. Geophys. Geosyst. 20 (11), 5148–5176.
Lawton, T.F., Amato, J.M., 2017. U-Pb ages of igneous xenoliths in a salt diapir, La Popa basin: Implications for salt age in onshore Mexico salt basins. Lithosphere 9 (5), 745–758.
Lawton, T.F., Solari, L., Urueña, J.E.R., Terrazas, C.M.T., Juárez-Arriaga, E., 2018. May. Pennsylvanian-Triassic magmatic flux in northern Mexico as indicated by detrital zircon data from Triassic-Lower Cretaceous strata. In: Joint 70th Rocky Mountain Annual section/114th Cordilleran Annual section Meeting-2018. GSA.
Lawton, T.F., Fitz-Diaz, E., Stockli, D.F., 2020. T12. Structural Evolution and Sedimentation along the Western Gulf of Mexico Margin. In: South-Central section-54th Annual Meeting-2020. GSA.
Lillie, R.J., Nelson, K.D., de Voogd, B., Drewer, J.A., Oliver, J.E., Kaufman, S., Brown, L., 1983. Crustal structure of Ouachita Mountains, Arkansas: a model based on integration of COCORP reflection profiles and regional geophysical data. AAPG Bull. 67, 907–931.
Lin, P., Bird, D.E., Mann, P., 2019. Crustal structure of an extinct, late Jurassic-to-earliest Cretaceous spreading center and its adjacent oceanic crust in the eastern Gulf of Mexico. Mar. Geophys. Res. 40 (3), 395–418.
Lisi, A.F., 2013. Provenance of the Upper Jurassic Norphlet and Surrounding Formations from U-Pb Detrital Zircon Geochronology.
Liu, M., Filina, I., Mann, P., 2019. Crustal structure of Mesozoic rifting in the northeastern Gulf of Mexico from integration of seismic and potential fields data. Interpretation 7 (4), T857–T867.
Lock, B.E., Duex, T.W., 1996. Xenolithic inclusions within the salt at Weeks Island, Louisiana, and their significance: Gulf Coast Association of Geological Societies. Transactions 46, 229–234. https://doi.org/10.1306/2DC40B23-0E47-11D7-8643000102C1865D.
Lovell, T., 2010. Detrital zircon U-Pb age Constraints on the Provenance of the Upper Jurassic Norphlet Formation, eastern Gulf of Mexico: Implications for Paleogeography.
Lovell, T.R., Weislogel, A., 2010. Detrital Zircon U-Pb age constraints of the provenance of the upper Jurassic Norphlet Formation, Eastern Gulf of Mexico: implications for paleogeography: Gulf Coast Association of Geological Societies. Transactions 60, 443–460.
Lundin, E.R., Doré, A.G., 2017. The Gulf of Mexico and Canada Basin: genetic siblings on either side of North America. GSA Today 27 (1), 4–11.
Lundin, E.R., Redfield, T.F., Péron-Pinvidic, G., 2014. Rifted continental margins: Geometric influence on crustal architecture and melting. In: Pindell, J., Horn, B., et al. (Eds.), Sedimentary Basins: Origin, Depositional Histories and Petroleum Systems – 33rd Annual Gulf Coast Section SEPM Foundation Bob F. Perkins Research Conference. Gulf Coast Section SEPM(GCSSEPM), Houston, TX, pp. 26–28.
Lundin, E.R., Doré, A.G., Redfield, T.F., 2018. Magmatism and extension rates at rifted margins. Pet. Geosci. 24 (4), 379–392.
MacRae, G., Watkins, J.S., 1995. Early Mesozoic rift stage half graben formation beneath the DeSoto Canyon salt basin, northeastern Gulf of Mexico. J. Geophys. Res. Solid Earth 100 (B9), 17795–17812.
Manatschal, G., Müntener, O., 2009. A type sequence across an ancient magma-poor ocean–continent transition: the example of the western Alpine Tethys ophiolites. Tectonophysics 473 (1-2), 4–19.
Mancini, E.A., Mink, R.M., Bearden, B.L., 1985. Upper Jurassic Norphlet Hydrocarbon Potential Along the Regional Peripheral Fault Trend in Mississippi, Alabama, and the Florinda Panhandle.
Mancini, E.A., Llinas, J.C., Parcell, W.C., Aurell, M., Badenas, B., Leinfelder, R.R., Benson, D.J., 2004. Upper Jurassic thrombolite reservoir play, northeastern Gulf of Mexico. AAPG Bull. 88 (11), 1573–1602.
Martini, M., Ortega-Gutiérrez, F., 2016. Tectono-stratigraphic evolution of eastern Mexico during the break-up of Pangea. Earth Sci. Rev. 183, 38–55. https://doi.org/10.1016/j.earscirev.2016.06.013.
Martini, M., Ramírez-Calderón, M., Solari, L., Villanueva-Amadoz, U., Zepeda-Martínez, M., Ortega-Gutiérrez, F., Elías-Herrera, M., 2016a. Provenance analysis of Jurassic sandstones from the Otlaltepec Basin, southern Mexico: Implications for the reconstruction of Pangea breakup. Geosphere 12 (6), 1842–1864.
Martini, M., Ramírez-Calderón, M., Solari, L., Villanueva-Amadoz, U., Zepeda-Martínez, M., Ortega-Gutiérrez, F., Elías-Herrera, M., 2016b. Provenance analysis of Jurassic sandstones from the Otlaltepec Basin, southern Mexico: Implications for the reconstruction of Pangea breakup. Geosphere 12 (6), 1842–1864.
Marton, G., Buffler, R.T., 1994. Jurassic reconstruction of the Gulf of Mexico Basin. Int. Geol. Rev. 36 (6), 545–586.
Marzano, M.S., Pense, G.M., Andronaco, P., 1988. A comparison of the Jurassic Norphlet Formation in Mary Ann field, Mobile Bay. In: Alabama to Onshore Regional Norphlet Trends.
Marzen, R.E., Shillington, D.J., Lizarralde, D., Knapp, J.H., Heffner, D.M., Davis, J.K., Harder, S.H., 2020. Limited and localized magmatism in the Central Atlantic Magmatic Province. Nat. Commun. 11 (1), 1–8.
Marzoli, A., Renne, P.R., Piccirillo, E.M., Ernesto, M., Bellieni, G., De Min, A., 1999. Extensive 200-million-year-old continental flood basalts of the Central Atlantic Magmatic Province. Science 284 (5414), 616–618.
Marzoli, A., Callegaro, S., Dal Corso, J., Davies, J.H., Chiaradia, M., Youbi, N., Bertrand, H., Reisberg, L., Merle, R., Jourdan, F., 2018. The Central Atlantic magmatic province (CAMP): a review. In: The Late Triassic World. Springer, Cham, pp. 91–125.
McBride, J.H., 1991. Constraints on the structure and tectonic development of the early Mesozoic South Georgia rift, southeastern United States; seismic reflection data processing and interpretation. Tectonics 10 (5), 1065–1083.
McHone, J.G., 2003. Volatile emissions from Central Atlantic Magmatic Province basalts: mass assumptions and environmental consequences. Geophys. Monogr. Am. Geophys. Union 136, 241–254.
Menard, H.W., 1967. Transitional types of crust under small ocean basins. J. Geophys. Res. 72 (12), 3061–3073.
Mickus, K., Stern, R.J., Keller, G.R., Anthony, E.Y., 2009. Potential field evidence for a volcanic rifted margin along the Texas Gulf Coast. Geology 37 (5), 387–390.
Miles, P.R., Verhoef, J., Macnab, R., 1996. Compilation of magnetic anomaly chart west of Iberia. In: Proceedings-Ocean Drilling Program Scientific Results. National Science Foundation, pp. 659–664.
Milliken, J.V., 1988. Late Paleozoic and Early Mesozoic Geologic Evolution of the Arklatex Area. Rice University, Houston. Unpublished MS thesis.
Minguez, D., Gerald Hensel, E., Johnson, E.A., 2020. A fresh look at Gulf of Mexico tectonics: Testing rotations and breakup mechanisms from the perspective of seismically constrained potential-fields modeling and plate kinematics. Interpretation 8 (4), SS31–SS45.
Minshull, T.A., Dean, S.M., Whitmarsh, R.B., 2014. The peridotite ridge province in the southern Iberia Abyssal Plain: Seismic constraints revisited. J. Geophys. Res. Solid Earth 119 (3), 1580–1598.
Miranda-Madrigal, E., Chávez-Cabello, G., 2020. Regional Geological Analysis of the Southern Deep Gulf of Mexico and Northern Yucatán Shelf. Geological Society, London, Special Publications, p. 504.
Miranda-Peralta, L.R., Cardenas-Alvarado, A., Maldonado-Villalon, R., Reyes-Tovar, E., Ruiz-Morales, J., Williams-Rojas, C., 2014. Play hipotetico pre-sal en aguas profundas del Golfo de Mexico: Ingeniería Petrolera, v. 54, pp. 256–266.
Mixon, R.B., 1963. Geology of the Huizachal Redbeds. Sierra Madre Oriental, Mexico.
Mjelde, R., Breivik, A.J., Raum, T., Mittelstaedt, E., Ito, G., Faleide, J.I., 2008. Magmatic and tectonic evolution of the North Atlantic. J. Geol. Soc. 165 (1), 31–42.
Mohn, G., Karner, G.D., Manatschal, G., Johnson, C.A., 2015. Structural and stratigraphic evolution of the Iberia–Newfoundland hyper-extended rifted margin: a quantitative modelling approach. Geol. Soc. Lond., Spec. Publ. 413 (1), 53–89.
Molina-Garza, R.S., Geissman, J.W., 1999. Paleomagnetic data from the caborca terrane, Mexico: implications for cordilleran tectonics and the mojave-sonora megashear hypothesis. Tecto 18 (2), 293–325.
Molina-Garza, R.S., Van Der Voo, R.O.B., Urrutia-Fucugauchi, J., 1992. Paleomagnetism of the Chiapas Massif, southern Mexico: Evidence for rotation of the Maya Block and implications for the opening of the Gulf of Mexico. Geol. Soc. Am. Bull. 104 (9), 1156–1168.
Molina-Garza, R.S., Pindell, J., Cortés, P.C.M., 2020. Slab flattening and tractional coupling drove Neogene clockwise rotation of Chiapas Massif, Mexico: Paleomagnetism of the Eocene El Bosque Formation. J. S. Am. Earth Sci. 104, 102932 https://doi.org/10.1016/j.jsames.2020.102932.
Montaron, B., Tapponnier, P., 2010. A quantitative model for salt deposition in actively spreading basins. Search Dis. 30117.
Moy, C., Traverse, A., 1986. Palynostratigraphy of the subsurface eagle mills formation (Triassic) from a well in east-central texas, USA. Palynology 10 (1), 225–234.
Mutter, J.C., Buck, W.R., Zehnder, C.M., 1988. Convective partial melting: 1. A model for the formation of thick basaltic sequences during the initiation of spreading. J. Geophys. Res. Solid Earth 93 (B2), 1031–1048.
Nakamura, Y., Sawyer, D.S., Shaub, F.J., MacKenzie, K., Oberst, J., 1988. Deep Crustal Structure of the Northwestern Gulf of Mexico.
Nelson, K.D., Arnow, J.A., McBride, J.H., Willemin, J.H., Huang, J., Zheng, L., Oliver, J. E., Brown, L.D., Kaufman, S., 1985. New COCORP profiling in southeastern United States; Part l, Late Paleozoic suture and Mesozoic rift basin. Geology 13, 714–718.
Nguyen, L.C., Mann, P., 2016. Gravity and magnetic constraints on the Jurassic opening of the oceanic Gulf of Mexico and the location and tectonic history of the Western Main transform fault along the eastern continental margin of Mexico. Interpretation 4 (1), SC23–SC33.
Nicholas, R.L., Waddell, D.E., Hatcher, R.D., Thomas, W.A., Viele, G.W., 1989. The Ouachita system in the subsurface of Texas, Arkansas, and Louisiana. The Appalachian-Ouachita Orogen in the United States 661–672.
Nirrengarten, M., Manatschal, G., Yuan, X.P., Kusznir, N.J., Maillot, B., 2016. Application of the critical Coulomb wedge theory to hyper-extended, magma-poor rifted margins. Earth Planet. Sci. Lett. 442, 121–132.
Norton, I.O., Carruthers, D.T., Hudec, M.R., 2016. Rift to drift transition in the South Atlantic salt basins: A new flavor of oceanic crust. Geology 44 (1), 55–58.
O'Reilly, C., Keay, J., Birch-Hawkins, A., Bate, D., Halliday, J., 2017. Regional play types in the Mexican Offshore.
Olson, H.C., Snedden, J.W., Cunningham, R., 2015. Development and application of a robust chronostratigraphic framework in Gulf of Mexico Mesozoic exploration. Interpretation 3 (2), SN39–SN58.
Padilla Sánchez, R.J., 2016. Late Triassic-Late Cretaceous Paleogeography of Mexico and the Gulf of Mexico.
Palmason, G., 1980. A continuum model of crustal generation in Iceland: kinematic aspects. J. Geophys. 47, 7–18.
Paton, D.A., Pindell, J., McDermott, K., Bellingham, P., Horn, B., 2017. Evolution of seaward-dipping reflectors at the onset of oceanic crust formation at volcanic passive margins: insights from the South Atlantic. Geology 45, 439–442.

Peel, F.J., 2019. Paleo-Oceanographic preconditioning promotes precipitation: how the global context is a key factor for understanding Bajocian Louann Salt deposition. In: GCSSEPM Foundation 37th Annual Perkins-Rosen Research Conference.
Peel, F.J., Travis, C.J., Hossack, J.R., 1995. Genetic Structural Provinces and Salt Tectonics of the Cenozoic Offshore US Gulf of Mexico: A Preliminary Analysis.
Peña, J.M.C., 2016. Revisión estratigráfica del Jurásico en el Cerro La Cruz, Aramberri, Nuevo León (Doctoral dissertation. Universidad Autónoma de Nuevo León).
Pérez-Gussinyé, M., 2013. A tectonic model for hyperextension at magma-poor rifted margins: an example from the West Iberia–Newfoundland conjugate margins. Geol. Soc. Lond., Spec. Publ. 369 (1), 403–427.
Péron-Pinvidic, G., Manatschal, G., 2009. The final rifting evolution at deep magma-poor passive margins from Iberia-Newfoundland: a new point of view. Int. J. Earth Sci. 98 (7), 1581–1597.
Péron-Pinvidic, G., Manatschal, G., Dean, S.M., Minshull, T.A., 2008. Compressional structures on the West Iberia rifted margin: Controls on their distribution. Geol. Soc. Lond., Spec. Publ. 306 (1), 169–183.
Pindell, J.L., 1985. Alleghenian reconstruction and subsequent evolution of the Gulf of Mexico, Bahamas, and Proto-Caribbean. Tectonics 4 (1), 1–39.
Pindell, J., Dewey, J.F., 1982. Permo-Triassic reconstruction of western Pangea and the evolution of the Gulf of Mexico/Caribbean region. Tectonics 1 (2), 179–211.
Pindell, J., Heyn, T., 2011. Rapid subsidence at outer continental margins and SDR packages during the rift-drift transition: the roles of landward dipping faults and "magmatic detachment". In: AAPG Annual Convention and Exhibition.
Pindell, J.L., Kennan, L., 2001. December. Kinematic evolution of the Gulf of Mexico and Caribbean. In Transactions of the Gulf Coast Section Society of Economic Paleontologists and Mineralogists (GCSSEPM). In: 21st Annual Bob F. Perkins Research Conference, Petroleum Systems of Deep-Water Basins, Houston, Texas, December, pp. 2–5.
Pindell, J.L., Kennan, L., 2009. Tectonic evolution of the Gulf of Mexico, Caribbean and northern South America in the mantle reference frame: an update. Geol. Soc. Lond., Spec. Publ. 328 (1), 1–55.
Pindell, J., Miranda, E., 2011. Linked Kinematic Histories of the Macuspana, Akal-Reforma, Comalcalco, and Deepwater Campeche Basin Tectonic Elements, Southern Gulf of Mexico.
Pindell, J., Radovich, B., Horn, B., 2011. Western Florida: A New Exploration Frontier in the Eastern Gulf of Mexico.
Pindell, J., Graham, R., Horn, B., 2014. Rapid outer marginal collapse at the rift to drift transition of passive margin evolution, with a Gulf of Mexico case study. Basin Res. 26 (6), 701–725.
Pindell, J., Miranda, C.E., Cerón, A., Hernandez, L., 2016. Aeromagnetic map constrains Jurassic-Early cretaceous synrift, break up, and rotational seafloor spreading history in the Gulf of Mexico. In: Mesozoic of the Gulf Rim and beyond: New progress in science and exploration of the Gulf of Mexico Basin: SEPM Society for Sedimentary Geology, 35, pp. 123–153.
Pindell, J., Weber, B., Elrich, W.H., Cossey, S., Bitter, M., Molina, R., Graham, R., Erlich, R., 2019. Strontium isotope dating of evaporites and the breakup of the Gulf of Mexico and Proto-Caribbean Seaway. In: 2019 AAPG Annual Convention and Exhibition.
Pindell, J., Villagómez, D., Molina-Garza, R., Graham, R., Weber, B., 2020. A Revised Synthesis of the Rift and Drift History of the Gulf of Mexico and Surrounding Regions in the Light of Improved Age Dating of the Middle Jurassic Salt. Geological Society, London, Special Publications, p. 504.
Planke, S., Symonds, P.A., Alvestad, E., Skogseid, J., 2000. Seismic volcanostratigraphy of large-volume basaltic extrusive complexes on rifted margins. J. Geophys. Res. Solid Earth 105 (B8), 19335–19351.
Quirk, D.G., Shakerley, A., Howe, M.J., 2014. A mechanism for construction of volcanic rifted margins during continental breakup. Geology 42, 1079–1082. https://doi.org/10.1130/G35974.1.
Radovich, B., Horn, B., Nuttall, P., Mcgrail, A., 2011. The Only Complete Regional Perspective: RTM Re-Processing Gives a New Look at the Gulf of Mexico Continental Margin.
Ramos, E.L., 1975. Geological summary of the Yucatan Peninsula. In: The Gulf of Mexico and the Caribbean. Springer, Boston, MA, pp. 257–282.
Ramos, J.R.R., Mercado, M.A.C., Mora, L.E.S., Ferrer, C.R.L.F.S., 2009. Continental-Oceanic Boundary Deep Structure in a Shear Margin: Western Main Transform, Offshore Veracruz, southern Gulf of Mexico.
Raymond, D.E., 1989. Eagle Mills Formation of the Alabama Coastal Plain.
Rigoti, C.A., 2015. Evolução tectônica da Bacia de Santos com ênfase na geometria crustal. In: Interpretação integrada de dados de sísmica de reflexão e refração, gravimetria e magnetometria Doctoral dissertation, Dissertação de mestrado. Universidade Federal do Rio de Janeiro).
Rives, T., Pierin, A.R., Pulham, A.J., Salel, J.F., Wu, J., Duarte, A., Magnier, B., 2019. The Sakarn Series: A Proposed New Middle Jurassic Stratigraphic Interval from the Offshore Eastern Gulf of Mexico.
Rodriguez, A.B., 2011. Regional Structure, Stratigraphy, and Hydrocarbon Potential of the Mexican Sector of the Gulf of Mexico.
Rojas-Agramonte, Y., Neubauer, F., Garcia-Delgado, D.E., Handler, R., Friedl, G., Delgado-Damas, R., 2008. Tectonic evolution of the Sierra Maestra Mountains, SE Cuba, during Tertiary times: From arc-continent collision to transform motion. J. S. Am. Earth Sci. 26 (2), 125–151.
Rowan, M.G., 2014. Passive-margin salt basins: Hyperextension, evaporite deposition, and salt tectonics. Basin Res. 26 (1), 154–182.
Rowan, M.G., Sumner, H.S., Huston, H., Venkatraman, S., Dunbar, D., 2012. Constraining Interpretations of the Crustal Architecture of the Northern Gulf of Mexico.
Rubio-Cisneros, I.I., Lawton, T.F., 2011. Detrital zircon U-Pb ages of sandstones in continental red beds at Valle de Huizachal, Tamaulipas, NE Mexico: Record of Early-Middle Jurassic arc volcanism and transition to crustal extension. Geosphere 7 (1), 159–170.
Sager, W.W., Weiss, C., Tivey, M.A., Johnson, H.P., 1998. Geomagnetic polarity reversal model of deep-tow profiles from the Pacific Jurassic Quiet Zone. Proc. ODP Sci. Results 124, 659–669.
Salvador, A., 1987. Late Triassic-Jurassic paleogeography and origin of Gulf of Mexico basin. AAPG Bull. 71 (4), 419–451.
Salvador, A., 1991. Origin and development of the Gulf of Mexico basin. In: Salvador, A. (Ed.), The Gulf of Mexico Basin. The Geology of North America, pp. 389–444.
Sandwell, D.T., Müller, R.D., Smith, W.H., Garcia, E., Francis, R., 2014. New global marine gravity model from CryoSat-2 and Jason-1 reveals buried tectonic structure. Science 346 (6205), 65–67.
Saunders, M., Geiger, L., Rodriguez, K., Hargreaves, P., 2016. The Delineation of Pre-Salt License Blocks in the Deep Offshore Campeche-Yucatan Basin.
Sawyer, D.S., Ebeniro, J.O., O'Brien Jr., W.P., Tsai, C.J., Nakamura, Y., 1986. Gulf of Mexico Seismic Refraction Study, Alaminos Canyon OBS Experiment (Final Technical Report). University of Texas Institute for Geophysics Technical Reports.
Sawyer, D.S., Buffler, R.T., Pilger Jr., R.H., 1991. The crust under the Gulf of Mexico Basin. The Gulf of Mexico Basin: Geological Society of America, The Geology of North America, pp. 53–72.
Schlager, W., Buffler, R.T., Angstadt, D., Bowdler, J.L., Cotillon, P.H., Dallmeyer, R.D., Halley, R.B., Kinoshita, H., Magoon, L.B., Mcnulty, C.L., Patton, J.W., 1984. Deep sea drilling project, leg 77, southeastern Gulf of Mexico. Geol. Soc. Am. Bull. 95 (2), 226–236.
Schmandt, B., Lin, F.C., Karlstrom, K.E., 2015. Distinct crustal isostasy trends east and west of the Rocky Mountain Front. Geophys. Res. Lett. 42 (23), 10–290.
Schouten, H., Klitgord, K.D., 1994. Mechanistic solutions to the opening of the Gulf of Mexico. Geology 22 (6), 507–510.
Scott, K.R., Hayes, W.E., Fietz, R.P., 1961. Geology of the Eagle Mills formation.
Shann, M.V., Vazquez-Reyes, K., Ali, H.M., Horbury, A.D., 2020. The Sureste Super Basin of southern Mexico. AAPG Bull. 104 (12), 2643–2700.
Sibuet, J.C., Srivastava, S., Manatschal, G., 2007. Exhumed mantle-forming transitional crust in the Newfoundland-Iberia rift and associated magnetic anomalies. Journal of Geophysical Research: Solid Earth 112 (B6).
Sibuet, J.C., Tucholke, B.E., 2013. The geodynamic province of transitional lithosphere adjacent to magma-poor continental margins. Geol. Soc. Lond., Spec. Publ. 369 (1), 429–452.
Smith, W.H., Sandwell, D.T., 1997. Global sea floor topography from satellite altimetry and ship depth soundings. Science 277 (5334), 1956–1962.
Snedden, J., Galloway, W., 2019. The Gulf of Mexico Sedimentary Basin: Depositional Evolution and Petroleum Applications. Cambridge University Press, Cambridge, p. 326. https://doi.org/10.1017/9781108292795.014. IBSN: 978-1-108-41902.
Snedden, J.W., Norton, I.O., Christeson, G.L., Sanford, J.C., 2014. Interaction of deepwater deposition and a mid-ocean spreading center, eastern Gulf of Mexico basin, USA. Gulf Coast Association of Geological Societies Transactions, 64, pp. 371–383.
Snedden, J.W., Norton, I.O., Hudec, M.R., Peel, F., 2019. Paleogeographic Reconstruction of the Louann Salt Basin. Proc. of GCSSEPM Foundation 37th Annual Perkins-Rosen Research Conference 24–27.
Snedden, J.W., Stockli, D.F., Norton, I.O., 2020. Palaeogeographical reconstruction and provenance of Oxfordian aeolian sandstone reservoirs in Mexico offshore areas: Comparison to the Norphlet aeolian system of the northern Gulf of Mexico. In: Davison, I., Hull, J.N.F., Pindell, J. (Eds.), The basins, orogens and evolution of the southern Gulf of Mexico and northern Caribbean: Geological Society, v. 504. Special Publications, London, p. 21. https://doi.org/10.1144/SP504-2019-219.
Snee, J.E.L., Zoback, M.D., 2020. Multiscale variations of the crustal stress field throughout North America. Nat. Commun. 11 (1), 1–9.
Steier, A., Mann, P., 2019. Late Mesozoic gravity sliding and Oxfordian hydrocarbon reservoir potential of the northern Yucatan margin. Mar. Pet. Geol. 103, 681–701.
Steltenpohl, M.G., Horton, J.W., Hatcher, R.D., Zietz, I., Daniels, D.L., Higgins, M.W., 2013. Upper crustal structure of Alabama from regional magnetic and gravity data: Using geology to interpret geophysics, and vice versa. Geosphere 9 (4), 1044–1064.
Stern, R.J., Dickinson, W.R., 2010. The Gulf of Mexico is a Jurassic backarc basin. Geosphere 6 (6), 739–754.
Stern, R.J., Anthony, E.Y., Ren, M., Lock, B.E., Norton, I., Kimura, J.I., Miyazaki, T., Hanyu, T., Chang, Q., Hirahara, Y., 2011. Southern Louisiana salt dome xenoliths: First glimpse of Jurassic (ca. 160 Ma) Gulf of Mexico crust. Geology 39 (4), 315–318.
Talwani, M., Ewing, J., Sheridan, R.E., Holbrook, W.S., Glover, L., 1995. The EDGE experiment and the US East Coast magnetic anomaly. In: Rifted Ocean-Continent Boundaries. Springer, Dordrecht, pp. 155–181.
Ten Brink, U.S., Lee, H.J., Geist, E.L., Twichell, D., 2009. Assessment of tsunami hazard to the US East Coast using relationships between submarine landslides and earthquakes. Mar. Geol. 264 (1-2), 65–73.
Thangraj, J.S., Quiros, D.A., Pulliam, J., 2020. Using ambient noise seismic interferometry and local and teleseismic earthquakes to determine crustal thickness and Moho structure of the northwestern Gulf of Mexico margin. Geochem. Geophys. Geosyst. 21 (7) e2020GC008970.
Tominaga, M., Sager, 2010. Revised Pacific M-Anomaly Geomagnetic Polarity Timescale: GJI, 182, pp. 203–232. https://doi.org/10.1111/j.1365-246X.2010.04619.x.
Trudgill, B.D., Rowan, M.G., Fiduk, J.C., Weimer, P., Gale, P.E., Korn, B.E., Phair, R.L., Gafford, W.T., Roberts, G.R., Dobbs, S.W., 1999. The Perdido fold belt, northwestern deep Gulf of Mexico, part 1: structural geometry, evolution and regional implications. AAPG Bull. 83 (1), 1320–1336.

Tugend, J., Gillard, M., Manatschal, G., Nirrengarten, M., Harkin, C., Epin, M.E., Sauter, D., Autin, J., Kusznir, N., Mc-Dermott, K., 2018. Reappraisal of the magma-rich versus magmapoor rifted margin archetypes. Geol. Soc. London 476.

Van Avendonk, H.J., Christeson, G.L., Norton, I.O., Eddy, D.R., 2015. Continental rifting and sediment infill in the northwestern Gulf of Mexico. Geology 43 (7), 631–634.

Wagner, L.S., Fischer, K.M., Hawman, R., Hopper, E., Howell, D., 2018. The relative roles of inheritance and long-term passive margin lithospheric evolution on the modern structure and tectonic activity in the southeastern United States. Geosphere 14 (4), 1385–1410.

Warren, J.K., 2006. Evaporites: sediments, resources and hydrocarbons. Springer Science & Business Media.

Weeks, W.B., 1938. South Arkansas stratigraphy with emphasis on the older coastal plain beds. AAPG Bull. 22 (8), 953–983.

Weislogel, A.L., Hunt, B., Lisi, A., Lovell, T., Robinson, D.M., 2015. Detrital zircon provenance of the eastern Gulf of Mexico subsurface: Constraints on Late Jurassic paleogeography and sediment dispersal of North America. Late Jurassic Margin of Laurasia—A Record of Faulting Accommodating Plate Rotation. Geol. Soc. Am. Spec. Pap. 513, 89–105.

White, R.S., Smith, L.K., 2009. Crustal structure of the Hatton and the conjugate east Greenland rifted volcanic continental margins, NE Atlantic. J. Geophys. Res. Solid Earth 114 (B2).

White, R.S., Spence, G.D., Fowler, S.R., McKenzie, D.P., Westbrook, G.K., Bowen, A.N., 1987. Magmatism at rifted continental margins. Nature 330 (6147), 439–444.

Whitmarsh, R.B., Manatschal, G., Minshull, T.A., 2001. Evolution of magma-poor continental margins from rifting to seafloor spreading. Nature 413 (6852), 150–154.

Wiley, K.S., 2017. Provenance of Syn-rift Clastics in the Eastern Gulf of Mexico: Insight from U-Pb Detrital Zircon Geochronology and Thin Sections. Graduate Theses, Dissertations, and Problem Reports, 6951. https://researchrepository.wvu.edu/etd/6951.

Williams-Rojas, C.T., Reyes-Tovar, E., Miranda-Peralta, L., Reyna-Martinez, G., Cardenas-Alvarado, A., Maldonado-Villalon, R., Muñoz-Bocanegra, V., Lora-delaFuente, C., 2011. Hydrocarbon Potential of the Deepwater Portion of the "Salina del Istmo" Province. Southeastern Gulf of Mexico, Mexico.

Winterer, E.L., 1991. The Tethyan Pacific during Late Jurassic and Cretaceous times. Palaeogeogr. Palaeoclimatol. Palaeoecol. 87 (1-4), 253–265.

Wood, G.D., Benson Jr., D.G., 2000. The north american occurrence of the algal coenobium plaesiodictyon'. paleogeographic, paleoecologic, and biostratigraphic importance in the Triassic. Palynology 24 (1), 9–20.

Woods, R.D., Addington, J.W., 1973. Pre-Jurassic Geologic Framework Northern Gulf basin.

Woods, R.D., Salvador, A., Miles, A.E., 1991. pre-Triassic. The Gulf of Mexico Basin. Colorado, Geological Society of America, Geology of North America, Boulder, pp. 109–129.